

**AEROSOL GEOCHEMISTRY IN
RAJASTHAN AND DELHI REGIONS AND
ITS ENVIRONMENTAL IMPLICATIONS**

*Thesis Submitted to the Jawaharlal Nehru University
for the award of the degree of*

Doctor of Philosophy

By

SUDESH YADAV



**School of Environmental Sciences
Jawaharlal Nehru University
New Delhi – 110067
INDIA
November, 2003**

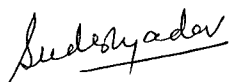



जवाहरलाल नेहरू विश्वविद्यालय
Jawaharlal Nehru University
SCHOOL OF ENVIRONMENTAL SCIENCES
New Delhi-110067

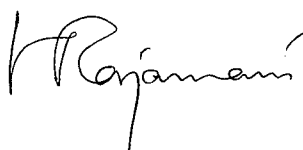
November 27, 2003

CERTIFICATE

The thesis entitled "*AEROSOL GEOCHEMISTRY IN RAJASTHAN AND DELHI REGIONS AND ITS ENVIRONMENTAL IMPLICATIONS*" embodies the original work, carried out at *School of Environmental Sciences, Jawaharlal Nehru University, New Delhi, India*. This work has not been submitted in full or partial for any other degree or diploma to any other university or institute.


SUDESH YADAV
(Candidate)


Prof. Kasturi Datta
(Dean, SES)


Prof. V. Rajamani
(Supervisor)

Dedicated to-----

My Father

&

Late Mother

ACKNOWLEDGEMENTS

The task of acknowledging the immense debt of gratitude, which one owes to so many people, is perhaps the most pleasant aspect of writing a dissertation. Words alone are inadequate to convey my deep sense of gratitude towards my supervisor, Prof. V. Rajamani, Professor of Geology, School of Environmental Sciences for his affectionate guidance, incessant inspiration and constructive criticism at all stages of this work. His intellectual brilliance, analytical skills, innovative ideas, overwhelming experience and enthusiasm had been the path of light to the objective of this study. I am highly indebted for the encouragement infused in me by him to do research.

I take this opportunity to acknowledge Prof. V. Rajamani, Prof. J. Subba Rao, Prof. D. K. Banerjee and Prof. Kasturi Datta, successive Deans, School of Environmental Sciences for providing the school facilities to me for this work.

I am thankful to Prof. V. K. Jain and Prof. A. K. Attri, SES, for their immaculate suggestions as well as for the affection shown towards me. Prof. Talat Ahmed, DU, Delhi, Prof. Balakrishnan, PU, Pondicherry and Prof. Ramesh, PRL Ahmedabad are thanked for their guidance and help during this work. I am grateful to Dr. Shiva Siddaiah, WIHG, Dehradun for helping me in the isotope data generation on his TIMS machine and for his time to time guidance. I acknowledge the help of Prof. D. C. Srivastava and his student in carrying out SEM-EDEX analysis at IIT, Roorkee. I heartily acknowledge my M. Sc. teacher Prof. Ishwar Singh, MDU, Rohtak for his care, affection and guidance at various stages of research career since my M. Sc. days. I am thankful to Dr. Ram Singh, Asst. Professor SCLG, JNU, for his affection and care given to me. The valuable and unflinching help and support of teachers always urged me to learn better.

I am thankful to my lab seniors Dr. Meenal Mishra and Dr. J. K. Tripathi, scientist, NFG, SES for their help and guidance at various stages of the work. The loving respectable attitude and their kind nature to help made me remember my juniors Rajneesh, Pankaj and Deepika. I am highly indebted to my lab senior Dr. K. L. Pruseth and juniors, Rajneesh and Pankaj, who

have helped me a lot in computer work and in organization of the thesis, especially during the last week of submission. I am also equally thankful to my former lab seniors Dr. Mohanta ji, Scientist, NML, Jamshedpur, Dr. Anupam, Scientist, BSIP, Lucknow, Dr. Pramod, PU, Pondicherry, Dr. Giritharan, GSI, Calcutta and Dr. K. P. for their cooperation and brotherly guidance during their stay here in the lab as well as from their working place.

Friends and colleagues have contributed so immensely in realizing my work, that it cannot be expressed in words alone. Work and stay in JNU became a pleasure during the companionship of Abhay, Anirudha and Ms. Sudesh Chaudhary. This trio of friends had their significant contribution in personal life than in academic, particularly when I badly needed recreation and relaxation. Friends and batchmates at JNU Anup Das, Chandu, Ravi, Rajesh and Somendu (now IPS), and Pramod are acknowledged for their company. Help of Mansi in proof reading is duly acknowledged. I am thankful to J. P. bhai sahab for just getting me relaxed out of tension at weak ends. I am grateful to Neelay, my neighbor in hostel, for his care and moral support during the last days of work. Dr. Jaibir deserves thanks for his brotherly guidance and care given to me since my M. Sc. days. I remain obliged to my Narnaul friends Ashok (Guruji), Rajesh, Dr. Rajeev, Dr. Surender, Virender secretary and DBDN who have always stood by me during my stay at my home town as well as at JNU.

I duly oblige the assistance extended to me by all the faculty members and staff of SES in my research work. Venket, B. D. Sharma are thanked for technical assistance during the work. Periswamy (Raju), Nukul and Babu Ram are thanked for their laboratory assistance and Ms. Maya for computer work. The refreshing tea and coffee served by Yunus in the lab deserve a mention here.

I express my sincere thanks to Mrs. Sushila Yadav, Mr Naresh Surelia, GPF Manager, Jhunjhunu, and Mr. Manish Dadu of Garhmuktesar for extending co-operation and help to me during the sampling at Udairamsar (Bikaner), Jhunjhunu and Garhmuktesar, respectively. I am grateful to Harish Gadhavi, PRL, Ahmedabad for calculating air back trajectories. The meteorological data and library help provided by Indian Meteorological Department, New Delhi and its Jaipur station are duly acknowledged.

I owe my thanks to my mamaji Shri Mahipal Singh and Rishi, and bhaiya Manoj Yadav for their supportive nature and for now and then asking me about my work and thesis submission. My father has always been supportive in my endeavors. I am indeed grateful to my father and brother 'Babbu' who have always encouraged me in pursuit of higher education. I owe my present status to my father for his enduring patience.

Lastly, financial assistance provided to me by the University Grants Commission, New Delhi and Jawaharlal Nehru University is gratefully acknowledged. I am solely responsible for any error in this thesis.

SUDESH YADAV

VITAÉ

PAPERS

- **Yadav S.** and Rajamani V. (2003a) Aerosols of NW India-a potential Cu source!
Curr. Sci. **84(3)**, 278-280.
- **Yadav S.** and Rajamani V. (2003b) Geochemistry of aerosols of northwestern part of India adjoining the Thar desert. *Geochim. Cosmochim. Acta* (accepted).

ABSTRACTS

- ◆ **Yadav S.** and Rajamani, V. (2000) Aerosol geochemistry: implications to surface earth processes and nutrient dynamics. In memoir the “*Annual convention of the Geological Society of India and the National symposium on Milestone in petrology at the end of millenium and future perspectives*” held at Banaras Hindu University between Nov. 14 to 16, 2000.
- ◆ **Yadav S.** and Rajamani, V. (2001) Geochemistry of aerosols in North-West India. *Eos Trans. AGU*, 82 (47), Fall Meet. Suppl, Abstract xxxxx-xx, 2001, Abstract published and accepted for Oral presentation..

PAPER PRESENTED

- ◆ **Yadav S.** (2000) Aerosol geochemistry: implications to surface earth processes and nutrient dynamics. A paper presented in “Annual convention of the Geological Society of India and the National symposium on Milestone in petrology at the end of millenium and future perspectives” held at Banaras Hindu University between Nov. 14 to 16, 2000.
- ◆ **Yadav S.** (2001) Geochemistry of dust in Delhi region – a Talk given in workshop on “Aerosol, cloud and climate” 9-13th July 2001 at IISc, Bangalore.

TRAINING COURSES ATTENDED

- ◆ Workshop on “*Aerosol, cloud and climate*” held at IISc, Bangalore from 9-13th July 2001 conducted by CAS, IISc. Bangalore and ISRO space cell, GOI.
- ◆ Training course on “*Theory and practice of Inductively Coupled Plasma Spectrometry*” held at NIO Goa from 3rd to 5th Feb. 2003, organized by GSI and International association of Geochemistry and Cosmochemistry.

ABSTRACT

The atmosphere is of cardinal importance in sustaining life system on our planet. Compositionally “atmosphere” is a conglomeration of gaseous, liquid and solid phases. The dispersion of liquid or solid phases in a gaseous phase (air) in the atmosphere make the “aerosols” which are there everywhere in the atmosphere and perhaps all through the geological time scale. Humans have lived with natural aerosols over the entire course of their history on earth. In contrast, we have been living with pollutant aerosols for a relatively short time in our history, since the beginning of industrial age. Population explosion and industrial growth together have disrupted the natural composition of the atmosphere. No air is found clean on planet earth even at the remote sites. This has resulted in global warming, climatic changes, environmental pollution and adverse health effects. Atmospheric aerosols have a variety of natural and anthropogenic causes. Natural sources include wind blown dust, soils, sea salt sprays, volcanic emissions, forest fires and anthropogenic include point industry sources, vehicular exhaust, biomass burning as well as secondary aerosol particles formed by physical and chemical interactions in atmosphere. Total aerosol emission from these sources have been estimated globally and known to vary between 1000-3000 Tg/year. Anthropogenic sources contribute 20 to 25% of total aerosol content of atmosphere and this is expected to further increase with increasing human activities in future. The total flux of natural aerosols averaged over the globe is about three to four times larger than the flux of aerosols generated by human activities. The global production of natural dust may also be increasing substantially due to desertification by human activity. However, on a regional scale, the flux of

anthropogenic aerosols can dominate over natural ones by three to four folds or vice versa.

Recently, there is a great deal of interest in the study of dust and aerosols because of their importance in climate change problems, nutrient dynamics, atmospheric pollution and environmental health and in the process of desertification. Most studies have shown that our present understanding of dust and aerosols with respect to physico-chemical-biological properties, diverse sources and mechanisms of transport and deposition is very limited considering their application potential. Any improvement to our knowledge of dust and aerosols requires more data on different aspects of aerosols from diverse geographic settings. The northwestern part of India witnesses frequent dust storms (locally known as “aandhi”) during summer months (April to July) before the onset of the monsoon. These dust storms transport a large quantity of sediments in this arid to semi arid regions. The famous Thar desert of Rajasthan lies in the westernmost part of India and the prevailing winds are strongly westerly during the summer months. No information is yet available on the physico-chemical nature of the dust/aerosols that are being transported, their proximal and distal sources, causes and consequences, and time duration of aeolian processes. A few chemical studies of rainwater and aerosols in this region point to the neutralizing effect of crustally derived cations on the pH of rainwater. Because of the lack of primary data on the dust and aerosols in this vast arid zone of India and also because of the regional and global importance of dust and aerosols in general, the present work on *“Aerosol Geochemistry in Rajasthan and Delhi Regions and its Environmental Implications”* was undertaken.

Four different sampling locations covering a total distance of 600 km along the dominant SW-W winds were selected for the study of aerosols in NW India. The

sampling sites are Bikaner (28.01°N and 73.22°E) in the Thar desert in west Rajasthan, Jhunjhunu (28.06° N and 75.25° E) and Delhi (28.38° N and 77.12° E) situated at the desert margins and Garhmuktesar (28.42° N and 77.8° E) in the Ganga alluvial plains in the east. This corridor was selected because the strong W-SW winds dominate dust storms. The Thar desert as well as most of Rajasthan and the Delhi region experience a hot, arid to semi arid climate. The prevailing SW-W surface winds attain their maximum strength of 25-30 km/h over west Rajasthan during June and raise a tremendous amount of dust from the loose sandy soil of the region and the dust is transported eastward over the neighboring states of India. Thus, the Thar desert and parts of western India become the center of intense dust activity before the onset of Monsoon.

Geologically, the study area includes the Thar desert, the Aravalli hill ranges and the Indogangetic alluvium represented by our specific sampling locations, Bikaner, Jhunjhunu and Delhi, and Garhmuktesar, respectively. In the Thar region a thick pile of loose sands is underlain by middle to late Proterozoic metasediments and acid volcanics and Mesozoic to Tertiary sandstones, limestones and gypsum. The Aravalli hills, which mark the eastern boundary of the Thar desert, consist of the Delhi Supergroup with high metamorphic grade metasediments. The Gangetic alluvium to the east is Quaternary in age and was deposited by the Himalayan rivers draining from the High Himalayan Crystalline (HHC) lithotectonic units of the Himalayan orogen. The Thar desert has an areal extent of nearly 320,000 sq. km in the NW part of India (a part of it lies in the Sind province of Pakistan) and has an undulating topography. The low lying (mean elevation of 500-600 m) Aravalli hills act as a barrier to the transport of sediments from the Thar by the prevailing winds. The region adjacent to active desert includes several saline lakes, of which Sambhar

(bolsan type) and Didwana (playa type) are the important ones. To the east of the Aravalli hills, the area is covered with river alluvium as well as wind reworked alluvium. The probable anthropogenic sources in the Thar region are clay mines and gypsum quarries in and around Bikaner and copper mining in Khetri, 60 km east of Jhunjhunu. Otherwise the region is very poorly industrialized compared to the eastern region. Vehicular emissions, thermal power plants and other small-scale industrial units are the major polluting sources. Biomass burning is another important source as wood is the most widely used fuel in this region in winter.

Three different size fractions of aerosols (free fall = FF, suspended particulate matter = SPM, particles less than 10 μm = PM_{10} and $>10\mu\text{m}$) were collected using different sampling techniques simultaneously at Bikaner, Jhunjhunu and Delhi stations using available instruments and limited logistics. Aerosol samples were collected for a few days in both summer and winter seasons between 19-26th May, 2000 and 17-27th Jan 2001, respectively. At Garhmuktesar, aerosol sampling during summer could not be performed due to non-availability of air samplers. However, free fall samples were collected for a longer duration (40 days) in May-June before the onset of the summer monsoon, and January-February in winter. FF samples were collected using marble dust collectors, which is a widely accepted international standard method of FF collection. SPM and PM_{10} samples were collected on high quality glass microfiber filter paper EPM 2000 by using High volume air samplers, which meet United States Environmental Protection Agency (USEPA) as well as Central Pollution Control Board, (CPCB) New Delhi norms. The surface sediments also were collected as channel samples and were used as reference material in this study. The FF as well as sediment samples were processed to -200 mesh size whereas SPM and PM_{10} were scraped off the filter papers with greater than 95% recovery. All

types of aerosols and sediment samples were characterized for their texture and mineralogy by using Fritsch Analysette 22 laser particle size analyzer and Philips X-ray diffractometer, respectively. All types of sample powders were put to solution by using standard acid dissolution methods for major and trace element analysis. Samples were digested by using NaOH-Na₂O₂ fusion method and Rare earth elements were separated and pre-concentrated by column chemistry using cation exchange resin (Dowex-50) in hydrogen form. All the major and trace elements including REE were analyzed on ICP-AES (JY make). The precision and accuracy of the analysis for major and trace elements was better than 5 and 2% respectively. ⁸⁷Sr/⁸⁶Sr isotopic ratios of a few bulk aerosol samples were obtained by using a multi collector solid source Thermal Ionization Mass Spectrometer VG 354 at the Wadia Institute of Himalayan geology, Dehradun. ⁸⁷Sr/⁸⁶Sr isotopic ratios of three carbonate leached aerosol samples (1.3 N HCl) were obtained by using TIMS, model MAT-262 installed at GEOMAR, Kiel, Germany. Electron micro-probe analysis for a few selected samples was done using SEM-EDX at IIT, Roorkee.

Different size fractions of aerosols (FF, SPM, PM₁₀ and >10µm) as well as the surface sediment samples, collected from Bikaner, Jhunjhunu, Delhi and Garhmuktesar situated along the dominant wind trajectory for about 600 km were characterized for their texture, mineralogy and geochemistry including REE and Sr isotopes. Within each size fraction, a bimodal distribution of grain size was observed. Quartz is the dominant mineral followed by K-feldspar, mica, calcite, chlorite and plagioclase. Garnet, amphibole, titanite and zircon are some of the identified heavy minerals. The geochemical nature of aerosols is a function of source (s), wind strength (speed and direction), particle size, and sampling site and season. The aerosols are generated from two dominant sources, crustal and anthropogenic activities. The

crustal materials themselves have two components, the Thar silicate sediments derived from the Himalayas and non silicate, such as, soil carbonates in the Thar sediments, and the dry lakebeds in desert regions. The anthropogenic sources again include contributions from vehicular exhaust, oil/coal combustion, metal and mining industry, and biomass burnings. Geochemical coherence among aerosols, deposited surface sediments and the Thar sands, and the limited Sr isotopic data indicate that the Thar sediments and certain lithotectonic units of the Himalayan orogen are the proximal and distal crustal sources, respectively, for the aerosols in this region. Prevailing aridity and strong summer winds, and the presence of river alluvium in the Thar act together to transport silt rich dust, the removal of which could be a possible mechanism of the ongoing desertification. The different sources identified contribute differently to the chemistry of different fractions of aerosols, for the different elements and in different seasons. Whereas crustal sources are dominant in all the size grades, anthropogenic components show up in the finer fractions; metal and mining industry to size fractions \leq free fall aerosols, coal/oil combustion and vehicular exhaust to particles of size \leq suspended particulate matter, and biomass burnings to fractions \leq PM₁₀. The crustal components are somewhat diluted by the anthropogenic inputs in the finer fractions, particularly in the winter season and vice versa is true in the summer season. The wind strength (speed and direction) acts as an intensive variable in deciding the chemistry of aerosols. Strong winds make the crustal component a very large part of the aerosols and therefore, result in the very homogeneous and uniform chemistry in different fractions of aerosols in different regions. During periods of low wind strength, the aerosols become heterogeneous in their chemistry, particularly in that of the trace elements which have been contributed by the anthropogenic sources and in the winter season. Wind strength also indirectly

controls the trace element chemistry of the crustal component in aerosols through differential lifting, transportation and deposition of the heavy minerals hosting the trace elements present in the silicate sediments. The observed aerosol chemistry has both positive and negative impact to the environment. The dominant crustal component would buffer the rain water pH by providing cation rich aerosols. Presence of some of the nutrient cations such as Ca, K and Mg in aerosols may be responsible for the enhanced or at least self sustained fertility of the soil system in the down wind region and for the removal of fertility in the upwind region. The high levels of accumulation of some of the toxic trace elements such as Ba, Pb, Zn, Ni and Cu in the soils of the semi arid and monsoonal climatic regions of N-NW India may get into the water and soil systems which are detrimental to terrestrial and aquatic life systems.

CONTENTS

ACKNOWLEDGEMENTS	i-iii
VITAÉ	iv
ABSTRACT	v-xi
CONTENTS	xii-xiii
LIST OF FIGURES	xiv-xvi
LIST OF TABLES	xvii
CHAPTER 1. INTRODUCTION	1-19
1.1 PHSYIO-CHEMICO AND BIOLOGICAL PROPERTIES OF AEROSOLS	
1.2 IMPORTANCE OF AEROSOLS	
1.3 SOURCES OF AEROSOLS	
1.4 WORLD SCENARIO	
1.5 INDIAN CONTEXT	
1.6 OBJECTIVES OF THE STUDY	
CHAPTER 2. STUDY AREA	20-39
2.1 SAMPLING LOCATIONS	
2.2 CLIMATE	
2.3 PHYSIOGRAPHY	
2.4 REGIONAL GEOLOGY	
2.5 SOIL	
2.6 VEGETATION	
2.7 ANTHROPOGENIC SOURCES	
2.8 RATIONALE FOR SAMPLING SITE SELECTION	
CHAPTER 3. METHODOLOGY	40-59
3.1 SAMPLE COLLECTION	
3.2 SAMPLE PROCESSING	
3.3 INSTRUMENTS AND APPARATUS	
3.4 CHEMICALS AND REAGENTS USED	
3.5 TEXTURE ANALYSIS	
3.6 MINERALOGICAL ANALYSIS	
3.7 SAMPLE DISSOLUTION	

3.8 DETERMINATION OF SILICA	
3.9 ⁸⁷ SR/ ⁸⁶ SR ISOTOPE RATIO	
3.10 SAMPLE ANALYSIS BY ICP-AES	
3.11 DETERMINATION OF CHEMICAL INDEX OF ALTERATION	
CHAPTER 4. AEROSOL GEOCHEMISTRY	60-94
4.1 ABSTRACT	
4.2 INTRODUCTION	
4.3 REGIONAL GEOLOGY AND METEOROLOGY	
4.4 SAMPLING AND ANALYTICAL TECHNIQUES	
4.5 RESULTS AND DISCUSSION	
4.6 CONCLUSIONS	
CHAPTER 5. ENVIRONMENTAL CHEMISTRY	95-116
5.1 INTRODUCTION	
5.2 DEPOSITIONAL FLUX AND THE AIR QUALITY	
5.3 TRACE METAL CHEMISTRY	
5.4 ENVIRONMENTAL CONSEQUENCES	
CHAPTER 6. AEROSOLS - A POTENTIAL Cu SOURCE!	117-124
CHAPTER 7. CONCLUSIONS	125-127
REFERENCES	128-143
APPENDICES	144-155

LIST OF FIGURES

Figure 2.1 Map of the study area showing aerosol-sampling locations, dominant wind direction and prominent physiographic features.

Figure 2.2 Various climatic zones in the study area.

Figure 2.3 (a) Wind rose diagram for Bikaner (A - April, B - May, C - June, D- July and E - December 2000). Number in circle indicates the percent calm period. Wind speed is given in Knots per hour. Data source: IMD, Jaipur.

Figure 2.3 (b) Wind rose diagram for Delhi (A - April, B - May, C - June, D- July and E - December 2000). Number in circle indicates the percent calm period. Wind speed is given in Knots per hour. Data source: IMD, Jaipur.

Figure 2.4 Air back trajectories during sampling period in summer, 2000 and winter, 2001 at different locations Bikaner, Jhunjhunu, Delhi and Garhmuktesar. Data source: FNL Meteorological data, National Oceanic Atmospheric Administration (NOAA), USA.

Figure 2.5 Schematic profile along 27° N showing general increase in altitude from mean sea level from west to east.

Figure 2.6 Geological map of the region around the sampling area.

Figure 2.7 Geological map of Rajasthan.

Figure 3.1 Various sampling techniques used for aerosol sample collection. (A) Trays containing marble bi-layers for free-fall collection. (B) High-volume air sampler for SPM collection. (C) High-volume air sampler for PM₁₀ collection.

Figure 3.2 Interior view of the dome-shaped cyclone chamber of the PM₁₀ high-volume air sampler.

Figure 3.3 Typical PM₁₀ cyclone collector depicting the principle for collection of only PM₁₀ aerosols on filter paper leaving behind the >10 μm fraction

Figure 4.1 Map of the study area showing aerosol-sampling locations, dominant wind direction and prominent physiographic features.

Figure 4.2 Major and trace element abundance in aerosols normalized to the abundance in average upper continental crust ($X_{\text{Aerosol}}/X_{\text{UCC}}$; UCC of Taylor and McLennan, 1985). Actual Ni concentration in Bikaner is 2.5 times to that shown in Figure 2f. FF-free fall; SPM-suspended particulate matter; PM_{10} – particulate matter less than 10 μm .

Figure 4.3 Chondrite normalized REE abundance and patterns of aerosol and sediment samples of NW India. Note the uniformity of REE chemistry of summer FF, SPM, PM_{10} , and $>10\mu\text{m}$ samples from different stations along the W-E wind corridor. In figure a, b and c, sample sites are not distinguished because of the closeness of abundance in samples collected from different sites. Data source: Loess (McLennan, 1995); Upper Continental Crust (UCC) and Post Archean Australian Shale (PAAS) (Taylor and McLennan, 1985).

Figure 4.4 Equiline plots of sediment samples and UCC. Note the uniformity of composition of wind deposited Delhi ridge sediments (DRS) and sediment samples from Jhunjhunu.

Figure 4.5 A-CN-K ($\text{Al}_2\text{O}_3\text{-CaO} + \text{Na}_2\text{O-K}_2\text{O}$ normalized molecular composition after Nesbitt and Young, 1984) plot of aerosol and sediment samples from NW India. Upper Continental Crust (UCC) and Loess from Taylor and McLennan (1985); Post Archean Australian Shale (PAAS) from McLennan (1995); Yamuna river alluvium from Tripathi et al. (2003).

Figure 5.1 Atmospheric loading of free fall (FF), suspended particulate matter (SPM), PM_{10} aerosols at different locations in summer and winter. Dashed line represents the dust storm event during sampling campaign. Horizontal lines in the error bar indicate geometric mean and the error bar indicate geometric standard deviation.

Figure 5.2 Trace element abundance and variations in abundances in aerosols and surface sediment samples of different locations. Closed and open symbols represent summer and winter samples respectively. Line connecting * represent the crustal abundance of trace elements.

Figure 5.3 Scatter diagram showing correlation between Pb and Ba in our sample population.

Figure 5.4 Scatter plot of Cu vs. Zn in our sample population.

Figure 5.5 Site and seasonal variations in the accumulation rates of trace elements at Bikaner (Bkr), Jhunjhunu (Jhun), Delhi (Del) and Garhmuktesar (Garh) in NW India.

Figure 6.1 Sample locations of the present study. Map also shows the dominant wind trajectory in summer and winter months in the study area.

Figure 6.2 Dependency of Cu concentration on the particle size of aerosols in NW India. Open and filled symbols represent summer and winter samples. Bikaner: ▽, Jhunjhunu: □, Delhi: O, Garhmuktesar: ◇.

Figure AF.2.1 X-ray diffractograms of sediment samples. Scans are shifted by 200 counts and $2^\circ 2\theta$ from each other for better comparison.

Figure AF.2.2 X-ray diffractograms of summer and winter FF samples. Scans are shifted by 200 counts and $2^\circ 2\theta$ from each other for better comparison.

Figure AF.2.3 X-ray diffractograms of summer and winter SPM samples. Scans are shifted by 200 counts and $2^\circ 2\theta$ from each other for better comparison. Note the significant drop of intensity in the winter samples.

Figure AF.2.4 X-ray diffractograms of summer and winter PM_{10} samples. Scans are shifted by 200 counts and $2^\circ 2\theta$ from each other for better comparison. Note the significant drop of intensity compared to FF and SPM samples from all sites.

Figure AF-2.5 Backscattered electron images of different free-fall grains collected from Jhunjhunu. (A) rounded amphibole, (B) rounded chlorite, (C) sphene.

Figure AF-2.6 Backscattered electron images of different free-fall (A) and SPM (B & C) grains collected from Jhunjhunu. (A) elongated calcite, (B) lathe-shaped feldspar, (C) diamond-shaped amphibole showing cleavage at 120 degree.

LIST OF TABLES

- Table 1.1** Characteristic elements emitted from various out door particle sources
- Table 1.2** Estimates of annual global production of aerosols.
- Table 2.1** General geological succession in and around the study area.
- Table 3.1** Methods of chemical analysis.
- Table 4.1** Textural and mineralogical data of aerosols and sediment samples, and dust loading of air during sampling period.
- Table 4.2** Representative Electron Probe Micro-Analysis (EPMA) data on selected aerosol grains. Digits in parentheses show the number of grains analysed.
- Table 4.3** Texture and chemical composition of aerosols from NW part of India. Major oxides are in % and trace elements (in ppm). REE ratios are on chondrite normalized basis.
- Table 4.4** Inter and intra sample variability in chemical composition of Delhi aerosols. Major oxides are in % and trace elements (in ppm).
- Table 4.5** $^{87}\text{Sr}/^{86}\text{Sr}$ isotopic ratio of the analyzed aerosol Samples.
- Table 5.1** Dry accumulation rates of FF aerosols and the air quality data on SPM and PM_{10} aerosols for NW India.
- Table 5.2** Reference standards for average ambient air quality.
- Table 5.3** Trace element concentration (in ppm) in different size fractions of aerosols and sediment samples collected from different locations.
- Table 5.4** (A) Bulk free fall as well as the trace metal accumulation rates in $\text{mg}/\text{m}^2/\text{day}$ on soil/ water surface in NW India; (B) Trace element abundance in surface sediments and the projected percent increase in soil metal contents in next 20 years.
- Table 6.1** Cu concentration (ppm) in the aerosol samples of NW India. (values in parentheses are in $\mu\text{g}/\text{m}^3$ of air).
- Table AT 2.1** Geochemical analysis of aerosols of NW India.

Introduction

1. INTRODUCTION

Our environment, the place where we live, is the planet Earth. The Earth is made up of three reservoirs; the solid Earth or geosphere, the liquid layer or hydrosphere, and the gaseous envelope or atmosphere. Living organisms (the biosphere) inhabit all the three spheres interacting with them as well as combining them complexly. Atmosphere, an integral component of our planet, is of cardinal importance in sustaining life on our planet. Compositionally, “atmosphere” is a conglomeration of gaseous, liquid and solid phases. The dispersion of liquid or solid phases in the gaseous phase (air) makes the “aerosols” which are there everywhere in the atmosphere and perhaps all through the geological time. Humans have lived with natural aerosols over the entire course of their history on earth. In contrast, we have lived with pollutant aerosols for a relatively short time in our history since the beginning of the industrial age. Population explosion and industrial growth together have disrupted the natural composition of the atmosphere. No air is found clean on the planet earth even at the remote sites. This has resulted in global warming, climatic changes, environmental pollution and adverse health effects. The question that now comes to one’s mind is “Why Aerosols?” To a common man, a dust storm is an event, which forces him to stay indoors and pray for it to get over. To a geochemist, it is time to go out in the open and collect the aerosol particles. This collection would help him to decipher the code sent by natural as well as man made activities regarding their sources, climate changes, global warming, surface earth processes, pollution aspects and nutrient dynamics.

Broecker (2000) remarked that “*Were I to select one aspect of the climate record on which to focus attention, it would be dust*”. Such is the importance of dust in climate studies.

Aerosols, the ubiquitous component of the atmosphere, are suspension of particulate matter; either solid or liquid droplets or both in a gaseous medium, i.e., air. Aerosols and dust are considered synonymous and are frequently substituted for each other. The term aerosol strictly applies to both the gaseous and particulate phases in a system, but it is widely used to refer to the particulate phase alone (Prospero et al., 1983). Dust is a type of aerosols, related to, but distinct from smoke, mists, fumes and fogs (see appendix A1).

1.1 PHSYIO-CHEMICO AND BIOLOGICAL PROPERTIES OF AEROSOLS

The physical attributes of airborne particulates include mass concentration and the size distribution. Particle size distribution determines particle behavior (aging, transport, and deposition) and that particle size and shape are clearly linked to the nature of their sources, source(s) history, processes of their entrainment and transport, and post formation processes. The particle size is characterized by particle diameter. Diameter is a characteristic of spherical objects, although only a small fraction of aerosol particles are perfectly spherical in nature. Therefore, to represent particles of irregular shapes, the term particle equivalent diameter has been introduced. The particle diameter determination mainly again depends on the choice of particle properties or the behavior to be measured. The different classes of equivalent diameters are aerodynamic diameter (mainly for particles larger than 0.05 μm), Stoke's diameter and equivalent volume diameter (for detail definitions see appendix A1). Aerodynamic diameter is the most commonly used scale for size classification; ambient levels of mass concentration are measured in micro gram of particles per cubic meter of air ($\mu\text{g}/\text{m}^3$).

Depending upon the source and production mechanism aerosol size varies and extends over about five order of magnitude from 10^{-3} and 10^2 μm . Aerosols being produced by a variety of natural and man made processes are poly-disperse in nature, which means, an aerosol population of different sizes. Airborne particulates have a log normal size distribution, i.e., particle concentration versus particle size curve is normal (bell shaped) on a logarithmic scale. Geometric standard deviation characterizes the width of the peak in the distribution. Particle size distribution often contains one or more distinct peaks, called mode of the distribution depending upon the nature of source. Nomenclature of aerosols depends on the size of the particle, and the particle property and behavior under study, as both are very closely related. Depending on size, aerosols are broadly classified into small, large and giant particles. Depending on the mode of the size distribution, aerosols are categorized into three groups namely nucleation mode, accumulation mode and giant particle mode. Detailed nomenclature of aerosols used for different studies and their respective sizes are provided in appendix A1. The nucleation mode aerosols are produced mainly by gas to particle conversion processes in atmosphere, the accumulation mode by coagulation and condensational growth of nucleation mode aerosols and coarse mode aerosols by mechanical processes. The residence time of aerosols is also a function of particle size. Coarser particles do not stay in atmosphere and settle back by gravity sedimentation processes. Particles below 100 μm in size can stay in atmosphere for hours to a day, depending on the wind conditions. Highest residence time varying between days to weeks is observed for particles below 10 μm in size. Particles below 16 μm can be transported to several thousand kilometers in the atmosphere from the source region by wind (Rahn, 1976a and 1979; Duce et al., 1980; Pye, 1987; Prospero, 1999; Prospero et al., 2002). Thus, the fine and coarse mode particles (a)

originate separately, (b) are transported separately, (c) have different chemical composition, (d) are removed from the atmosphere by different processes and (e) have different impact on the environmental quality.

It is, however, not only the number or mass of particles in a particular size range that is important, but also the composition of particles. Chemically, aerosols are dominantly in homogenous mixture of different chemical species. The elemental composition also strongly depends on the particle formation and post formation processes just as the particle size. The large particles carry compounds and elements mainly of crustal origin, and produced from natural processes. Some particles (largely stone or clay-based particulates emitted particularly by cement industry) act as carrier or adsorbate for the trace elements. The fine particles generally come from man made activities such as industry, vehicular exhaust and biomass burnings, and are rich in toxic metals (Natusch et al., 1974; Hlavay et al., 1992; Singh et al., 2002). Table 1.1 present examples of the most common suit of the elements related to common outdoor particle sources.

Biological content of aerosols include pollen grains, fungal spores, mites, insects, plant fragments and animal biomass, and such aerosols are called bioaerosols. The health effects of bioaerosols are also determined by their particle size. Airborne particulate matter causes adverse health effects through the inhalation of particles below 10 μm in size which can be deposited in the tracheobronchial and alveolar region of the lungs (Hileman, 1981). It is now well established that the fine aerosols are carrier of pollens, bacteria, fungal spores and cause allergic diseases (Lewis, 1984; Singh and Malik, 1994; Singh and Singh, 1994).

Table 1.1 Characteristic elements emitted from various out door particle sources*

Emission Sources	Characteristic Elements Emitted
Resuspended soil	Si, V, Cr, Ca, Ti, Sr, Al, Mn, Sc
Road transport Motor vehicle emissions Engine wear Catalytic converters Tyre wear Road side dusts	Br, Pb, Ba, Mn, Cl, Zn, V, Ni, Se, Sb, As Fe, Al Rare earths Zn C, Al, Si, K, Ca, Ti, Fe, Zn
Small combustion Refuse incineration Wood smoke	Zn, Sb, Cu, Cd, Hg, K, Pb Ca, Na, K, Fe, Br, Cl, Cu, Zn
Industrial facilities Oil fired power plants Coal combustion Refineries Nonferrous smelters Iron and steel mills Copper refinery	V, Ni Se, As, Cr, Co, Cu, Al, S, P, Ga V As, In, Cu, Zn Pb Cu
Minerals and material processing	Mg, Al, K, Sc, Fe, Mn
Sea spray	Na, Cl, S, K

* Morawska and Zang (2001) modified

1.2 IMPORTANCE OF AEROSOLS

There is an increasing interest in the study of aerosols because of their importance in many areas of environmental concern. Aerosols play an important role in the global climate system by altering the earth's radiation budget in the atmosphere through scattering and absorption of radiations (Tegen et al., 1996; Broecker, 2000; Haywood and Boucher, 2000; Harrison et al., 2001). Dust generation is a highly nonlinear process that is very sensitive to climate changes. There could even be a feedback between the climate and dust generation processes, and the climate forcing effects of dust. Mineral dust could also affect climate indirectly by affecting cloud nucleation and optical properties (Levin et al., 1996; Wurzler et al., 2000). In addition, dust can

serve as reactive surface for reactive gas species in the atmosphere (Dentener et al., 1996) and for moderating the photochemical processes (Dickerson et al., 1997). These heterogeneous secondary interactions are also responsible for the global ozone depletion (Subbaraya et al., 2000). Dust also has an important role in paleoclimate studies. The composition of wind blown dust in deep sea sediments (Rea, 1994; Kohfeld and Harrison, 2001), ice cores (Yung et al., 1996; Kreutz and Sholkovitz, 2000; Kohfeld and Harrison, 2001), Quaternary paleosols (Herwitz et al., 1996) and in Quaternary soils (Reheis et al., 1995) is often used as proxy indicator of paleoclimate aridity on the continents, and of global climate change records.

The generation, transport and deposition of aerosols have major environmental consequences and human economic benefits. Mineral dust plays an important role in the biogeochemical cycling of some nutrient elements (Michaels et al., 1996; Prospero et al., 1996; Reynolds et al., 2001) and toxic elements (Wood, 1974; Larocque and Rasmussen 1998; Rasmussen, 1998). Wind transported dust could be a dominant source of Fe, an essential micronutrient for phytoplanktons in many oceanic regions (Donaghay et al., 1991; DiTullio et al., 1993; Guerzoni and Chester, 1996; Falkowski et al., 1998; Fung et al., 2000). Moreover, certain cyanobacteria utilize Fe in their metabolism and play significant role in nitrogen chemistry of ocean; rate of production of nitrate and ammonia by these organisms is strongly influenced by the rate of input of dust to oceans (Michaels et al., 1996; Falkowski et al., 1998). The other groups of limiting nutrients, nitrate and phosphate for phytoplanktons are also directly influenced by the dust inputs to the oceans (Michaels et al., 1996; Prospero et al., 1996). Dust from distant sources is a major component of soils in arid and humid regions on the continents (Yaalon and Ganor, 1973; Reheis et al., 1995). This dust provides nutrients needed for plant growth and enhances the soil fertility after

deposition (Swap et al., 1992; Drees et al., 1993). Loess, the most fertile farmlands of the world, are formed by the deposition of wind blown dust (Pye, 1987; Tsoar and Pye, 1987). Selective lifting, transport and deposition of silt sized dust by winds are dominant processes of loess formation (Taylor et al., 1983; Pye, 1987). Massive loess deposits are found throughout Europe and Asia in the regions that have seen many of the early civilizations. Such wind blown dust deposits, i.e., loess cover approximately 10 % of the total land surface. On the other hand, dust also has a close relationship with desertification processes in the source regions. Desert regions are the cause of dust generation and the desertification (in terms of expansion of existing desert boundaries and loss of fertility) is the consequence of desert forming processes (Thomas and Middleton, 1994; Mortimore, 1998). However, the question of causation of dust over the globe is far from being resolved (Prospero et al., 2002). Geologically, dust deposition plays a role in hardening of rocks, desert varnish formation, duricrust development and cementation of sediments (Walker et al., 1982; Pye and Tsoar, 1987). Dust deposition also leads to the stabilization of sand dunes and other mobile surfaces in arid regions by formation of cohesive dust-rich crust. Goudie (1983) emphasized the general importance of wind as a geomorphological agent and identified several major geomorphological consequences of dust storms. Mechanics and geological implication of dust transport and deposition in deserts have been reviewed by Pye and Tsoar (1987) and Tsoar and Pye (1987). Within their composition, these wind born crustal sediments preserve a record of their source (provenance) and consequently allow us to examine the relationship between composition of upper crustal sources and the nature and distribution of sediments.

Acid rain has been the rallying cry for the past three decades in most parts of the industrialized world. Crustally derived aerosols strongly influence the acidity of

precipitation by neutralizing the acidic species such as SO_x and NO_x present in the atmosphere. Neutralization processes take place either through the dissolution of the dust particles in the acidic cloud of water droplets or through direct combination with gaseous sulphate and nitrate oxides (Gillette and Sinclair, 1990; Hedin and Likens, 1996). Among the aluminosilicate minerals, hydrolysis of feldspar is extremely slow even under mild acidic conditions (Lasaga, 1984), whereas carbonate minerals such as calcite and dolomite, on the other hand dissolve, rapidly. Birkeland (1974), Applin and Jersak (1986) and Young et al. (1988), in their study observed that calcium is by far, the most concentrated dissolved constituent in rainfall samples, which suggest the importance of carbonate component of dust in lowering of acidity of precipitation. Base cations of the dust also neutralize the acid when they reach the ground, although the chemistry remains different (Likens et al., 1996).

The dust after being deposited onto the soils and surface waters also affects human health and the life of terrestrial and aquatic ecosystems (Molnar et al., 1993). Inhalation of fine dust enriched in toxic metals such as Pb, Cd, Hg, Cu, Zn, Ni and As, the majority of which is considered anthropogenic (Galloway et al., 1982; Hlavay et al., 1992; Rasmussen, 1998; Singh et al., 2002), is very deleterious to human health compared to silicate dust (Ross et al., 1993). Recent studies show a close relationship between respiratory related mortality and morbidity and levels of particulate matter with diameter less than 10µm (Dockery et al., 1993; Adler and Fischer, 1994; Dockery and Pope, 1996). It is now well established that the fine aerosols are the carriers of pollens, bacteria and fungal spores (Lewis, 1984; Singh and Malik, 1994; Singh and Singh, 1994) and have higher concentrations of toxic elements such as Pb, Cu, Ni and Zn (Hlavay et al. 1992; Yadav and Rajamani, 2003 a). Recently, United States Environmental Protection Agency (USEPA) has reviewed and brought down

the standard of PM₁₀ to 50 µg/m³. This agency has suggested a great need to study the particles below 10 µm especially, PM₅ and PM_{2.5} aerosols to monitor the health effects (USEPA, 1996). Recent epidemiological evidences (Schwartz 1991; Schwartz and Dockery, 1992; Ostro, 1994) suggest that there is no safe limit for fine particles and the effects are linearly related to the concentration of toxic elements. The reduced visibility and corrosion of the monuments by dust activity are other causes of concern.

1.3 SOURCES OF AEROSOLS

Atmospheric aerosols have a variety of natural and anthropogenic causes. Natural sources include wind blown dust, soils, sea salt sprays, volcanic emissions, forest fires, etc. and the anthropogenic sources include point industry sources, vehicular exhaust, biomass burning as well as secondary aerosol particles formed by physical and chemical interactions in the atmosphere. Large quantities of aerosol particles are continually being put into the atmosphere by these sources-natural as well as anthropogenic. Total aerosol emission from these sources have been estimated globally and known to vary between 1000-3000 Tg/year (Andreae, 1995; Duce, 1995; IPCC 1995). Anthropogenic sources contribute 20 to 25% of total aerosol content of the atmosphere and with increasing human activities, this is expected to further increase with time (Andreae, 1995). The total flux of natural aerosols averaged over the globe is about three to four times larger than the flux of aerosols generated by human activities. The global production of natural dust may also be increasing substantially due to desertification by human activity (Sheehy, 1992). However, on a regional scale, the flux of anthropogenic aerosols can dominate over natural ones by three to four folds or vice versa (Srinivasan and Gadgil, 2002). The variety of

dominant aerosol sources with their respective contribution to the total annual global atmospheric aerosol budget is summarized in table 1.2.

Table 1.2 Estimates of annual global production of aerosols.

NATURAL SOURCES	QUANTITY (Tg/Yr)
Rock and soil debris	100-500
Forest fire	3-150
Sea salt	300
Volcanic debris	25-150
Particles by gas to particle conversion:	
Sulphate from hydrogen sulphite	10-200
Nitrate from nitrogen oxides	60-430
Hydrocarbon from plants	75-200
<i>Sub-total (natural)</i>	<i>693-2630</i>
ANTHROPOGENIC SOURCES	
Directly emitted particles	10-90
Particles by gas to particles conversion:	
Sulphate from sulphur dioxide	130-200
Nitrate from nitrogen oxides	30-35
Hydrocarbon	15-90
<i>Sub-total (anthropogenic)</i>	<i>185-415</i>
GRAND TOTAL	878-3045

Data source: Nambi and Sapra, 1998

1.4 WORLD SCENARIO

Soil dust is a major constituent of the air borne particles in the global atmosphere. Its annual global emission is estimated to account for 20–50 % (~1500 Tg) of the total global dust load, which could be even higher (Tegen and Fung, 1994; IPCC, 1995). The global distribution of the major atmospheric dust sources and the related environmental characteristics responsible for dust generation have been studied and reviewed by Prospero et al. (2002). The largest and the most persistent sources are located in the northern hemisphere, mainly in the broad “dust belt” that extends from the west coast of North Africa, over Middle East, Central and South Asia, to China.

The dominant source regions are arid and semiarid zones in these continental areas. To name a few of them are, Tunisia and North Algeria, the Eastern Libyan desert, the Sahara desert in North Africa, the Taklamakhan and Gobi desert in China, the Thar desert in India, arid belts defined by Sierra Nevada in the western United States, Lake Eyre and the Great Altesian basin in Australia and the arid belts of South America. The interesting fact about the dominant global sources is, that these regions have been intermittently flooded through the Quaternary and action of water for dust production is evident from such arid and sub arid regions (Prospero et al., 2002). It has been well documented that all year long, large quantities of soil derived aerosols are emitted into the atmosphere from arid and semiarid continental areas and that a substantial quantity can be carried to great distances (Duce et al., 1980; Prospero, 1981; Uematsu et al., 1983; Pye, 1987; Prospero et al., 1989; Goudie and Middleton, 1992).

The long range transport of aerosol particles from continents to oceans as well as from continent to continent has been studied world wide in southeastern United States (Reheis and Kihl, 1995; Prospero, 1999; Reheis et al., 2002), in Japan (Sadayo et al., 2002; Shinji, 2002), in China (Wang et al., 1982; Chen et al., 1999; Xiaoqing et al., 2002), in Korea (Choi et al., 2001; Chun et al., 2001), in north Indian ocean (Satheesh et al., 1999; Prospero et al., 1989; Leon, 2001; Leon and Legrand, 2003), in Indian ocean and Western South Pacific ocean (Prospero, 1981; Leo et al., 2001), in central north pacific (Prospero et al., 1989; Arimoto et al., 1996; Uematsu, 1998), in north Atlantic ocean (Michaels et al., 1996; Prospero et al., 1996), in India (Pant, 1993; Yadav and Rajamani, 2003 b), in Canada (McKendry et al., 2001) and in the Pacific ocean (Andreae et al., 1986). Aerosol studies carried out over the past several decades have documented spatial and temporal variabilities of dust transport (Duce et

al., 1980; Arimoto et al., 1995; Duce, 1995; Prospero, 1996a and 1996b; Gao et al., 2001).

The physical presence of dust plumes/clouds have been studied through satellite products using various physical techniques like, Thermal Ozone Mapping Spectrometer (TOMS; Herman and Celarier, 1997; Ginoux et al., 2001; Prospero et al., 2002), Infrared Difference Dust Index (Ackerman, 1997; Husar et al., 1997; Brooks and Legrand, 2000; Legrand et al., 2001; Leon and Legrand, 2003) and Multiwave Radiometer (Subbaraya et al., 2000). But these techniques cannot be readily used to identify sources of aerosols because of difficulties associated with the large temporal and spatial variability of the albedo of land surface as they are based on the light reflectance or absorbance by aerosols present in the atmosphere. Also, it is difficult to resolve the immediate aerosol sources in natural or anthropogenic terms or to locate the ultimate source by such physical techniques (Hausar et al., 1997). Although on a global scale, dust mobilization appears to be dominated by natural sources and processes, the aerosol input due to man made activities can not be ignored. The total contribution to the global aerosol budget by anthropogenic activities tends to increase from the present contribution of between 20 and 25 % with increasing industrialization (Andreae, 1995). Moreover, the emission of particularly fine particles rich in toxic elements such as As, Pb, Cd, Hg, Zn, Cu, etc. into the atmosphere from anthropogenic sources poses a potential threat to the living organisms, and terrestrial and aquatic ecosystems (Galloway et al., 1982; Hlavay et al., 1992; Rasmussen, 1998; Singh et al., 2002). This fine fraction of aerosol can be easily subjected to long range transport or can stay in suspension in the atmosphere for longer durations even under low wind conditions and thus, degrade the environmental quality both at the proximal as well as distal sites from their sources.

The chemical composition of different species in the atmospheric aerosol is a function of sources, natural or anthropogenic or both, time and site (proximal or distal) of sampling. The dust studies on micro-meteorological scale have shown that dust generation is extremely sensitive to a wide range of factors including the composition of soil, its moisture content, the surface condition (degree of disturbance) and wind velocity (Gillette, 1981 and 1999). The physical and chemical properties of natural aerosols greatly depend on the weathering history in the source region and the subsequent modifications that occur during transit in the atmosphere (typically a period of a week or more; Prospero, 1999). While progress has been made in characterizing the importance of mineral dust in global scale processes, there has been little progress in identifying the sources of large scale dusts, the environmental processes that affect dust generation in source regions and the meteorological factors that affect the subsequent transport and deposition (Prospero et al., 2002). The study of geochemical characteristics (major and trace elements including the REEs) of aerosols make it possible to evaluate their sources even at remote sites (Rahn, 1976 a; Darzi and Winchester, 1982; Knap, 1990; Choi et al., 2001). The mineralogy of aeolian dusts in different size fractions is also a helpful tool of understanding the nature of aerosols and their sources (Leinen et al., 1994). Rahn (1976 b and 1979) have studied the crust-air fractionation of elements in aerosols and have argued that elemental concentrations in aerosols and their enrichment ratios with respect to the Earth's crust are indicative of the sources of aerosols. Naturally derived elements have enrichment ratios between 1 and 2 with respect to the crust whereas, anthropogenically emitted elements show a value between 2 and 10 or even more. Some trace elements including the REEs are being used as tracers for the sources of aerosols. Because of the consistencies in the chondrite normalised patterns and in the

inter elemental ratios among the REE during dust formation and following processes, REE can be a good indicator to the geochemical nature of the dust and its natural crustal sources (Kreutz and Sholkovitz, 2000; Reheis et al., 2002). REE are also considered as better source tracers for the anthropogenic activities, such as oil fired power plants and refineries than V and Ni (Olmez and Gordon, 1985; Wang et al., 2000). Quantitative estimation and the major source inventories of various trace elements of environmental interest on global scale has been studied and reviewed by Nriagu and Pacyna (1988) and Nriagu (1989). Recently, isotopes of many elements such as lead, cesium, strontium, beryllium and their ratios are being used as powerful tools to resolve the complex nature of aerosols and their ultimate sources ($^{206}\text{Pb}/^{207}\text{Pb}$: Sturges and Barrie, 1989; Monna et al., 1997; ^7Be , ^{131}Cs and ^{90}Sr : Igarashi et al., 2001; $^{87}\text{Sr}/^{86}\text{Sr}$: Grousset et al., 1992; Yadav and Rajamani, 2003 b). However, Rasmussen (1998) has reviewed the scientific literature of the past 25 years on trace metal chemistry in aerosols and found a lack of consensus over the relative significance of natural and anthropogenic sources of aerosols and the related environmental consequences. Therefore, geochemical perspectives are needed to address the large uncertainties and information gaps associated with attempts to understand the sources (natural and anthropogenic, as well as proximal and distal) of aerosols, the processes responsible for their generation, transportational modifications and the post depositional changes.

1.5 INDIAN CONTEXT

The north and northwestern parts of India witness frequent dust storms during summer months (April to July) before the onset of summer monsoon. During the summer months a well-defined spot of dust activity remains centered over the Thar

desert in the western parts of Rajasthan (Leon and Legrand, 2003; Ackermann and Cox, 1989). The prevailing strong SW-W winds in this region transport a large quantity of dust from the Thar desert in the upwind direction to its marginal areas within Rajasthan and to the neighboring states of Haryana, Punjab, Delhi and Uttar Pradesh. However, anthropogenic sources also make a significant contribution to the total aerosol budget in the northern India (Prospero et al., 2002). The population density in this region is one of the highest in the world. Also much of India's heavy industries and mining activities are located here. Because of the lack of pollution controls, there are very large emissions of poorly combusted fuels of all types (petrol, diesel, wood, coal and cattle dung). All such sources (natural as well as anthropogenic) result in the worst visibility conditions in the Indian subcontinent in the world (Husar et al., 1997). Unfortunately, work on aerosols in the Indian subcontinent has started only in the last two decades, particularly due to the rapid deterioration of environmental indicators.

Much of the research remained concentrated on the suspended particulate matter in the major cities where SPM level ranges between 80 to 1400 $\mu\text{g}/\text{m}^3$ (Sharma et al., 1983; Mahadevan et al., 1989; Kulshrestha et al., 1995, 1996 and 1998; NEERI, 1995, 96 and 97). These studies are restricted to the determination of a few major elements of crustal origin, heavy metals of anthropogenic origin and acid radicals in the SPM samples collected over different regions by different workers. Also, it is not possible to assess the quality of the reported data from the described methodology of sample collection and analysis. Surface erosion of soils appears to be a major source of crustal elements in many of the areas studied. Dusts from arid and semiarid tracts of India, especially from the great Indian Thar desert, have additional impact on the aerosols and on the wet precipitation chemistry in the atmosphere over northern India

(Handa et al., 1982; Khemani, 1985 and 1989; Verma, 1989 a and 1989 b; Saxena et al., 1996; Kulshrestha, 1996 and 1999). A few chemical studies on rain water and aerosols in this region point to the neutralizing effect of crustally derived cations (Ca and Mg) on the pH of rain water (Khemani, 1989; Verma, 1989 a and 1989 b; Kulshrestha et al., 1998; Pillai et al., 2001). It has been hypothesized that the prevailing SW-W summer winds in this region are responsible for the cation-rich dust transport from the Thar desert. The neutralization processes are so overwhelming that any possibility of acid rain over the northern part of India is ruled out, even in future, in spite of its rapid and heavy industrialization. However, we lack primary geochemical data on aerosols of different size ranges in the vast arid zones of India. Very limited data sets are available for the chemical composition of PM₁₀ aerosols (Sharma, 1992) and their levels in the atmosphere (Kumar et al., 2001). They need immediate attention, as they are dominantly emitted by anthropogenic activities and as potent carriers of toxic elements can impose adverse health impacts by spreading diseases in the source region and at sites far away from their sources. Recently, a genetic link between the desert-forming processes in Rajasthan and the build-up of fertile soil in the downwind direction, has been suggested by Tripathi and Rajamani (1999). However, no information on the geochemical nature of aerosols of different size fractions, their immediate and ultimate sources, causes and consequences and time duration of aeolian processes is available. Therefore, the present study was undertaken on *“Aerosol Geochemistry in Rajasthan and Delhi regions and its environmental implications”*. The present study is concentrated on mainly four different size fractions of aerosols, namely free fall, suspended particulate matter, >10 µm fraction and PM₁₀, as defined below:

Free Fall is defined as a suspension of only solid particles in a gas phase, or deposits of such particles (Pye, 1987). This includes particles greater than 20 μm in size (mostly silt size) which settle back to the surface quickly due to gravity sedimentation processes.

SPM includes the entire domain of particulate matter, which remains in suspended form in the atmosphere. This includes all the air borne solid or liquid particles except water, ranging in size from approximately 0.005 μm to 100 μm in diameter.

PM₁₀ refers to the particulate matter less than 10 μm aerodynamic diameter. They are commonly referred to as inhalable or thoracic particles as they can penetrate into the human respiratory tract. Such particles are thought to cause direct adverse impact on human health by spreading diseases.

1.6 OBJECTIVES OF THE STUDY

The present study was undertaken with the aim of **“understanding aerosol geochemistry in the dominant SW-W wind corridor passing through Rajasthan, Haryana and Delhi states of NW India and its environmental implications.”** This study on geochemistry of aerosols in NW India has been aimed at understanding the following aspects:

1. The immediate and ultimate source of present day aerosols in this region.
2. Impact of SW-W winds on aerosol transport in the downwind direction on a real time sampling basis.
3. Crust-air fractionation of various elements and the behavioral changes during dust generation, transport and deposition.

4. Aeolian earth processes taking place in this region, the ongoing desertification processes in the upwind region and the self-sustaining fertility in the downwind direction.
5. Impact of the anthropogenic activities on the aerosol chemistry in terms of heavy metals and the related environmental consequences.
6. Last but not the least, to develop a reliable database, first of its kind in India, on complete geochemical characterization (texture, mineralogy, major and trace elements including REEs and isotope chemistry) of different size fractions of aerosols for future researchers in this field.

FOLLOWING OBJECTIVES WERE SET TO ADDRESS THE ABOVE QUESTIONS

- Simultaneous sampling of aerosols in different size fractions at four different stations located along the dominant SW-W wind trajectory covering a distance of 600 KM in NW India. Deposited surface sediments were also collected and used as reference materials.
- To study the impact of SW-W winds on atmospheric aerosol loading and its seasonal variability under different wind conditions through the estimation of the relative proportions of the FF, SPM and PM₁₀ in summer and winter seasons at selected sites in NW India.
- To study the texture, mineralogy and geochemistry (Major, Trace, REE chemistry) of the FF, SPM and PM₁₀ aerosol samples and deposited sediments.
- To establish the immediate source of the aerosols through comparison of the geochemistry of the present day aerosols with the deposited sediments.

- To study the strontium $^{87}\text{Sr}/^{86}\text{Sr}$ isotopic systematics to understand and pin down the ultimate source of aerosols in this region.
- To study the long range transport (LRT) of aerosols in different size fractions in the selected domain and the related environmental impacts such as desertification and nutrient dynamics.
- To observe the seasonal (Pre-monsoon/summer and Post-monsoon/winter) and temporal variations in the chemistry of the FF, SPM and PM_{10} at these study sites.
- To study the heavy metal concentration with respect to the impact of anthropogenic activities on the chemistry of the FF, SPM and PM_{10} ; how they modify the chemistry and related health impacts.
- To obtain the secondary meteorological data, particularly wind speed and direction and to draw the wind back trajectory during the sampling period.

Study Area

2. STUDY AREA

2.1 SAMPLING LOCATIONS

The study area for the present work includes the part of the Thar desert in western Rajasthan and its northeastern and eastern marginal regions extending up to Garhmuktesar and then merging into the Gangetic alluvial plains in the further east. Sampling of the aerosols in different size fractions was planned along the dominant

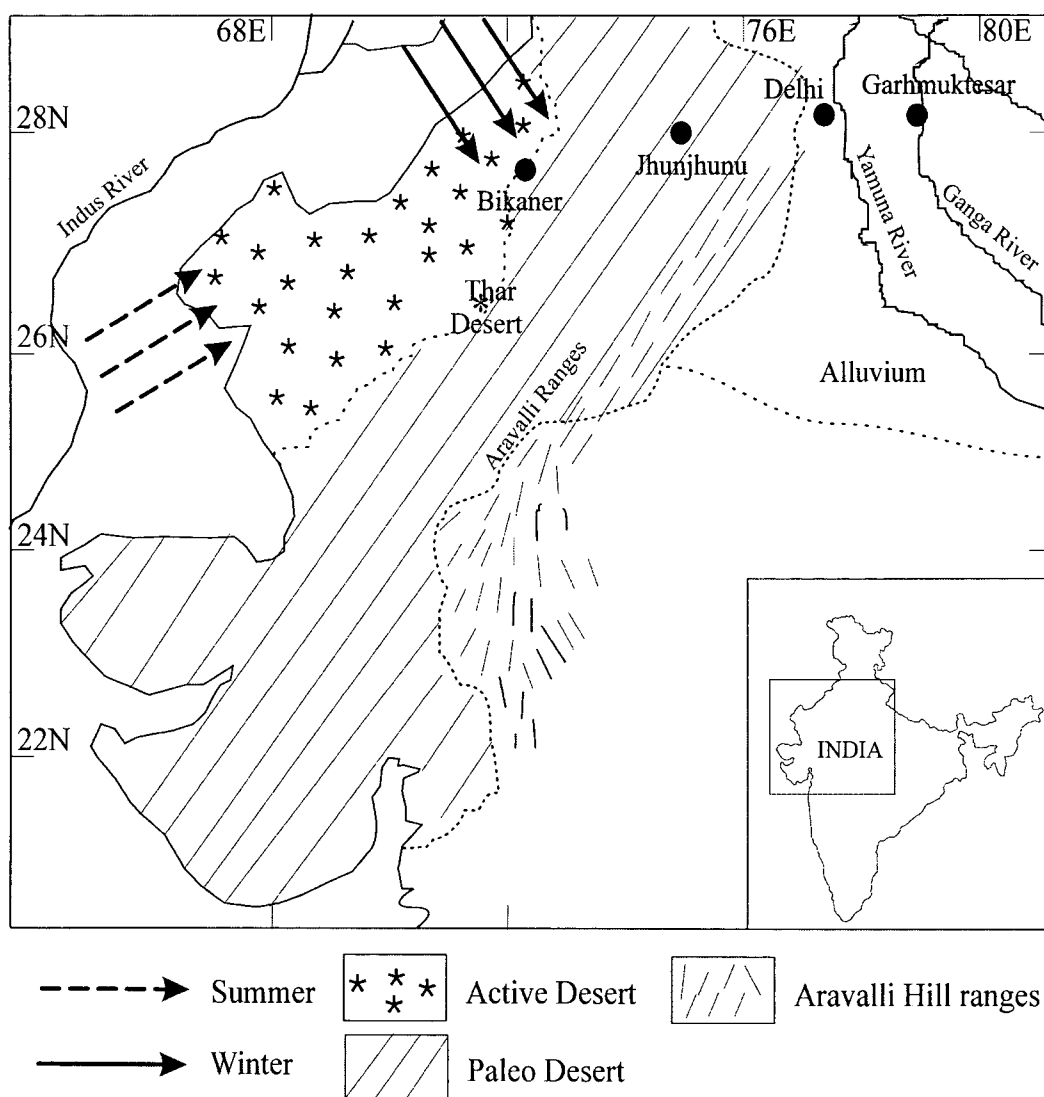


Figure 2.1 Map of the study area showing aerosol-sampling locations, dominant wind direction and prominent physiographic features.

west to east wind corridor of about 600 km starting from Bikaner in the Thar desert in

the west through Jhunjhunu and Delhi in the eastern fringe area of the Thar to Garhmuktesar, 100 km east of Delhi, located on the bank of the river Ganga. The sampling sites chosen for the aerosol study are Bikaner (28.01°N and 73.22°E) in the Thar desert, Jhunjhunu (28.06° N and 75.25° E) and Delhi (28.38° N and 77.12° E), located in the eastern boundary of the Thar desert in the downwind direction to Garhmuktesar (28.42° N and 77.8° E) in the Ganga alluvial plains in the east (Fig.2.1). Bikaner, Jhunjhunu and Delhi are separated from each other roughly by a distance of 250 Km. In Bikaner aerosol samples were collected from Udairamsar, 15 km south of Bikaner city in western Rajasthan. Aerosol sampling was done at Jawaharlal Nehru University, south of New Delhi, the National Capital Territory, at district secretariat in Jhunjhunu and at canal guest house in Garhmuktesar.

2.2 CLIMATE

The Thar, the western part of Rajasthan and the Delhi region experience dry, hot, arid to semi arid climate (Fig. 2.2). Three different seasons are recognized in our study area, a dry hot summer from March to June, a wet monsoon from July to September and a dry cold winter from October to February. The summers are very hot and uncomfortable with a mean temperature of 42°C to 43°C and the highest temperature reaching as high as 50°C. The weather tends to be oppressive during summer due to high humidity and temperature. The winters are severe with minimum temperature varying from 8.5°C to 6°C, occasionally dropping to near zero. Vertical temperature inversions have also been reported from this region, which make the atmosphere more stable and lowers down the mixing height for the pollutants. The net effect of this result in the winter maxima of pollutants, particularly heavy metals emitted by anthropogenic sources in fine particulate mode (McDonald and Duncan, 1979;



JH - 11101

Murthy, 1984). Comparable to many deserts in the world, the Indian Thar desert also receives considerable rainfall, 100-300 mm/yr. The Thar desert region extending from

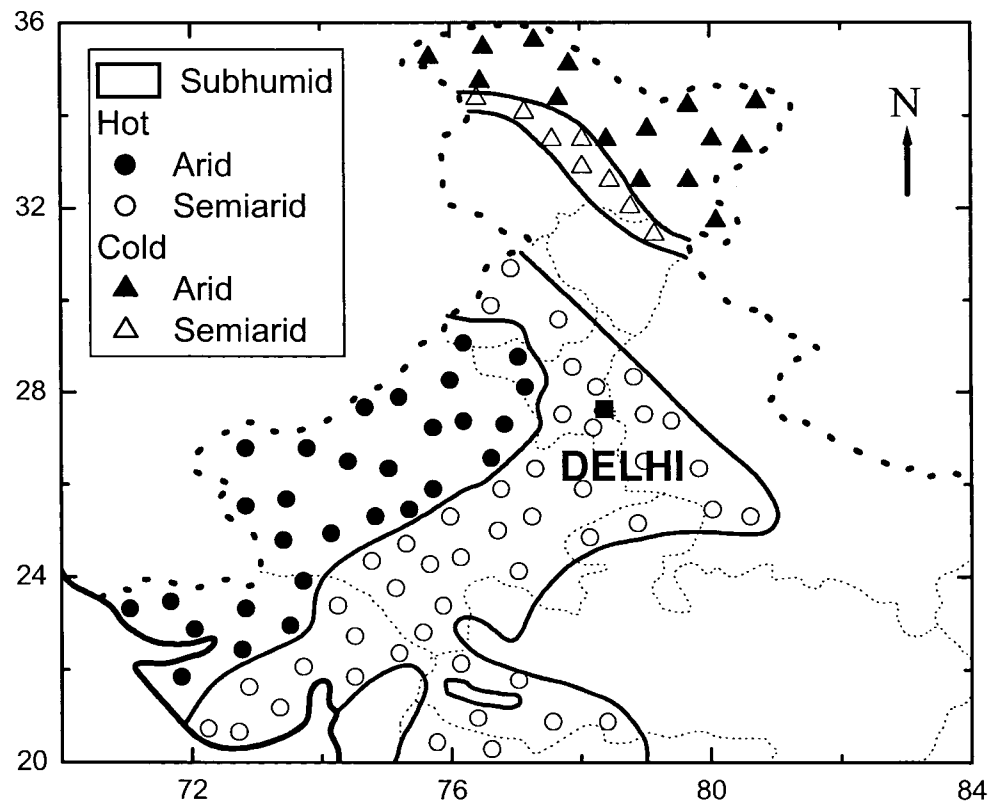


Figure 2.2 Various climatic zones in the study area.

the Sindh province of Pakistan to western Rajasthan regions of India is a meteorologically homogenous region where physiographic and anthropogenic conditions are somewhat comparable to that of the Sahara region in north Africa. The average annual rainfall at Delhi is about 710 mm, 80% of which is received during July to September, the summer monsoon period.

The climate of the western part of India is dominantly controlled by the summer heat low over Sindh-west Rajasthan region and the Siberian anticyclone at surface level in winter. The seasonal variation of atmospheric pressure over the state takes place in a systemic manner with a maximum in winter (January) and minimum in monsoon season (July). During winter, the high pressure is to the north and

decreases from west to east in summer months. Accordingly, the N-NW light winds blow through the region in winter. From January onwards, the winds turn gradually anticlockwise and are replaced by light northwesterly to westerly winds in April. With the advance of summer, pressure gradient increases and correspondingly the winds from west to southwest also get strengthened reaching their maximum strength of 25-30 km/h over the Rajasthan region during June. The pressure decreases from west/southwest to east/northeast over the state in July resulting in more and more westerly winds. October is the month of transition with weakest pressure gradient. From October onwards, change over of the pressure gradient and wind pattern commences. Monthly variations in wind pattern in terms of speed and direction during the year observed at Bikaner and Delhi are well depicted by the wind rose diagrams (Fig. 2.3 a and b). The summer winds at Delhi (Fig. 2.3 b) are somewhat north and northwesterly because of the location of the IMD data acquisition center in Delhi. The S-SW wind pattern in summer and N-NW wind pattern in winter at the different sampling locations can be better understood from the online air back trajectories drawn for the sampling duration by using National Oceanic and Atmospheric Administration (NOAA), USA satellite data (Fig. 2.4).

Depending upon the prevailing wind pattern, dust activity starts in March-April and picks up by the month of May-June in Rajasthan in NW India (Prospero et al., 2002). By July, dust activities remain confined to NW India because of the onset of the SW monsoon. The mountain ranges to the north, the Himalayas and the Hindukush, impart a strong topographical control on the dust sources and the subsequent transport of dust. The strong SW winds blowing towards NE become low speed north westerly after hitting these mountain ranges and drops the significant part of dust in the northern plains of India (Ackerman and Cox, 1989; Middleton, 1986).

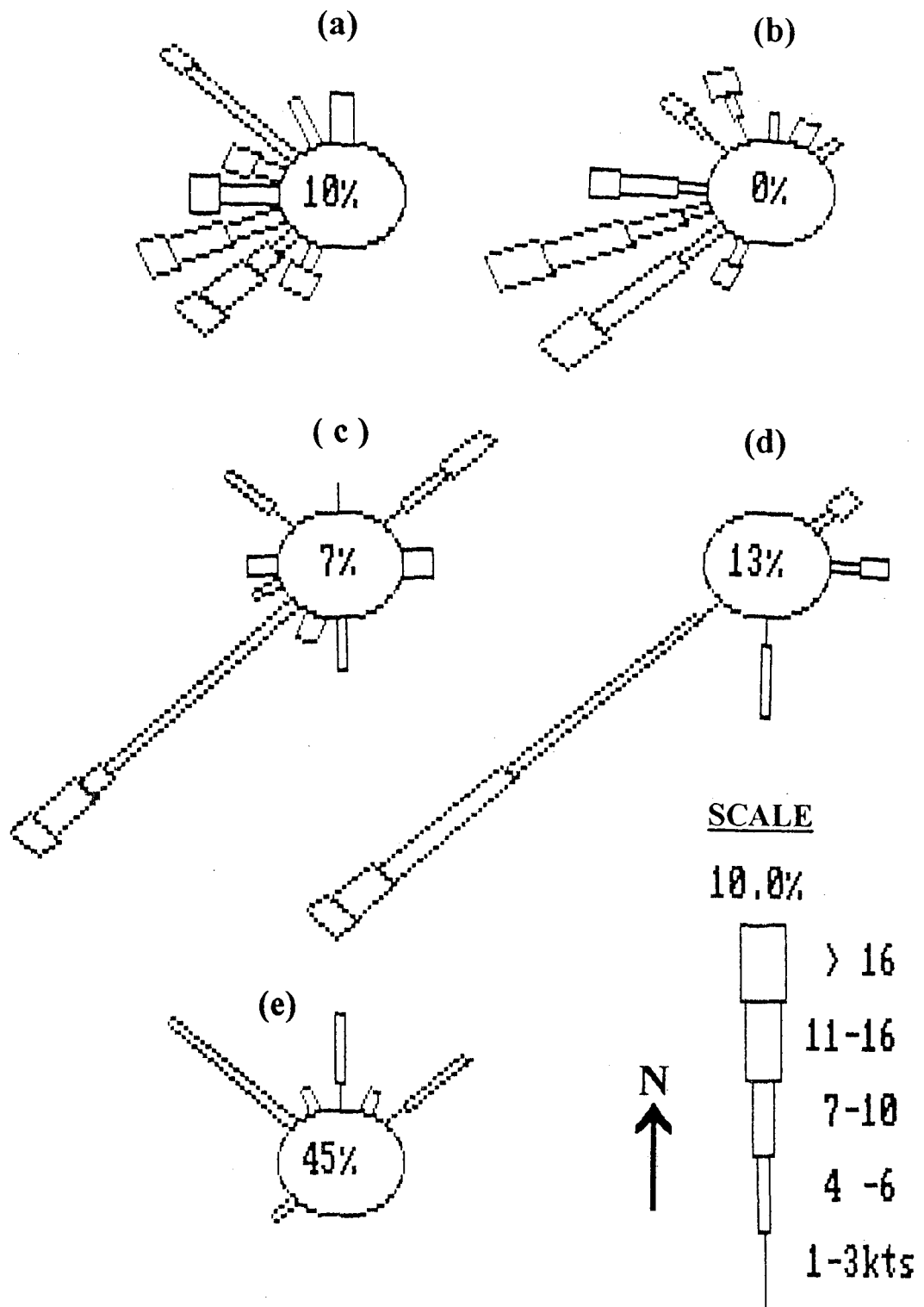


Figure 2.3 (a) Wind rose diagram for Bikaner (A - April, B - May, C - June, D- July and E - December 2000). Number in circle indicates the percent calm period. Wind speed is given in Knots per hour. Data source: IMD, Jaipur.

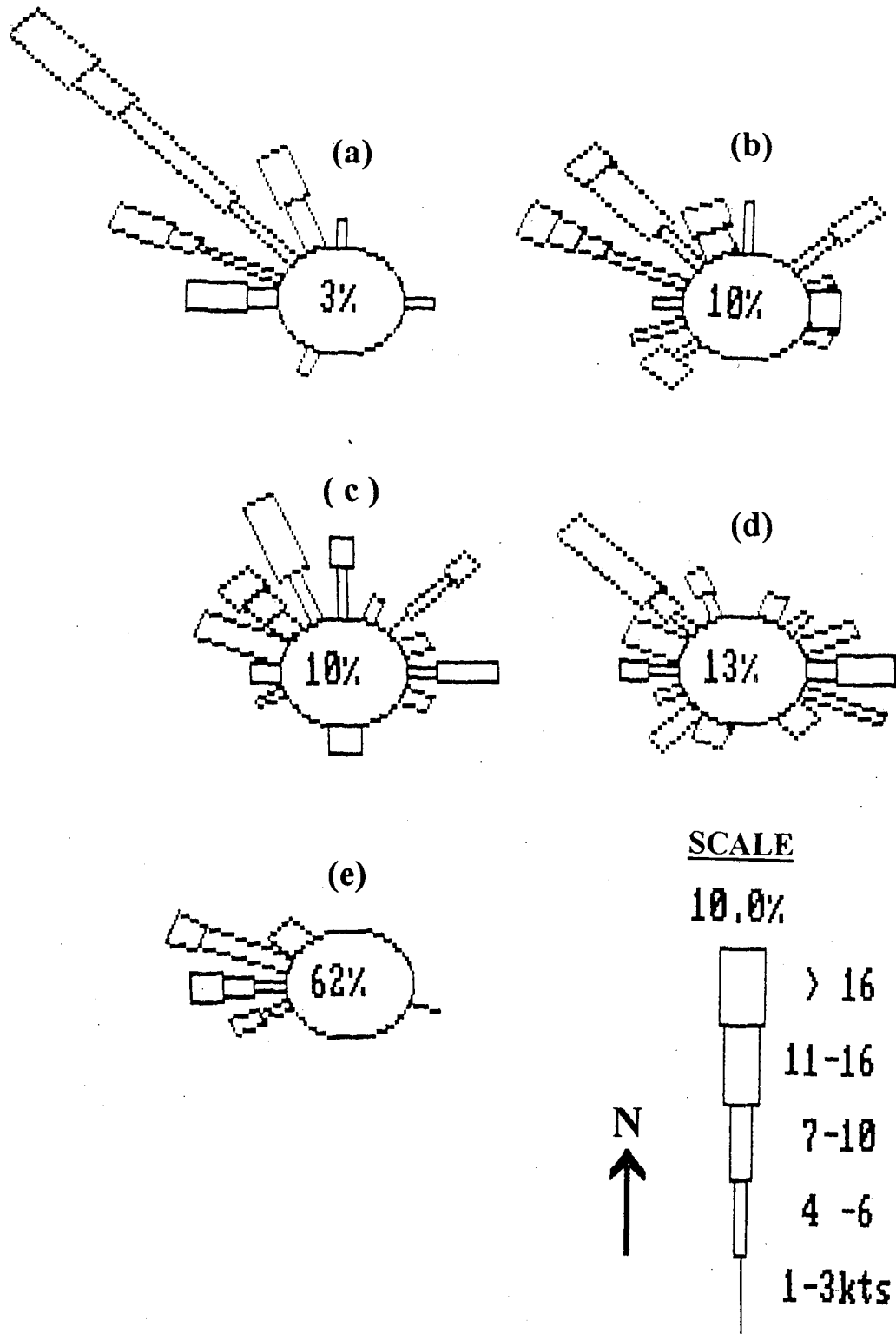


Figure 2.3 (b) Wind rose diagram for Delhi (A - April, B - May, C - June, D- July and E - December 2000). Number in circle indicates the percent calm period. Wind speed is given in Knots per hour. Data source: IMD, Jaipur.

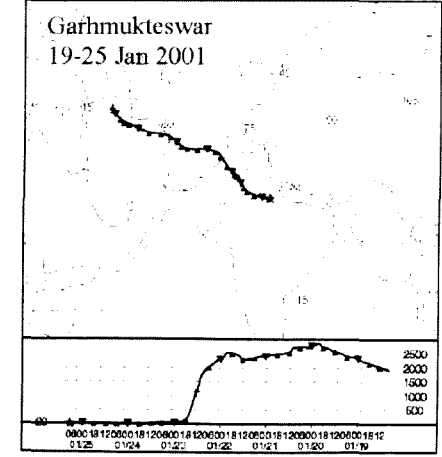
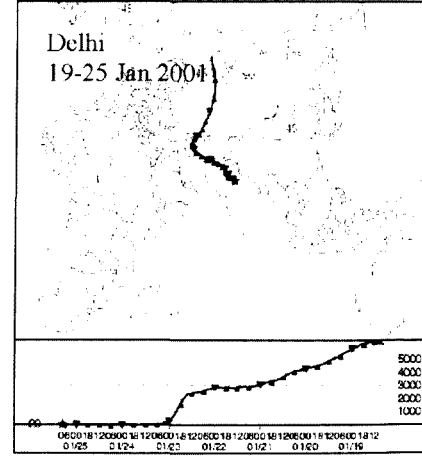
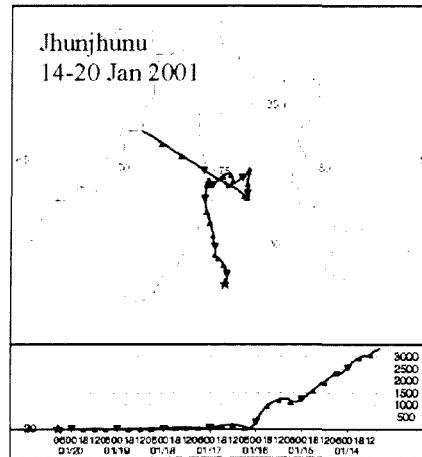
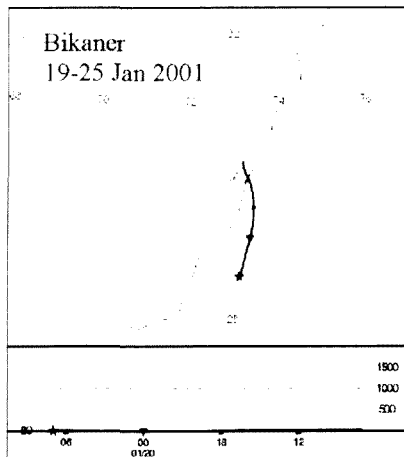
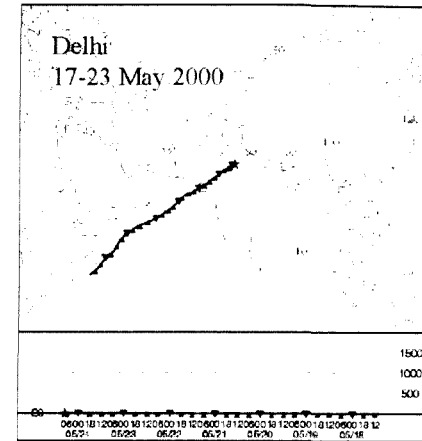
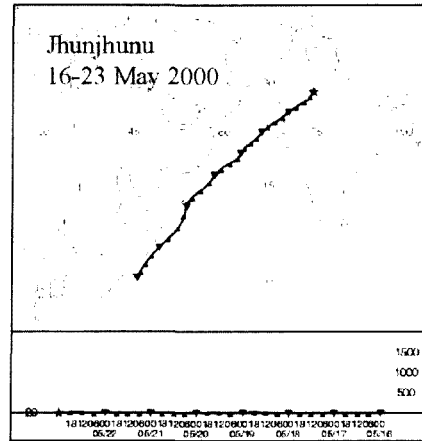
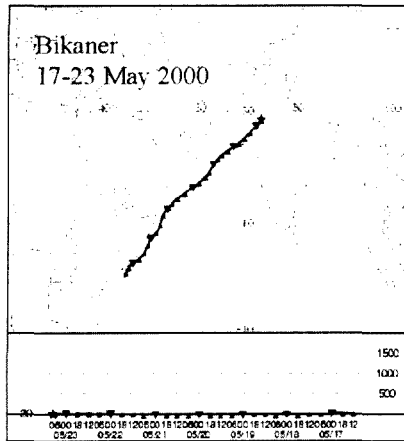


Figure 3.4 Air back trajectories calculated from FNL Meteorological data, obtained from National Oceanic Atmospheric Administration (NOAA), USA for Bikaner, Jhunjhunu, Delhi and Garhmukteswar in winter 2001.

Dust storms occur more frequently in Ganganagar (17 days), followed by Bikaner (15 days), Jodhpur (6 days) and Jaisalmer (2-3 days) in western Rajasthan than over the eastern Rajasthan during April to July. During the summer season, a dust layer from the ground up to 8-9 km height is built up gradually from March to June over western Rajasthan, which affects the horizontal and vertical visibility, even the Sun has obscured visibility during the mid-day (Husar et al., 1997). Dust storms also occur to the east of the Thar desert over the Gangetic plains, although frequency decreases (at Delhi, 8 per year; Middleton, 1986). Dust storms are often accompanied by thunderstorms (dry and wet). The annual number of thunderstorm days is about 10 over west Rajasthan and increases to about 40 over east Rajasthan (Sikka, 1997). The dust raising capacity of the surface winds is proportional to the cube of the wind speed and hence the capacity of the winds to raise sand from the desert increases sharply after a wind speed of 10 km/h. The average annual soil loss by the dust storms in the Thar desert varies between 30-60 Kg/m² per day during April to June (Sikka, 1997).

2.3 PHYSIOGRAPHY

Physiographically the northwestern part of India includes the Thar deserts, the Proterozoic Aravalli ranges and the Quaternary Indo-Gangetic alluvium. The great Indian Thar desert extends from the Sind province of Pakistan to the states of Rajasthan, parts of Haryana, Punjab and Gujarat occupying an area of about 320,000 sq. kms in NW India. The low lying Aravalli hill ranges, trending NE-SW, form the major eastern boundary of the Thar, while the flood plains of Gagger - Sutlej constitute the northern periphery. In the southwest, the Great Rann of Kachchh is its limit. Average elevation of this undulating desert terrain is about 200 m above the

mean sea level, with a regional slope towards the west and southwest. Figure-2.5 depicts, that from the extreme west of the Thar desert altitude (from mean sea level) increases eastward along 27°N combined with change in geology. The gradual thickening of aeolian and fluvial sediments can also be noticed as increasing height of hills, which act as obstacles in the way of aeolian sediment transport in the down wind direction eastwardly. Fluvial and aeolian actions are still dominant in that region. Aeolian processes dominate in the western parts of Rajasthan just as fluvial regime in the eastern marginal areas. Most common landform sequences produced by fluvial action within desert are the hilly-rocky/gravelly pediment, flat buried pediment, older and younger alluvial plain and river bed. The Aravalli hill ranges formed of metamorphic and intrusive igneous rocks are the major hilly tracts along the eastern margin. At micro level the desert hill slopes exhibit typical features of physico-chemical weathering. The most recent landforms are the narrow younger alluvial plains along the major streams in the Luni basin and along the dry valley of the river Saraswati. The spatial extent of fluvial landforms has reduced over time due to their burial by aeolian sands. Most spectacular among these landforms in west Rajasthan are the sand dunes, the interdune plains and the sandy undulating plains, which cover 50% of the area in the region. Some dunes are stabilized while others supply dust to the marginal areas of the Thar through SW-W winds (Sikka, 1997). Exposed plant roots, calcretes or bowl shaped cultivated fields and high fence line ridges provide an evidence of net aeolian erosion, although it lacks quantitative studies (Singh, 1978). Sambhar and Didwana lakes are the important saline depression in the desert and are examples of Bolson and Playa, respectively.

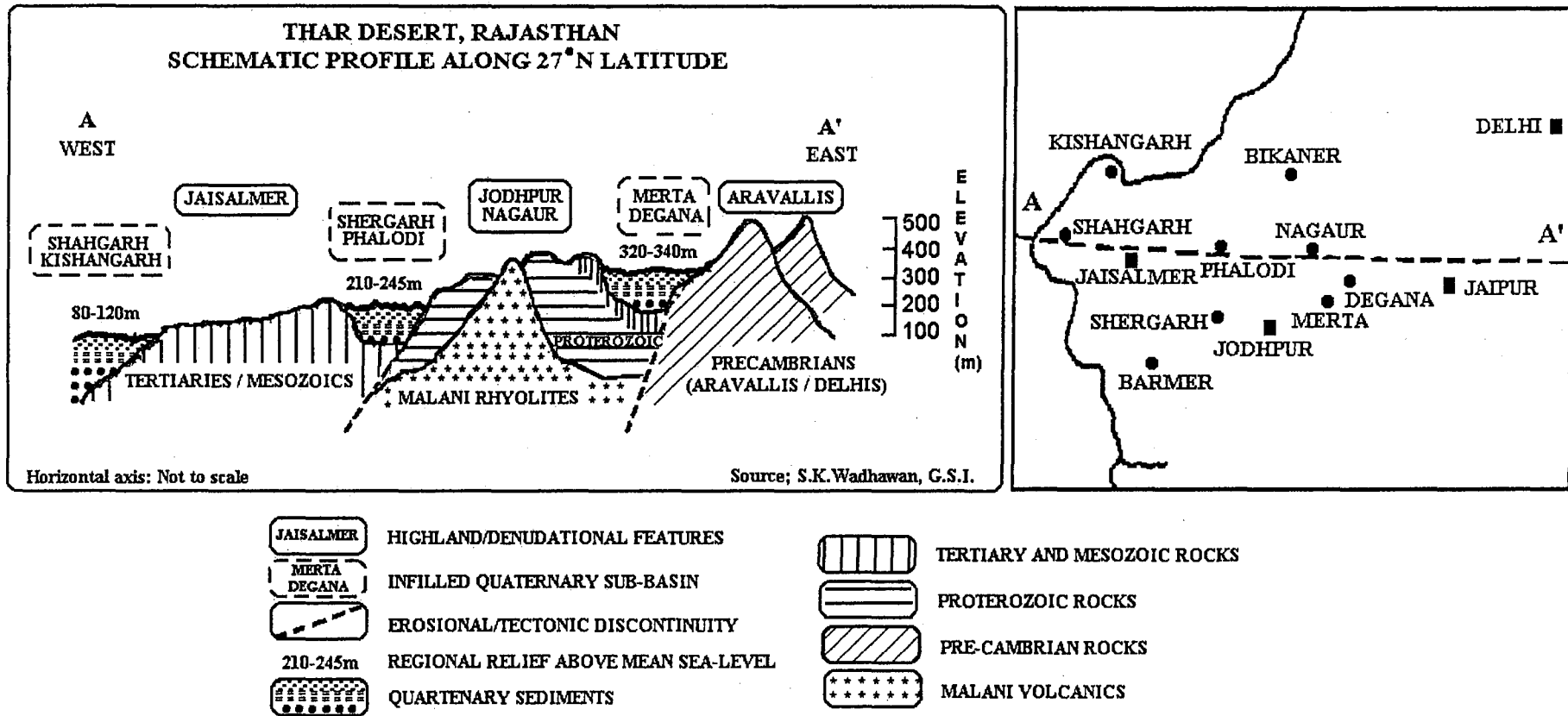


Figure 2.5 Schematic profile along 27° N showing general increase in altitude from mean sea level from west to east.

In the east of Thar desert, the entire area has a cover of unconsolidated sediments. The south and south western part of Delhi is a plateau of 250-300 meters height, rising about 100 meters above the surrounding area, known as the famous Delhi ridge. It has been reported that the bedrock in the surrounding areas of the Delhi ridge is overlain by aeolian silt, which is further overlain by alluvial material of Yamuna river (Srivastava, 1988). Although the exposed sediments surrounding the Delhi ridge are predominantly the floodplain alluvium of the Yamuna river (Thussu, 1995), those occurring within local depressions on the ridge are probably of aeolian origin. This is because the river inundation to the top of the ridges, which are on an average 100 m above the adjoining river flood plain, is less likely. Recently, an aeolian origin and the Thar desert source have been proposed for the sediments deposited on the Delhi ridge by Tripathi and Rajamani (1999). Extending from the Delhi ridge, the Ganga alluvium forms the major geomorphic feature in further east. The Ganga alluvium covers an area of 250,000 sq. km located between long. 77° E and 88° E and lat. 24° N and 30° N, have a regional slope towards the southeast. A few major rivers originating in the Himalayas and flowing southward characterize the present day drainage pattern of the Ganga plain. After entering into the flood plains these rivers swing in easterly and southeasterly directions. Essentially two types of deposits and geomorphic regional features are identified. The Older alluvium (Bhangar) makes the regional high surface, while the newer alluvium (Khadar) refers to the valley deposits and present day flood plain deposits.

2.4 REGIONAL GEOLOGY

The area of the present study includes western Rajasthan, part of Delhi and western part of Uttar Pradesh as Ganga plain (Garhmuktasar) (Fig.2.1). Supra crustal sequence

in Rajasthan records a fairly long history of earth beginning from the Archean to the Recent. The four-fold classification (Heron, 1936 and 1953) envisages the evolution of this terrain through three major orogenic cycles, now represented by the rocks of Banded Gneissic Complex (BGC), the Aravalli system and the Delhi system. In order of succession these super groups are: Bhilwara super group (3200-2500 m.y.); the early Proterozoic Aravalli super group (2500-2000 m.y.); the mid to late Proterozoic Delhi super group (2000-800 m.y.) (Table 2.1; Gupta et al., 1980). The three units are separated by regional unconformities/structural discordances (Fig. 2.6).

The Bhilwara Supergroup represents the oldest rock sequences in Rajasthan. These form the northwestern part of the Indian Peninsular craton. It consists of a variety of rock types such as granites and hornblende granitic gneisses with subordinate metasediments, amphibolites, migmatites, schists and pegmatites. It has unconformable relation with the overlying Delhi and Aravalli Supergroup wherever exposed. The Aravalli Supergroup rocks do not form the Aravalli mountains. They are thick sequences of metamorphic pelitic limestones, greywackes and orthoquartzites and some metavolcanics exposed to the east of the mountains. Metamorphic grade within the Aravalli metasediments increases from southeast to northwest. The contact between the Aravalli and Delhi Supergroup has been interpreted as a major tectonic suture or a structural discordance. Highly folded and metamorphosed rocks of the Delhi Supergroup (mid to late Proterozoic) form the main part of the Aravalli mountain, which is the principal physiographic feature striking northeast across the state. The Delhi ridge constitutes the northern most extension of the Aravalli range in the form of two ridges, i.e. Sohna ridge in Haryana, nearly 45 km from Delhi, and west of it is Harachandpur ridge which is also known as Delhi ridge. The Delhi Supergroup is sub-divided into Alwar and Ajabgarh Series. The rocks of Alwar series

are arkosic schists, quartzites and metaconglomerates whereas the Ajabgarh Series comprises biotitic schist, calc schist and calc gneisses. The Delhis are succeeded to the east of the Aravallis by rocks of the Vindhyan Supergroup, after a time interval marked by distinct erosional unconformity. The Vindhyan Supergroup comprises conglomerates, sandstones, grits, shales, porcellanites and limestones.

Table 2.1 General geological succession in and around the study area*.

Geological Era		Lithology		Important Granitic Bodies
Recent		Recent sand, silt and clay, Cal-and gyprecete, limestone, sandstone, Bentonite, Fullers Earth, variegated clays and lignite		
Mesozoic		Deccan Trap Sedimentary sequences of Jaisalmer, Barmer Basins and Palana-Ganganagar shelf		
Paleozoic		Bap Boulder Bed	Pebbles, cobbles and boulders, sand, clay, dolomites and minor shales	
Protero- zoic		Marwar Supergroup	Sandstones, limestones, evaporites and conglomerates	Jalor & Siwana Granites
		Malani Volcanic / Plutonic	Tuffs, welded tuffs, rhyolite, mafic dikes and granites	
		Vindhyan Supergroup	Conglomerates, sandstones, grits, shales and porcellanites limestones	
	Delhi Geological Cycle 2000-800 My	Delhi Supergroup	Arkosic schists, quartzites, meta-conglomerates, biotic schists, calc-schists and calc-gneisses	Erinpura, Sendra, Ambaji Granites, Kishengarh Syenite
	Aravalli Geological Cycle 2500-2000 My	Aravalli Supergroup	Phyllites, schists, limestones, greywacke, orthoquartzite and meta-volcanics	Udaipur, Darval Granites
Archea-n	Bhilwara Geological Cycle 2500 My	Bhilwara Supergroup (Banded Gneissic Complex)	Granites, hornblende granite, gneisses, subordinate meta sediments, amphibolites, migmatites, schists and pegmatites (BGC), dolomitic marbles, etc.	Berach, Untala, Gingla Granites

*after Gupta et al., 1980.

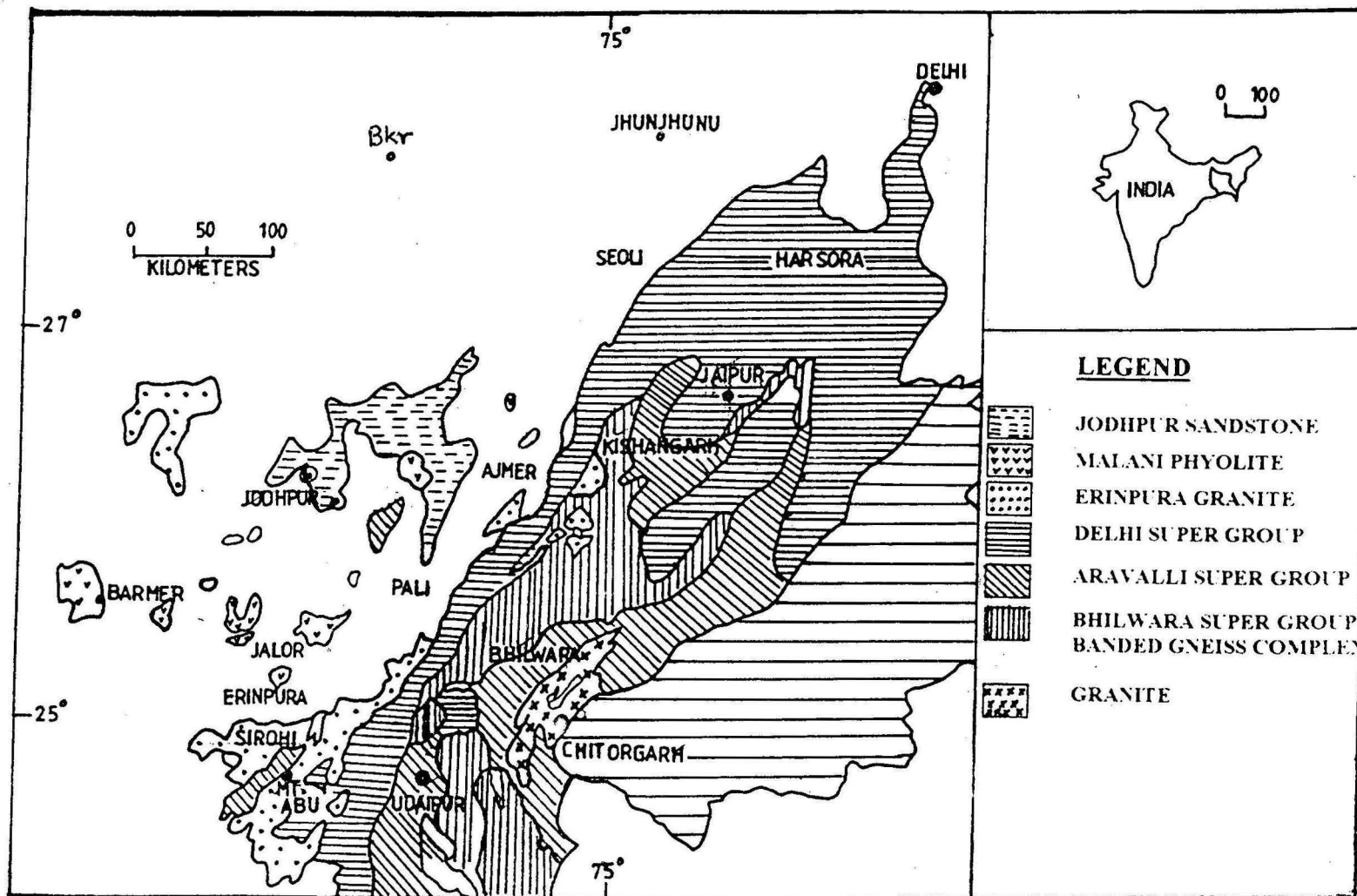


Figure 2.6 Geological map of the region around the sampling area (after Choudhary et al., 1984).

A widespread acidic volcanism at the end of the Proterozoic in western Rajasthan (Malani Igneous Suite) was marked by felsic lava outpouring and plutonic intrusions. These effusives and intrusives are cut by a number of felsic, intermediate and mafic dykes. The Malani Igneous Suite comprises an extrusive phase consisting of tuffs, welded tuffs, rhyolites, rhyolite porphyry and mafics (745 M.y.) and a dyke phase.

The late Proterozoic to early Paleozoic is represented by sandstones and limestones, which rest unconformably over the denuded and rugged terrain of the Malanis. These rock sequences form the Marwar Supergroup. The Proterozoic rocks are mostly directly overlain by Mesozoic rocks, except for isolated oval-shaped remnants of thick sedimentaries, occupying about 100 sq. km. in aerial extent, about 125 km SW of Pokharan. These sediments, comprising dolomite and minor shales, overlie the Malani basement rocks and underlie the sandstones of Jurassic period, and have been tentatively assigned a Paleozoic age (Misra et al., 1962)

The Mesozoic, the post-Permian period is marked by the Jurassic sequence overlying the Malani Igneous Suite. These comprise a sequence of coarse-grained sandstone, gritty sandstone, pebbly sandstone, gritty pebbly sandstone, conglomerate, arkose, lithic arenite, siltstones, shale, ferruginous shale and clay. The Mesozoics mentioned here are represented by the sedimentary sequences of the Jaisalmer, Barmer and Palana-Ganganagar shelf (Narayanan, 1964; Dasgupta, 1975; Pareek, 1981). Tertiary rocks are represented by the basins of Barmer (Akli Bentonite, Mandai sandstone and Kapurdi Fuller's earth, with associated lignite bands), Palana-Ganganagar (Palana shales, continental Marh Sandstones and Marine Jogira Fuller's earth) and Jaisalmer (Khuiyala-Bandah Limestone, variegated clays and ferricreted sandstone with grits).

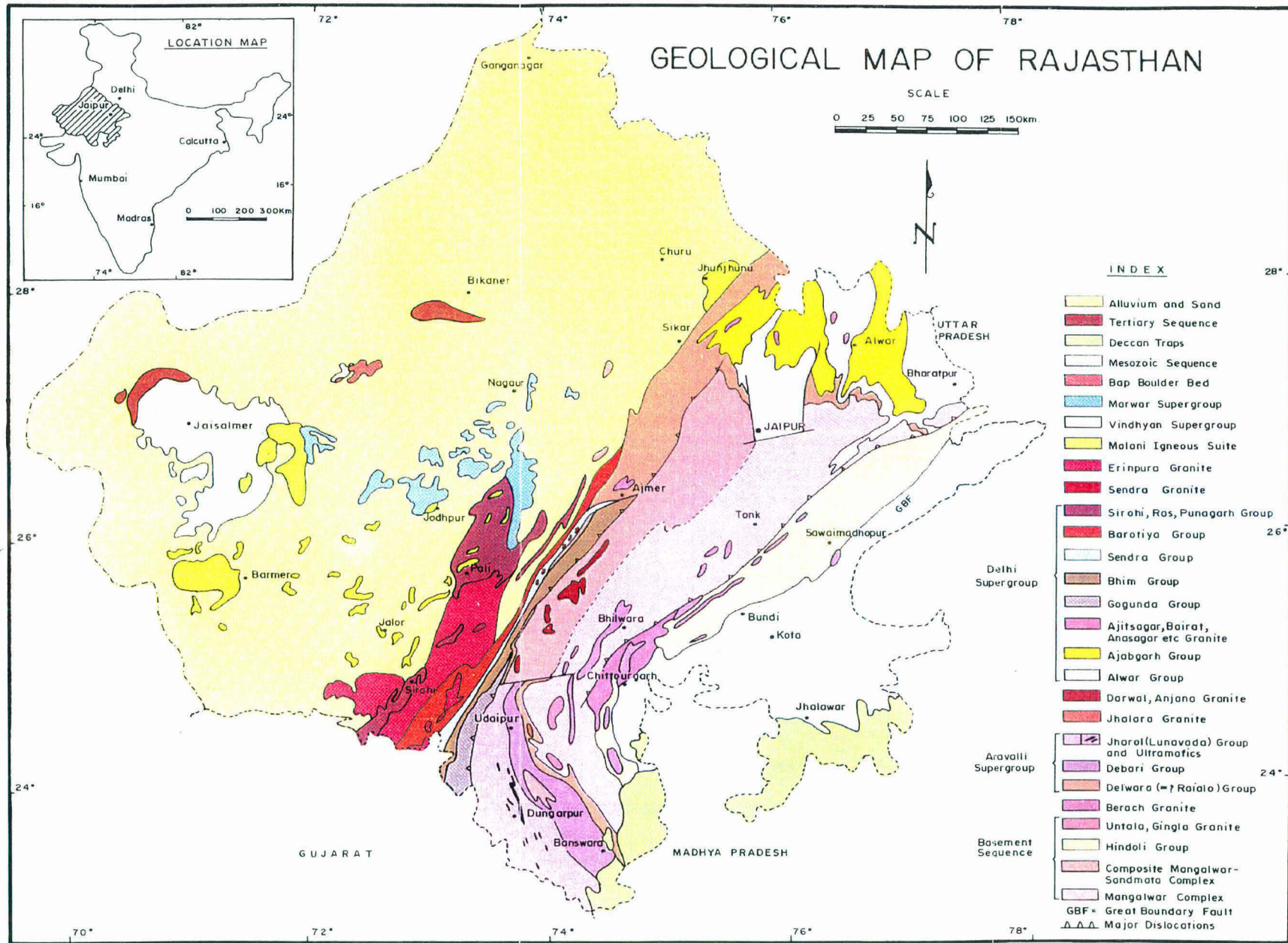


Figure 2.7 Geological map of Rajasthan (source: Singhvi and Kar, 1992).

These sandstones and shales are succeeded by Quaternary deposits. The Quaternary sequence is represented by a succession of fluvial, fluvio-lacustrine and aeolian deposits which were deposited in various basins that are formed due to the effect of various tectonic activities and changing climatic conditions. These Quaternary deposits now represent the all-famous Thar desert which is now thought to be major source of the atmospheric dust generated over western Rajasthan. Table-2.1 provides a generalized rock succession record of the study area. Figure 2.6 and 2.7 provide a generalized geological map of western Rajasthan, along with Delhi. East of the Thar desert occurs the Ganga alluvial plain which includes the Yamuna alluvium in the western side. The Quaternary alluvium in the north is mainly derived from the Himalayas. In the marginal areas of the Thar desert, the Delhi-Haryana region, aeolian sediments are found to intercalate with the alluvium (see table 2.1). In the Ganga alluvial plain sediments mainly occur as Older alluvium and Younger alluvium.

2.5 SOIL

Regional and local soil types have got importance in dust studies. Change in soil accumulation rates provides insight into the interplay of paleoclimate and dust supply and soil forming processes. Most researchers now agree that dust is a ubiquitous and important component of soil in arid, sub-humid and humid regions (Gardner, 1972; Reheis et al., 1995). Soils of arid regions show considerable variation in terms of morphological and physio-chemical properties depending upon the parent material, age and evolutionary history of landscape on which they occur, the same being true for soils of the Thar desert too. The soil of the aggregated alluvial plains has a medium to fine texture and is brown to light grayish brown in colour. The

calcareousness of the solum is variable but most soils are underlain by well developed lime nodular strata. Soils are classified as camborthids and some as calciorthids (yermosils and calcic yermosils). Previously these soils were classified as gray brown loams or as brown alluvial soils (Raychaudhury, 1963; Dhir, 1977). Central Arid Zone Research Institute, Jodhpur reported 20 soil associations ranging from coarse loamy to fine loamy depending upon their chemical composition. Soils of this region are fertile. Phosphorous, potassium and various micronutrients are generally adequate even in coarse textured soils of dunes (Sharma et al., 1985). The soil type on the Delhi ridge has been reported as sandy loam to loam and grouped into 15 soil series (Chibber, 1985). About 15% of this area is affected by salinity or alkalinity and about 64% of the total area is irrigated. Soils of the Delhi region are generally low in available nitrogen, low to medium in phosphorous, medium to high in potassium, adequate in calcium, magnesium and sulfur. Zinc deficiency has been noted in coarse textured soils.

2.6 VEGETATION

The Thar desert is sparsely vegetated and has a limited number of trees and shrubs species, dominantly xerophytic in nature. A close relationship exists between habitat and vegetation. Saxena (1977) have briefed the major vegetation of the Thar in ten categories, depending upon soil type, rainfall and climatic conditions. Hardy evergreen and spinuous xerophytic trees and shrubs, characteristic of arid climate are the most common vegetation of Delhi ridge. They are *Prosopis spicigera*, *Acacia arabica*, *Balanites roxburghi*, *Butea monosperma*, *Anogeissus pendula*, *Cassia fistula*, *Albizia lebbec* etc. *Capparis sepiaria* is common among large thorny shrubs. Other shrubs and undershrubs are *Grevia tenax* and *Adhatoda vasica*. In the alluvial plain,

the only timber tree is *Dalbergia sisoo*. Other trees like *Acacia arabica*, *Ficus bengalensis*, *Prosopis juliflora*, *Eucalyptus sp.* are found along roadsides. In the soils of recent alluvium, shrubs like *Calotropis procera* and grasses like *Erianthus avennae* and *Saccharum spontaneum* are commonly observed.

2.7 ANTHROPOGENIC SOURCES

The probable anthropogenic sources in the upwind region are the clay mining and gypsum quarrying in and around Bikaner, copper mining in Khetri, 60 km east of Jhunjhunu. Otherwise the region is very poorly industrialized compared to the eastern region. Delhi, the national capital territory is known as one of the most polluted cities of the world. Vehicular emissions, thermal power plants and other industrial units are the major polluting sources. The maximum contribution is from vehicles (72%), which are growing rapidly. Total number of vehicles running in the capital have just doubled to 3456579 in the last decade from 1812967 in 1990-91. Thermal power plants account for 13% whereas 12% comes from the industrial sector (Economic Survey of Delhi, 2002). Fly ash generation and fugitive emissions from two thermal power plants (Inderprastha and Badarpur) are main causes of air pollution. There are 28 recognized industrial areas with a total of 1,29,263 industrial units operating in them. Metal plating, electrical industry, food processing, pulp and paper, and small-scale leather industry are some common and dominant units. Most of these units do not have individual facility to monitor and reduce air pollution in the capital. Biomass burning is also important sources of aerosols in this zone as wood is the most widely used fuel in this region in the winter. The common major pollutant emitted from all these sources being dust, SPM levels were being observed to be much beyond the permissible levels.

2.8 RATIONALE FOR SAMPLING SITE SELECTION

The meteorological regime represented by high intensity SW-W winds in the north western parts of India was considered as the first and foremost criteria for the selection of the sampling sites in the present work. These winds are responsible for the occurrence of '*Aandhi*' and dust transport in this region during the summer season as explained earlier. The four sampling locations selected (Bikaner, Jhunjhunu, Delhi and Garhmuktesar) occur in a traverse nearly from west to east along the down wind direction of the dominant SW-W winds. This was another important parameter for the selection of sites in studying the impact of aerosols transported by these winds. The aerosols are transported in an eastwardly direction, thus simultaneous sampling was done at the selected locations. The systematic variations in the wind situation from high speed SW-W in summer to relatively low speed N-NW in winter aided in understanding the seasonal variations in aerosol chemistry under two different wind velocity conditions at the same sampling locations. The sampling sites Bikaner and Delhi contrast each other in terms of nature and quantitative estimates of anthropogenic sources to the aerosols. This assists in understanding the effects of anthropogenic sources on aerosol chemistry and a comparison of two different situations could be made. The sampling locations were also based on the available logistics facilities, particularly availability of electricity, protection and security of the equipments in the field. It must be pointed out here that neither the school was well equipped for an elaborate sampling campaign nor there was any fund to support the sampling. The struggle that was gone through for air sampling is beyond description here.

Methodology

3. METHODOLOGY

3.1 SAMPLE COLLECTION

Aerosol samples of four different sizes i.e. free fall (FF), suspended particulate matter (SPM), PM₁₀ (< 10 µm) and >10 µm were collected using different sampling techniques at four different sites Bikaner, Jhunjhunu, Delhi and Garhmuktesar as explained previously in the study area. Due to limitation of equipment, conveyance, electrical power and funds only a short sampling campaign was possible. However, the results are relevant because of the timely sampling at different places along the dominant SW-W wind trajectory. Despite encountering numerous difficulties in monitoring the instruments, a remarkable feature of the study was that the aerosol sampling in different size fractions was carried out simultaneously at all sampling locations. At each site aerosol sampling was done in summer and winter between 17-25th May 2000 and 19-26th Jan 2001, respectively. However, free fall samples were also collected for a longer duration (40 days) in May-June before the onset of summer monsoon, and January-February in winter. A longer duration was found essential to collect sufficient quantity of dust for geochemical analysis. At Garhmuktesar, aerosol sampling during summer could not be performed due to non-availability of air samplers. We have also collected surface sediments from these sites, which are used as reference materials.

3.1.1 Free Fall Aerosol Samples (FF)

Coarser aerosol particles, called as free fall (FF) settle down freely under gravity compared to the finer particles, which remain in suspension for longer duration in the atmosphere. Free fall aerosol samples were collected from all the stations using

plastic trays filled with two layers of glass marble balls (Fig. 3.1) kept at a height of 20 meters from the ground level. The purpose of putting a bilayer of marble balls in trays was to trap the freely falling dust particles in between the marble balls and the trays so that the dust particles cannot escape easily. The depth of 6" of the plastic trays was adequate enough to prevent the escape of once settled particles with the blowing air (Reheis and Kihl, 1995). Samples collected by this method essentially represent only dry samples, as there was no rain during sampling. After sampling, marble balls were removed from trays and dry powder deposited in trays was scraped out. The marble balls as well as the trays were washed with quartz distilled water to remove the sticking particles. The water was evaporated at 50⁰ C to get the sample in the dry powder form. Scraped dry powder and water dried powder were mixed very well and stored in plastic vials for chemical analysis.



Figure 3.1 Various sampling techniques used for aerosol sample collection. (A) Trays containing marble bi-layers for free-fall collection. (B) High-volume air sampler for SPM collection. (C) High-volume air sampler for PM₁₀ collection.

3.1.2 Suspended Particulate Matter (SPM)

The second type of aerosols, the suspended particulate matter were collected on EPM 2000 glass micro fiber filter paper (Whatman make) using High Volume Sampler Model-PEM-HVS-1 (Polltech instruments, Mumbai) (Fig.3.1b), which meets the standard norms of United States Environmental Protection Agency (USEPA) and Central Pollution Control Board (CPCB), New Delhi for SPM sampling. The design of the sampler allows total suspended particulate matter with diameter less than 100 μm (Stokes equivalent diameter) present in the atmosphere to be collected on glass

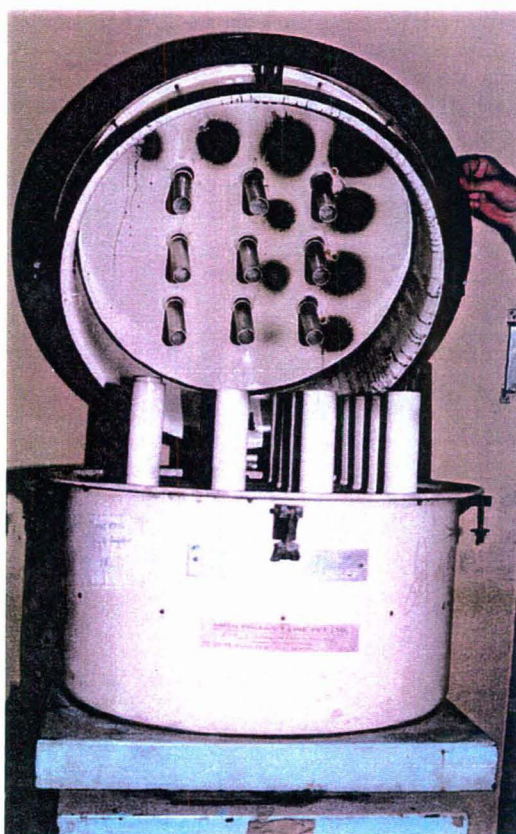


Figure 3.2 Interior view of the dome-shaped cyclone chamber of the PM_{10} high-volume air sampler.

microfiber filter paper. The Air samplers have a conical housing at the top to protect aerosol samples from contaminations like bird droppings, rain, and free fall dust. The HV samplers for collection of SPM were kept at a height of approximately 20 meters above the ground level at all stations and were operated at an average airflow rate of 1.2 lit/min.

3.1.3 Particulate Matter $<10\mu$ (PM_{10})

The third type of aerosols, the particulate matter less than $<10\mu$

(PM_{10}) were also collected on EPM 2000 glass micro fiber filter paper (Whatman

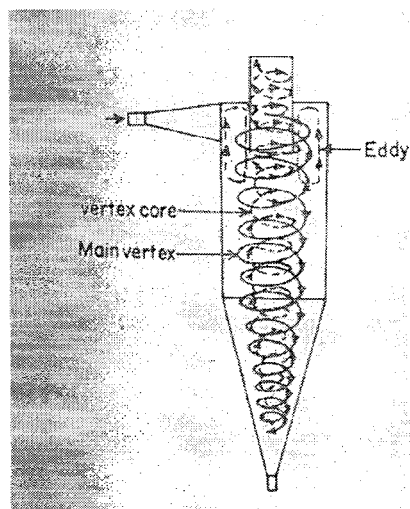


Figure 3.3 Typical PM_{10} cyclone collector depicting the principle for collection of only PM_{10} aerosols on filter paper leaving behind the >10

velocity of an inlet stream into a double vortex confined within the cyclone. In the double vortex the entering air spirals downward at the outside and spirals upward at the inside of the cyclone outlet (Fig. 3.3). The heavier particles ($>10 \mu m$), because of their inertia, tend to move towards the outside wall from which they, assisted by gravity, are led downwards and drop into a dust tight bin attached to the cyclone outlet. The lighter particles ($<10 \mu m$), however, travel upward with the inner spiral at the inside of the cyclone outlet. Thus, the design of cyclone chamber allows particles only with diameter less than $10 \mu m$ (Stokes equivalent diameter) to be collected on glass fiber filter paper. Particles, greater than $10 \mu m$ size, are collected on the cyclone plate and can be scraped off from the cyclone plate and stored for chemical characterization. The top housing also protects aerosol samples from contaminations like rain, bird droppings and free fall dust. PM_{10} sampling was also done at a height of approximately 20 meters above the ground level at all locations. The instrument has a microprocessor control and therefore, airflow rate can be kept constant at an average of 1.2 lit/min throughout the whole sampling campaign. This mode of aerosol

make) using the High Volume Sampler Model-PEM-HVF-1 (Polltech instruments, Mumbai), which meets standard norms of USEPA and CPCB, New Delhi for sampling of PM_{10} aerosols. These samplers have a dome shaped housing at the top having cyclone chamber inside (Fig.3.2). Cyclone separates particulate matter from the air or any carrier gas by transforming the

sampling simulates, to a reasonable degree, the dust collecting characteristics of the human respiratory system.

Because the filters got choked within a period of 24 hrs or less, we could collect different samples for the same size fraction from a given site and this enabled us to see the day to day variability of aerosol chemistry in a matter of a few days. EPM 2000 glass micro fiber filter papers, used in the present study have 99.9% collection efficiency for SPM and are recommended by USEPA as well as CPCB, New Delhi for aerosol collection. These glass fiber filters were desiccated at 40-50° C for 24 hrs in an oven before and after sampling to avoid weight gain or loss due to moisture. The difference in weight of filter paper before and after sampling was taken as the weight of aerosols collected. Although Teflon filters are recommended for SPM as well as PM₁₀ sampling to avoid the artifact formations during aerosol collection (Harrison, 1986), the non-availability of Teflon filters in India and their prohibitive import cost restricted our choice to glass fiber filters

3.1.4 Surface Sediment samples

Surface sediment samples were collected as channel samples ~10 cm below the surface, from the sand dunes at Bikaner and on top of small hills at Jhunjhunu.

3.2 SAMPLE PROCESSING

The two finer types of aerosols SPM and PM₁₀ collected on glass microfiber filter papers were in dry powder form and could be scraped off easily from the filter paper due to high strength and quality of the filter papers. Based on the weight differences in the blank filter paper before sampling and sample removal, we found that the recovery of SPM and PM₁₀ samples from filter papers by this scarping method was

better than 95% and filter paper fibers did not contaminate the samples. These aerosol samples were stored as such in plastic vials for further geochemical analysis. The FF dust samples collected from all sites were divided into two equal halves by coning and quartering after homogenization. The first half was differentiated in A and B fractions of $<75 \mu$ and $>75 \mu$ grain size, respectively, with the help of 75μ pore size sieve (-200 mesh size). The second half, used as bulk FF sample, and B fraction ($>75 \mu$) were crushed to -200 mesh size with the help of an agate mortar and pestle. Hundred gms of local surface sediment samples were taken from the total sample collected from Bikaner and Jhunjhunu by coning and quartering after homogenizing. These sediment samples were also ground to -200 mesh size. All the processed samples were stored in plastic vials for further use. At every step, care was taken to keep contamination at the minimum possible level.

3.3 INSTRUMENTS AND APPARATUS

Weighing balance: For weighing of the samples and chemicals, an electronic balance (METTLER) with digital display and minimum-weighing capacity of 10^{-5} gms was used.

Furnace: The Thermolyne 10500 model muffle furnace was used for fusion of samples. This furnace could attain a temperature of up to 1200°C and was provided with good thermocouple control on the attained temperature.

Inductively coupled Plasma atomic emission Spectroscopy (ICP-AES): LABTAM-8440 model, ICP-AES manufactured by Labtam Limited, Australia equipped with both simultaneous and sequential detection system was used for geochemical analysis. The instrument is equipped with a Czerny Turner type monochromator and a vertically mounted Poschem-Runge polychromator with 10 channels in vacuum for

simultaneous determination of 10 REEs. We used Argon as plasma, coolant and sample gas. All the elements except silica, sodium, potassium, rubidium and lead were quantitatively analyzed by this instrument at the characteristic wavelengths for each element (Table 3.1).

Flame Photometer: A microprocessor based Chemito 1020 flame photometer, with a sensitivity for potassium up to 1ppm, and a range of operation from zero to 100 ppm was used for sodium and potassium analysis.

Spectrophotometer: Spectronic 20 spectrophotometer, manufactured by Bausch and Lomb was used for calorimetric analysis of Silica.

Centrifuge: Refrigerated Automatic Hitachi Himac CR20B2 model was used for centrifuging samples at 9000 rpm and 4^o C during REE separation.

Teflon beakers: Teflon beakers, procured from Nalgene, USA, were used for REE separation and pre-concentration.

Others: Ultra 'F' pure graphite crucibles procured from Ultra Carbon corporation, Michigan, USA, were used for LiBO₂ fusion in muffle furnace for Zirconium and Y analysis. Quartz crucibles of 50 ml capacity, procured from Vitrosil, England were used for determination of loss on ignition (LOI). Teflon crucibles manufactured by JNU-USIC using high class teflon rods were used for preparing 'B' solution. Locally made high purity Nickel crucibles were used for sample fusion for REE and silica analysis. 'A' grade Borosil glassware was used for whole chemical work. Ashless filter papers of grade 41 and 42 (Whatman, England) were used for filtration at various steps during chemical analysis. Tarson make 500ml centrifuge bottles were used to centrifuge the solution during REE separation. Plastic vials and storage bottles used here were also of Tarson make.

3.4 CHEMICALS AND REAGENTS USED

Water: Triple distilled water was used for the preparation of standards, dilution of digested samples and rinsing, etc. The last two distillations were done in a pure quartz distillation plant.

Acids: The acids used were analytical grade HNO_3 (69%GR), HCl (35%GR), HF (48%GR), HClO_4 (70%GR) and H_2SO_4 (95-98%GR) procured from E.Merck (India) Ltd.

Resin: Cation exchange resin used for REE separation was AG50-X8, 100-200 mesh size and in hydrogen form, procured from BIO RAD laboratories, USA.

Other Reagents: Lithium Metaborate (LiBO_2) supplied by E.Merck Darmstadt, H_2O_2 (30%) and Na_2O_2 powder from Qualigens, NaOH pellets, Ammonia solution (25%AR), phenol red (20%), tartaric acid, Sodium Sulphite, Sodium bisulphite, Ammonium molybdate and Amyl alcohol from E.Merck (India) Limited, 1-Amino-2-naphthol-4-sulphonic acid of Sarabhai M. Chemicals and Sodium peroxide of Biosol laboratories were used. Only GR grade chemicals were used during whole chemical work.

3.5 TEXTURAL ANALYSIS

Particle size analysis of a few selected SPM, PM_{10} , FF aerosol samples and surface sediments was done by using Fritsch particle sizer analysette 22 Laser particle size analyzer. The homogeneously dispersed solution phases were prepared by mixing samples with water in 1:20 ratio using ultrasonic stirrer. This solution was fed into the laser particle analyzer chamber and the digitized optical data were automatically processed by the software provided by the company.

3.6 MINERALOGICAL ANALYSIS

3.6.1 X-Ray Diffractometer

Mineralogical analysis of selected SPM, PM₁₀, dry deposition samples and surface sediments collected from all sites was done by using a Philips X-ray diffractometer. Various specifications of instrument used during XRD analysis are as follows: Radiation: Cu K- α ; Filter: Ni; Acceleration voltage: 25 KV; Current: 15 mA; Goniometer speed: 1° 2 θ /min.; Scan range: 5° to 70° 2 θ . The mineral identification was done using the diffractogram after Carrol (1970) and Griffin (1971).

3.6.2 ELECTRON PROBE MICRO ANALYSIS (EPMA) OR SCANING ELECTRON MICROSCOPE ENERGY DISPERSIVE X-RAY ANALYSIS (SEM-EDX)

The EPMA provides mineralogical data with the chemical composition of the minerals identified in the samples. The minerals, which could not be observed in samples by X-ray diffractogram due to their low abundance, could be identified by this technique while doing the chemical probe of sample grains one by one. The micro probe analysis of a few FF, SPM and PM₁₀ samples was performed using a semi-automatic JEOL JXA-8600M electron probe X-ray micro analyzer with three channel wavelength dispersive spectrometers (WDS) at IIC, IIT Roorkee, Roorkee, India. The instrument was operated at an accelerating voltage of 15 kV and at a sample current of 20 nA. The beam size was 2 μ m in all cases keeping in view the small size of aerosol grains. All types of aerosol samples were fixed in Epoxy ring (15mm diameter and 15 mm thickness) and were polished using .5, .3, and .1 μ m Alumina powder successively. After polishing, samples were coated with carbon to a thickness of about

100 Å. Natural mineral standards (SPI standard, Canada) such as almandine, biotite, chlorite, feldspar and plagioclase were utilized in analysis. Wherever necessary multi mineral standards were used in analysis. ZAF corrections regarding X ray absorption, X ray fluorescence effect, atomic number effect, back scatter and ionization penetration losses were applied to the raw data and corrected using the program supplied by JEOL through DEC LSI-11/23 and 11/73 computers.

3.7 SAMPLE DISSOLUTION

We followed wet chemical method for geochemical analysis of aerosols, since it is essential to bring the dry sample into a solution form before feeding to analytical instruments. Sample dissolution was done by

- (a) Acid digestion method for “B” solution preparation
- (b) LiBO₂ fusion method for Zirconium analysis
- (c) NaOH-Na₂O₂ fusion method for Rare Earth Elements (REE) analysis

In acid digestion method, we used HF, HNO₃ and HClO₄ acids and did not add any matrix element through flux. In this method, Silicon the major interfering element was completely removed by using HF. Nitric acid was used to decompose carbonates and sulfides and to oxidize many elements of variable valency including iron into higher valence state. HClO₄ oxidizes organic matter present in samples. The “B” solution method gives low blank value, which in turn increases the sensitivity of the instrument. Keeping in view these merits, this method of sample dissolution was followed. ‘B’ solutions were used for the analysis of all major and trace elements except Si, Zr and those hosted by refractory minerals since this method does not digest the refractory minerals effectively. Alkali fusion is an effective method of

digesting refractory minerals, which include high field strength elements like Nb, Ti, Zr, Y and REE. We followed $\text{Na}_2\text{O}_2\text{-NaOH}$ fusion method for the REE analysis, which are present in very low concentration levels. LiBO_2 method was adopted for Zr and Y only as it digests the refractory minerals completely and gives good recovery of these elements for analysis.

3.7.1 Preparation of 'B' solution by acid Digestion method

'B' solution preparation procedure reported by Shapiro and Brannock (1962), modified in our laboratory, was followed for sample digestion. 0.5 gms of aerosol sample or sediment sample powder (-200 mesh size) was digested with 10 ml conc. HF, 5 ml conc. HNO_3 and 1-2ml HClO_4 in a 60 ml Teflon crucible on hot plate at a temperature range of $85\text{-}90^\circ\text{C}$ with the lid on for 4 hours to ensure complete reaction. After 4 hours the lid was removed and solution was heated to complete dryness. In the second step, 5 ml conc. HF, 10 ml conc. HNO_3 and 1-2 ml HClO_4 was added and heated at 90°C to complete dryness. Purpose of using HF was to remove silica as silicon fluoride, which is a highly volatile compound. In the third step, only 5 ml concentrated HNO_3 was added to remove traces of fluoride from solution and heated again to dryness. Then finally 20 ml of 1N HCl was added and heated to 100°C to bring the digested sample into solution. After regular swirling, the solution was transferred to a 100 ml volumetric flask. The teflon crucible was rinsed several times with 1N HCl and quartz distilled water to ensure complete recovery of sample and was poured into the volumetric flask. Then the flask was warmed on hot plate to ensure complete dissolution of crystalline material, if any. The solution in the flask was cooled and the volume was made up with QDW. The so prepared solution was 200 times diluted and used for analysis of trace elements by ICP-AES. This solution

was further diluted to 4000 times in a separate 100 ml volumetric flask by adding 5 ml of it (200x) and used for major elements analysis by ICP-AES. The same 'B' solution was used for Na₂O and K₂O analysis by flame photometer after diluting it to required dilution.

3.7.2 Carbonate leaching

Calculation of chemical index of alteration (CIA) for aerosols and sediment samples requires determination of calcium oxide present in the silicate phase only i.e. on carbonate free basis. Therefore, leaching experiment was performed with 1.3 N HCl acid in 1:10 ratio (Gale and Hoare, 1991). Leachate as well as the residue was collected and analysed for Ca in carbonate and residual silicate phases receptively.

3.7.3 LiBO₂ fusion method

For fusion by LiBO₂, sample to LiBO₂ flux ratio was maintained at 1:5. One gm of flux (LiBO₂) was taken in pre-ignited cleaned ultra 'F' pure graphite crucible and 0.2 gm of sample powder was transferred and mixed thoroughly by a steel wire. Due care was taken at this step to avoid sticking of sample on to the wall of the crucible and to ensure sample remains embedded in LiBO₂ flux only. The graphite crucible duly covered by quartz dome was kept in a muffle furnace for 10–15 minutes at a temperature of 1050 – 1100⁰C. The fused sample was poured into a flat-bottomed teflon beaker containing 40 ml 1 N HNO₃ acid (Walsh, 1980). The Teflon beaker was kept on magnetic stirrer for about 2 hours till complete dissolution of glassy fused material. After complete dissolution, it was transferred to a 50 ml volumetric flask and the volume was made 50 ml by adding QDW. This 500x-diluted solution, was used for Zirconium and Yttrium analysis by ICP AES. The LiBO₂ method has a

superior ability to dissolve refractory trace phases (Abbey et al., 1977; Johnson and Maxwell, 1981). Zr analysis by LiBO_2 was done for only a few selected FF, SPM and PM_{10} aerosol samples where adequate sample was available.

3.7.4 Na_2O_2 -NaOH fusion Method for REE analysis

One gram of NaOH (pellets) and 1.25 gm of Na_2O_2 (granular) was taken in a nickel crucible. 0.5 gm of sample (-200 mesh size) was added to the flux in nickel crucible (sample: NaOH: Na_2O_2 – 1: 2: 2.5) and the lid was put on. The sample and flux were then fused by heating the crucible on a bunsen burner for 10-15 minutes continuously swirling it. Crucible was allowed to cool and filled with QDW up to 3/4th level. After 8-10 hours, the digested sample was thoroughly scraped with the help of a teflon rod and transferred to 500 ml glass beaker. The crucible and teflon rod were washed repeatedly with 6N HCl followed by QDW to ensure the complete transfer. The solution in the beaker was heated over a hot plate (90-100°C) to evaporate until the viscous gel of silica started forming. Solution was left to cool and silica gel was filtered through Whatman-42 and 41 filter papers (two papers were used). The residue of gelatinous silica on filter paper was washed several times by 6N HCl, finally followed by QDW till no trace of acid remained in the gel (gel became completely white).

The filtrate was transferred to a 500 ml beaker and the filtration flask was washed several times with 6N HCl and QDW. The 500 ml beaker was kept on the hot plate at 80-85°C until complete dryness. This residue was picked up in solution with 30 ml 1N HCl by slight warming and transferred to tarson 500 ml centrifuge bottle by repeated washing. To this, 10-14 drops of phenol red indicator were added. Then 1:1 ammonia solution was added to it by dropping bottle till the precipitate forms and the

colour of the solution changes from yellow to red. At this stage, pH was nearly 8 and the trivalent and tetravalent cations were precipitated with divalent cations remaining in the solution. The matrix of Na was also scavenged by the precipitation with NH_4OH . The solution with precipitates in centrifuge bottle was centrifuged at 9000 rpm at 4°C for 45 minutes. The supernatant was discarded and the precipitates were picked with 6N HCl and QDW and transferred to a teflon beaker. This solution was kept on hotplate at 80°C until complete dryness.

This residue was dissolved in 30 ml of 1N HNO_3 (calibrated) by slightly warming it on the hot plate. The HNO_3 resin column was kept ready for loading the solution into it after regenerating, cleaning, agitating and finally equilibrating with 5 ml of 1N HNO_3 . The cation exchange resin used in the HNO_3 column was AG50-X8, in hydrogen form, 100–200 mesh size, procured from Bio-Rad laboratories, USA. This solution was loaded to the column through a Whatman 42 filter paper to filter off precipitated silica, if any. After passing this solution through the column, 60 ml of 1.8 N HNO_3 (calibrated) was passed and thus collected solution was discarded. Then column was loaded with 180 ml of 6N HNO_3 in three steps of 60 ml each and filtrate, which contains REE in it, was collected in teflon beakers. This solution was dried completely on a hot plate at 85°C . The dried residue was picked up with 30 ml 1N HCl and loaded to regenerated HCl resin column. Once loaded solution had passed, 80 ml of 1.8N ($< 2\text{N}$, calibrated) HCl was passed through column and the collect was discarded which contains Fe and Al cations. Then 220 ml of 6N HCl was passed through column again in three steps of 90 ml, 90 ml and 40 ml. The passed solution was collected in teflon beaker and dried completely.

The finally dried residue was picked up with 5 ml of 2N HNO_3 and used for analysis of rare earth elements by ICP-AES in polychromator, i.e. simultaneous

determination of 10 REE. During this whole procedure, utmost care had been taken to avoid any contamination or loss of sample at any step. Various acids of different normality, used for passing through the resin column were calibrated with respect to their densities.

3.8 DETERMINATION OF SILICA

For some selected SPM and PM₁₀ samples, where the quantity of sample was less, silica analysis was done by gravimetric method. Whereas for the remaining samples, silica analysis was done using A solution method described later.

3.8.1 Gravimetric Method

The silica gel separated during REE separation using ashless Whatman filter papers was ignited in a pre dried and weighed platinum crucible with lid on at 1000°C for 1 hour in muffle furnace. Then it was subjected to cooling for over night in a dessicator to avoid moisture absorption. Platinum crucible was again weighed to get silica weight. Care was taken during separation and filtration of silica from solution to avoid loss.

3.8.2 Colorimetric Method

The dissolution of the sample for the colorimetric determination of silica was done by ‘A-solution’ method after Shapiro and Brannock (1962).

3.8.2.1 Preparation of A- Solution

In a series of nickel crucibles cleaned with 1:1 HCl and washed with water, 10 ml of 15% NaOH was taken and evaporated to dryness under IR lamps. To these, 0.05 gm of –200 mesh samples were added and fused over a Bunsen burner at red hot

condition for 10 minutes. The crucibles were cooled and 2/3 part of each crucible was filled with water and kept covered overnight. The contents of the crucibles with washings were transferred to 500 ml plastic beakers containing 300 ml water and 10 ml of 12N HCl. The solutions in the beakers were quantitatively transferred to a series of 1000 ml volumetric flasks and were warmed up, if required till the solution become clear. The volume was made up to 1000 ml on cooling and 100 ml solution from each flask was further transferred to plastic bottles and preserved as 'A' solution for SiO₂ determination. The whole process was followed with no time lag in between to avoid much contact of solution with glassware, which can add extra silica to solution by acid leaching.

3.8.2.2 Reagents

Reagents used, were 7.5% ammonium molybdate solution, 8% tartaric acid solution and a reducing solution. 7.5% Ammonium molybdate solution was prepared by dissolving 7.5 gms of reagent grade (NH₄)₆ Mo₇O₂₄·H₂O in 75 ml of water in 100 ml volumetric flask with gentle heating and a subsequent addition of 10 ml of 1:1 H₂SO₄ on cooling. The volume was made up to the mark and stored in plastic bottle. Reducing solution was prepared by dissolving 40 gms of reagent grade anhydrous sodium sulphate in 10 ml water with subsequent addition of 0.15 gm of 1-amino-2-naphthol-4-sulphonic acid and stirring till complete dissolution. Solution of 9 gm of reagent grade sodium bisulphite in 80 ml water was added to the first solution and mixed thoroughly. After mixing, volume was made 100 ml and stored in plastic bottle in dark place.

3.8.2.3 Procedure

10 ml of 'A' solution of each sample, standard and blank were pipetted out and transferred to 100 ml volumetric flasks to which 1 ml of ammonium molybdate

solution (7.5%) was added and stirred. This solution was allowed to stand for 10 minutes. Afterwards 5 ml of tartaric acid solution (8%) was added, followed by addition of 1 ml reducing solution. The solution was stirred well so that blue color started developing. The volume was made up to 100 ml and the solution was allowed to stand for 30 minutes in order to develop full coloration. Then the absorbance of each solution was measured at 650 nm by a spectrophotometer using blank 'A' solution as zero reference. This was compared with the absorbance of 'A' solution of rock standards by plotting graph and SiO₂ % was calculated. To calculate it numerically, factor for each of the two standards was computed and average is taken.

$$\text{Factor} = \frac{\% \text{SiO}_2 \text{ of Standard}}{\text{Absorbance of Standard}}$$

Now % of SiO₂ of each sample was calculated using the formula:

$$\text{SiO}_2 = \text{Average factor} \times \text{absorbance of sample solution}$$

3.9 ⁸⁷Sr / ⁸⁶Sr ISOTOPE RATIO

3.9.1 Sr separation and concentration

50-100 mg of dry aerosol sample (-200 mesh size) was taken in Nalgene Teflon vials and digested with HNO₃, HF and HCl acid combination at 80⁰ C in a clean fume hood fitted with clean air system. High purity distilled acids were used in the dissolution of aerosol samples. Finally dried samples were picked up with 1 ml of 2N HCl. Sample solutions were centrifuged, in case of PM₁₀ samples only, to remove traces of undigested carbon particles. After centrifuge, sample solution was loaded in quartz column packed with Dowex 50 resin (-100 mesh size) and equilibrated with 2N HCl. Once the first one ml of HCl passed out, 16 ml of 2N HCl was added to remove Rb traces. After this whole elution, 22 ml of 2N HCl was added and the first 15 ml cut

was discarded. Final 7 ml cut containing strontium was collected in clean vials and dried on a hot plate at 100⁰ C. Resin columns were cleaned with 6N HCl in four successive steps of 30 ml each and final addition of 15 ml. After cleaning, the column was equilibrated with 1 ml of 2N HCl for further use.

3.9.2 ⁸⁷Sr / ⁸⁶Sr analysis

The dried samples in vials were loaded on Rhenium filament for ⁸⁷Sr / ⁸⁶Sr isotope ratio analysis by a multi collector solid source Thermal Ionisation Mass Spectrometer VG 354 installed at Wadia Institute of Himalayan geology, Dehradun. Strontium isotope standard SRM 987 was used to monitor peak shape, stability, fitness, resolution and reproducibility of TIMS. The average ⁸⁷Sr / ⁸⁶Sr ratio in SRM 987 was 0.710235, which is comparable with the ratio obtained in international laboratories elsewhere within experimental error.

3.10 SAMPLE ANALYSIS BY ICP-AES

The “B” solution, LiBO₂ and NaOH-Na₂O₂ digested samples of aerosols and sediments were analysed by ICP-AES and flame photometer. Quantitative analysis of major and trace elements was done by ICP-AES in monochromator using 4000 times and 200 times dilutions, respectively. Separated and pre-concentrated samples with 8-10 times dilutions were used for REE analysis. The REE analysis was done in a polychromator i.e. simultaneous determination of 10 REE by ICP-AES. The instrument was calibrated against USGS rock standards BHVO-1, STM-1, RGM-1 and our own laboratory standards 21-6, 22-22, 22-7, VM-9 were used as control during major and trace element as well as REE analysis. The precision was found to be higher than 95% and 90% for major and trace elements, respectively.

Table 3.1 Methods of chemical analysis.

Element	Wavelength (nm)	Solution	Instrument	% Error
Si	-	-	Gravimetry	1.5
Si	650	"A"	Spectrophotometer	2.5
Ti	336.121	"B"	ICP-AES	1.78
Al	396.152	"	"	0.65
Fe	259.940	"	"	1.52
Mn	257.610	"	"	1.78
Mg	285.213	"	"	0.18
Ca	317.933	"	"	1.10
Na	588.995	"	Flame Photometer	0.56
K	766.5	"	"	1.3
P	213.620	"	ICP-AES	6.02
Y	371.029	"	"	13.2
Y	371.021	LiBO ₂	"	1.23
Zr	339.198	"B"	"	10.6
Zr	339.198	LiBO ₂	"	4.8
Ni	231.604	"B"	"	6.72
Cr	267.716	"	"	2.25
Ba	455.403	"	"	1.98
Sr	407.771	"	"	3.95
Cu	324.754	"	"	1.0
Zn	213.856	"	"	4.5
Pb	220.353	"	"	6.0

Element	Wavelength (nm)	High Ref. Standard (ppm)
Ce	399.924	10
Nd	430.357	"
Sm	442.435	1
Eu	381.965	"
Gd	342.246	"
Dy	353.170	"
Er	326.478	"
Yb	328.937	"

The accuracy of the major element was better than 95%. The digestion procedure and wavelengths used for various elements and the percentage error between analysis done in our laboratory and standard values are given in table 3.1 above.

3.11 DETERMINATION OF CHEMICAL INDEX OF ALTERATION (CIA)

Nesbitt and Young (1984) suggested a parameter known as chemical index of alteration (CIA), to be calculated from the chemical analysis of the sediments. In this we use the molar proportions of oxides of Al, Ca, Na and K and this index is defined

as:

$$\text{CIA} = [\text{Al}_2\text{O}_3 / (\text{Al}_2\text{O}_3 + \text{CaO}^* + \text{Na}_2\text{O} + \text{K}_2\text{O})] * 100$$

CaO* represents the Ca in silicate phase only. Usually this CaO* is calculated by leaching the samples with cold diluted HCl (Gale and Hoare, 1991) and corrected for P₂O₅. The other elements should make 100% and can be used for calculations. But in study of aerosols, sample quantity was the biggest constraint, so we could make this CaO* calculation for only a few selected samples. To deal with such problem McLennan (1993), suggested that values of Na₂O can be taken for CaO* when CaO > Na₂O or CaO* has not been determined.

The molar proportions of Al₂O₃, CaO + Na₂O and K₂O are plotted on Triangular plots, called as A-CN-K diagram (Nesbitt and Young, 1984 and 1989). For the determination of palaeo-weathering index of alteration, a line is plotted from the K origin in A-CN-K plot through the sample to the weathering trend of the crustal rocks (Fedo et al., 1996). CIA index, between 45-55 indicates virtually no weathering whereas the value of 100 represents intense weathering with complete removal of alkali and alkaline earth elements.

Aerosol
Geochemistry

4. AEROSOL GEOCHEMISTRY

4.1 ABSTRACT

The northwestern part of India, which includes the Thar desert on its western side, is a hot and arid region with intense aeolian activity and transport of aerosols by the prevailing SW-W summer winds. Different size fractions of aerosols (free fall = FF, suspended particulate matter = SPM, $PM_{10} = <10\mu\text{m}$, and $>10\mu\text{m}$) from air were sampled simultaneously at four locations along the dominant wind trajectory for about 600 km. These aerosols and deposited surface sediments were characterized for their texture, mineralogy and geochemistry including REE and Sr isotopes. Within each size fraction, a bimodal distribution of grain size was observed. Quartz is the dominant mineral followed by K-feldspar, mica, calcite, chlorite and plagioclase. Garnet, amphibole, titanite and zircon are some of the identified heavy minerals. All samples, particularly those collected during summer, are compositionally homogeneous, including in their REE geochemistry, and are similar to average upper continental crust (UCC). However, in the winter aerosol samples, large deviations from the UCC composition are observed. This is attributed to meteorological parameters such as low wind velocity and temperature inversions in the winter season. During winter, secondary non-silicate and anthropogenic materials become important sources to Ca, Na, Mg, K, Ba and Ni budget; also reduction in the uptake and transport of heavy minerals lowered the concentration of Ti, Zr, Y, Cr, and REE in the aerosols. Geochemical coherence among aerosols, deposited surface sediments and the Thar sands, and the limited Sr isotopic data indicate that the Thar sediments and certain lithotectonic units of the Himalayan orogen are the proximal and distal crustal sources, respectively, for the aerosols in this region. Prevailing aridity and strong summer winds, and the presence of river alluvium in the Thar act together to transport

silt rich dust, the removal of which could be a possible mechanism of ongoing desertification.

4.2 INTRODUCTION

Recently, there is a great deal of interest in the study of dust and aerosols because of their importance in climate change problems (Broecker, 2000; Mikami, 2000), nutrient dynamics (Yaalon and Ganor, 1973; Drees et al., 1993; Reheis et al., 1995; Buseck and Posfai, 1999), atmospheric pollution and environmental health (Young et al., 1988; Pinnick et al., 1993; Ross et al., 1993; Wilson and Spengler, 1996; Prospero, 1999; Allen et al., 2001) and in the process of desertification (Lundholm, 1979; IPCC, 1995; Reynolds et al., 2001). Most studies have shown that our present understanding of dust and aerosols with respect to physico-chemical-biological properties, diverse sources and mechanisms of transport and deposition is very limited considering their application potential (Pye, 1987; Reheis et al., 1995; Prospero, 1999). Any improvement to our knowledge of dust and aerosols requires more data on different aspects of aerosols from diverse geographic settings (Prospero et al., 2002).

The northwestern part of India witnesses frequent dust storms (locally known as "aandhi") during summer months (April to July) before the onset of the monsoon. These dust storms transport a large quantity of sediments in this arid to semi arid region. The famous Thar desert of Rajasthan lies in the westernmost part of India and the prevailing winds are strongly westerly during the summer months. Although a suggestion has been made that the removal of silt from the Thar region by SW-W winds must have been responsible for its desertification (Tripathi and Rajamani, 1999), no information is yet available on the physico-chemical nature of the dust/aerosols that are being transported, their proximal and distal sources, causes and

consequences, and time duration of aeolian processes. A few chemical studies of rainwater and aerosols in this region point to the neutralizing effect of crustally derived cations on the pH of rainwater (Verma, 1989a and b; Khemani, 1989; Kulshrestha et al., 1998; Pillai et al., 2001). Because of the lack of primary data on the dust and aerosols in this vast arid zone of India and also because of the regional and global importance of dust and aerosols in general, we have undertaken a geochemical study of dust and aerosols in the NW part of India adjoining the Thar desert. Along a W-E wind corridor of about 600 km, we have characterised the texture, mineralogy and geochemistry (major and trace elements including REE and Sr isotopes) of three different size fractions of aerosols, (free Fall (FF) = dry deposition only excluding wet sampling; suspended particulate matter (SPM) and $<10 \mu\text{m}$ particulate matter (PM_{10}), as well as the deposited sediments. Our study shows that the distal sources for the dust and aerosols are dominantly Himalayan crustal rocks by way of the alluvium deposited in the Thar region and that wind velocity plays an important role in determining the geochemistry of the dust and aerosols, especially trace element content.

4.3 REGIONAL GEOLOGY AND METEOROLOGY

The sampling sites chosen for the aerosol study are along the west-east wind corridor of about 600 km from the Thar desert (Bikaner: 28.01°N and 73.22°E) in the west through the desert margin (Jhunjhunu: 28.06°N and 75.25°E ; Delhi: 28.38°N and 77.12°E) to the Ganga alluvial plains (Garhmuktesar: 28.42°N and 77.8°E) in the east (Fig.4.1). This corridor was selected because the strong W-SW winds dominate dust storms. Selection of the sampling points was also based on the availability of logistics such as electricity and security of the instruments during air sampling.

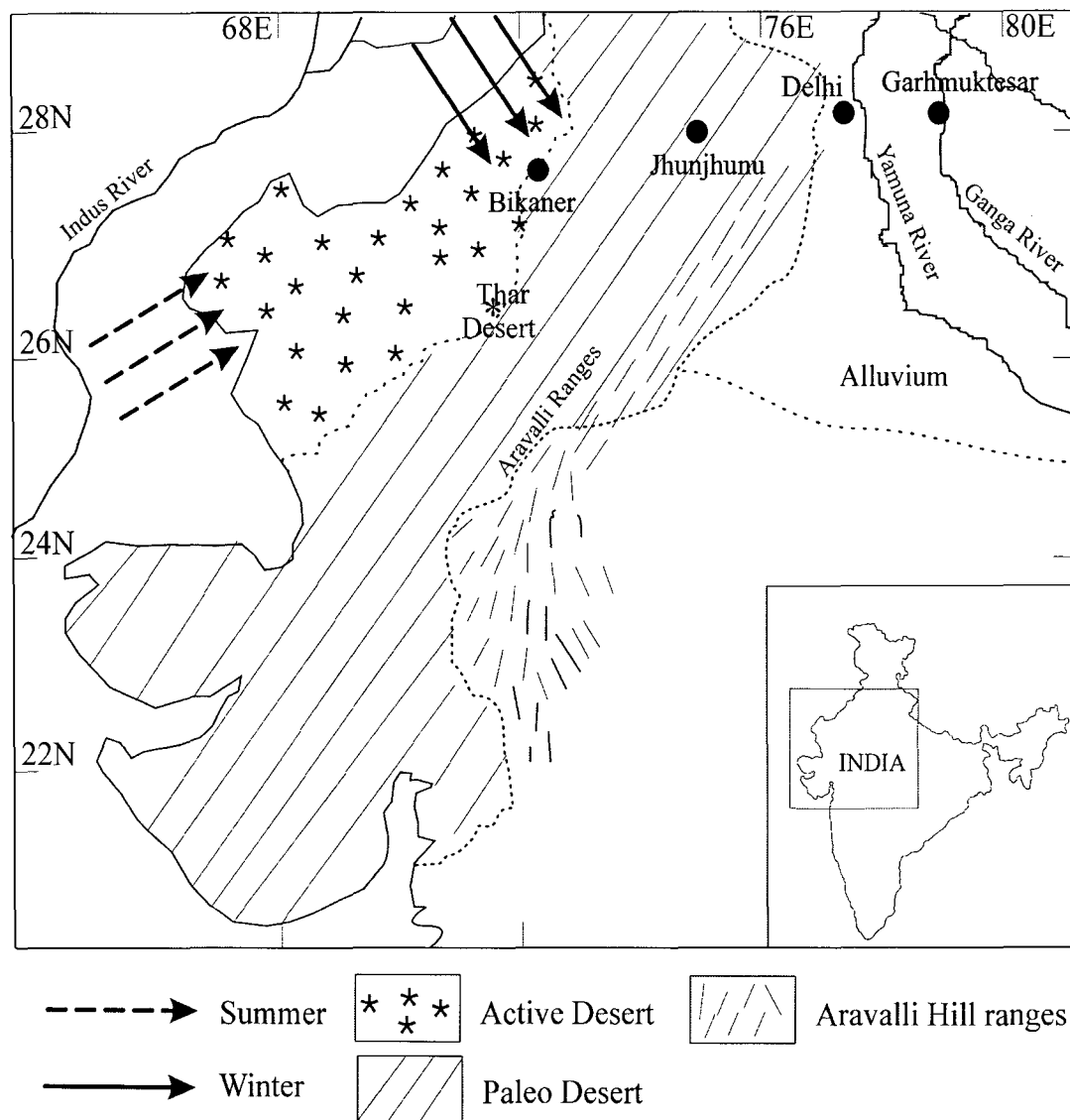


Figure 4.1 Map of the study area showing aerosol-sampling locations, dominant wind direction and prominent physiographic features.

Geologically, the study area includes the Thar desert, Aravalli hill ranges and Indogangetic alluvium represented by our specific sampling locations, Bikaner, Jhunjhunu and Delhi, and Garhmuktesar, respectively. In the Thar region a thick pile of loose sands is underlain by middle to late Proterozoic metasediments and acid volcanics and Mesozoic to Tertiary sandstones, limestones and gypsum. The Aravalli hills, which mark the eastern boundary of the Thar desert, consist of the Delhi

Supergroup with high metamorphic grade metasediments. The Gangetic alluvium to the east is Quaternary in age and was deposited by the Himalayan rivers draining from the High Himalayan Crystalline (HHC) lithotectonic units of the Himalayan orogen (Tripathi et al., 2003)

The Thar desert has an areal extent of nearly 320,000 sq. km in the NW part of India (a part of it lies in the Sind province of Pakistan) and has an undulating topography. The low lying (mean elevation of 500-600 m) Aravalli hills act as a barrier to the transport of sediments from the Thar by the prevailing winds. The region adjacent to active desert includes several saline lakes, of which Sambhar (bolsan type) and Didwana (playa type) are the important ones. To the east of Aravalli hills, the area is covered with river alluvium as well as wind reworked alluvium (Thussu, 1995). However local depressions on top of resistant Aravalli hills, such as, for example, Delhi Quartzite, have accumulated wind blown sediments with uniform texture and chemistry (Tripathi and Rajamani, 1999).

The Thar desert as well as most of Rajasthan and the Delhi region experience a hot, arid to semi arid climate. Through out the entire sampling domain, summers (April-June) are very hot with a mean temperature of 42-43° C and the highest day temperature reaching up to 50° C. The winters (October to February) are also severe with minimum temperature varying between 6-0° C. In recent years, vertical temperature inversions in winter months have been reported (Murthy, 1984). The desert region receives an annual rainfall of 100-300 mm, a feature not common to many deserts in the world. The region around Delhi, located at the eastern most point of the desert, receives an average annual rainfall of about 710 mm, 80% of which falls during July to September, the summer monsoon period. The climate of the western part of India is dominantly controlled by the summer low over the Sind and west

Rajasthan region and the Siberian anticyclone at surface level in the winter. During winter, the high pressure is to the north and therefore N-NW light winds blow through Bikaner and Jhunjhunu, and through Delhi and Garhmuktesar, respectively in this region. From January onwards, the winds turn gradually anti-clockwise and are replaced by light northwesterly to westerly winds in April. With the advance of summer, the west to east pressure gradient increases and the winds from west to southwest also strengthen reaching their maximum strength of 25-30 km/h over west Rajasthan during June. Surface winds raise a tremendous amount of dust from the loose sandy soil of the region and the dust is transported eastward over the neighboring states of India. Thus, the Thar desert and parts of western India become the center of intense dust activity before the onset of Monsoon (Leon and Legrand, 2003; Ackerman and Cox, 1989). The average soil loss in the Thar desert is estimated to vary between 30-60 Kg/m² per day during April to June (Sikka, 1997). In many areas, soil profiles are marked with caliche horizons. The desert region is sparsely vegetated and has a limited number of mostly xerophytic trees and shrub species.

The probable anthropogenic sources in the Thar region are clay mines and gypsum quarries in and around Bikaner and copper mining in Khetri, 60 km east of Jhunjhunu. Otherwise the region is very poorly industrialized compared to the eastern region. The Delhi region around the national capital is known as one of the world's most polluted urbanized areas. Vehicular emissions, thermal power plants and other industrial units are the major polluting sources. Biomass burning is another important source as wood is the most widely used fuel in this region in winter.

4.4 SAMPLING AND ANALYTICAL TECHNIQUES

Three different size fractions of aerosols (free fall = FF, SPM, PM₁₀ and >10µm) were collected using different sampling techniques. Sampling was done for all size

fractions simultaneously at Bikaner, Jhunjhunu and Delhi stations using available instruments and limited logistics. Aerosol samples were collected for a few days in both summer and winter seasons between 19-26th May, 2000 and 17-27th Jan 2001 respectively. However, free fall samples were collected for a longer duration (40 days) in May-June before the onset of summer monsoon, and January-February in winter. A longer duration was found essential to collect sufficient quantity of dust for geochemical analysis. At Garhmuktesar, aerosol sampling during summer could not be performed due to non-availability of air samplers. Dust samples falling freely due to gravity were collected in all the stations using plastic trays of 6" depth, filled with two layers of glass marbles kept at a height of 20 meters from the ground level (Reheis and Kihl, 1995). All free fall samples collected here represent dry only samples, as there was no rain during the sampling period. After sampling, dry aerosols were scraped off the trays and marbles, and trays were washed with triple distilled water to recover the sticking particles. The water was evaporated slowly at 50° C and the residue was mixed and homogenized with the scraped sample. This method of collection and processing of free fall samples have also been used by other workers and have been reported to be reliable for geochemical analysis (Reheis and Kihl, 1995). The bulk sample was divided into two halves after coning and quartering. One part was passed through the -200 mesh size sieve to separate <75µm and >75µm size fractions and the other half was used as the bulk FF sample for all the analyses. The second type of aerosols, suspended particulate matter (SPM, with a size range of 0.1-100µm) was collected using high volume air samplers, model PEM HVS-1 (Polltech instruments) fitted with EPM 2000 glass microfiber kept at a height of 20 meters from the ground level. The airflow was kept at an average rate of 1.2 l/min. A similar procedure was adopted for the finest size fraction PM₁₀ (<10µm in size) using

a microprocessor-based PM₁₀ air sampler, model PEM HVF-1 (Polltech instruments) fitted with EPM 2000 glass microfiber kept at the same height and at a constant flow rate of 1.2 l/min. In the summer season, we could also collect a fraction of >10µm size from these samplers. Because the filter papers got choked during the period of sampling at different times depending on the dust load at the given site and season, we could collect several samples (Table 4.1) of the same size fraction from a given site and this enabled us to see the variability of aerosol chemistry over several days. At each site we have also collected surface sediments, which were used as reference materials (Table 4.1). Surface sediment samples were collected as channel samples ~10 cm below the surface, from the sand dunes at Bikaner and on top of small hills Jhunjhunu. In Delhi, the accumulated sediments on quartzite ridges in several profiles were studied in detail by Tripathi and Rajamani (1999) for their texture, mineralogy and geochemistry and we use this data for the purpose of comparison. We did not collect the surface sediments from Garhmuktesar because of the dominance of local river alluvial materials on the surface. The two finer types of aerosols, SPM and PM₁₀ collected on glass microfiber filter papers were in dry powder form and therefore were easily scraped off the filters. Based on the weight differences in the blank filter paper before sampling and sample removal, we found that the recovery of SPM and PM₁₀ samples from filter papers by this scarping method was better than 95% and filter paper fibers did not contaminate the samples. SPM and PM₁₀ and <75µm fraction of FF samples, and powdered bulk FF, >75µm fraction samples and deposited bulk surface sediments (-200 mesh size) were stored in clean vials for geochemical analysis. Grain size analysis of aerosol samples as well as bulk surface sediments was done on separate aliquots using a Fritsch Particle Size Analysette-22 (Germany). Samples were dispersed in water with the help of an ultrasonic magnetic stirrer before

feeding into the instrument. X-ray diffraction and electron probe microanalysis (EPMA) of particles were done using a Philips XRD (PW1140) and JEOL JXA-8600M, respectively. A set of natural mineral standards (SPI standards Canada) such as almandine, biotite, chlorite, feldspar and plagioclase were used in the EPM analysis.

All types of samples were digested in open beakers using a combination of HF+HNO₃+HClO₄. Lithium metaborate fusion method was adopted for refractory elements like Zr and Y, as acid digestion did not result in complete dissolution of their host phases. Carbonate free Ca in aerosol samples was determined by the same acid digestion method after leaching the samples with 1.3 N HCl (Gale and Hoare, 1991). The alkali hydroxide and peroxide fusion method was followed for digestion of samples for REE determination. REE separation and pre-concentration was done using a cation exchange resin (Dowex 50, 100-200 mesh size, H form) column chemistry (for details see Singh and Rajamani, 2001). All the elements except Na and K were analyzed by using a Labtam 8440 ICP-AES. Na and K were determined by JY ultima-2 ICP-AES and flame photometer respectively. Silica was analyzed by a Bausch and Lomb Spectronic-20 spectrophotometer following the colorimeter method (Shapiro and Brannock, 1962). The precision and accuracy of analysis for major and trace elements including REE were monitored using USGS rock standards (BHVO, STM and RGM) as well as in house rock and sediment standards and found to be better than 5% and 2%, respectively. Ce and Nd have a precision of 5-10% for samples low in LREE content (<10 times chondrite). Multielemental standards prepared from pure REE metal standards (Johnson Mathey, USA) were used for instrument calibration. The efficacy of our sample dissolution procedures were checked by analyzing different aliquots of the same sample wherever possible. Blank

filter papers were also analyzed following the same procedure to apply corrections for possible contamination from filters, if any. These EPM 2000 filter papers were observed to have dominantly silica, minor amounts of Al, Ca, Mg; other trace elements particularly transition metals, were present either below the detection limit of ICP-AES or well within the error limits of our analysis. $^{87}\text{Sr}/^{86}\text{Sr}$ isotopic ratios of a few bulk aerosol samples were obtained by using a multi collector solid source Thermal Ionization Mass Spectrometer VG 354 at the Wadia Institute of Himalayan geology, Dehradun. Strontium isotope standard SRM 987 was used to monitor peak shape, stability, fitness, resolution and reproducibility of TIMS. The average $^{87}\text{Sr}/^{86}\text{Sr}$ ratio in SRM 987 was 0.710235, which is comparable to the ratio obtained in international labs elsewhere, within experimental error. $^{87}\text{Sr}/^{86}\text{Sr}$ isotopic ratios of three carbonate leached aerosol samples (1.3 N HCl) were obtained by using TIMS, model MAT-262 installed at GEOMAR, Kiel, Germany.

4.5 RESULTS AND DISCUSSION

4.5.1 Texture

Relevant textural data of aerosols and bulk surface sediments collected in this study are presented in table 4.1. We observe a bimodal distribution of particle size in all samples studied. The size maxima in FF, SPM and PM_{10} observed here are similar to those reported by other workers elsewhere in the world (Chan et al., 2000; Feng et al., 2002; Goossens et al., 2001; Sadayo et al., 2002). In some winter PM_{10} samples, sample amount was insufficient for textural analysis. The mean grain size of all the three textural types of aerosols in the summer is greater than of the winter at all stations. There is also a small decrease of mean size of FF samples along the downwind direction. Such a decrease in size is not seen in SPM and PM_{10} samples

because of small sampling domain (<1000 km) and high wind strength. Also, the physical sorting of particles during aerosol transport seems to be better for FF and SPM as compared to PM₁₀ during the summer season. FF samples during winter show a size reduction and poor sorting relative to the summer samples. These textural changes are attributed to low wind speed and relatively more calm atmosphere during the winter. This has resulted in more anthropogenic contributions to aerosol budget in the winter samples relative to the summer samples (see discussion later). Surface sediments at all stations, particularly at Bikaner, are slightly coarser than the FF samples in respective areas, a feature suggestive of winnowing processes on the surface (Pye, 1987; Nickling, 1983).

4.5.2 Mineralogy

The mineral composition of all three types of aerosols as well as sediments from all sites, studied by X-ray diffraction and electron microprobe methods, shows a dominance of quartz followed by K-feldspar, mica, calcite, chlorite and plagioclase (Table 4.1). Microprobe data also revealed the presence of biotite, amphibole, garnet, titanite and zircon. These heavy minerals are more frequently encountered in windward direction (Bikaner and Jhunjhunu) and more so in the summer samples. Representative mineral grain compositions in a few samples of aerosols are given in table 4.2. At all sites and in all seasons, coarse aerosols have a higher abundance of quartz compared to finer samples. Also the relative proportions of micaceous minerals increase and that of quartz decreases in winter samples which we attribute to lower wind strength in the winter. Details of mineralogy of aerosols with representative X-ray diffractograms, back scattered electron images of a few grains and relevant explanations are provided in appendix A-2.

Table 4.1 Textural and mineralogical data of aerosols and sediment samples, and dust loading of air during sampling period.

	Bikaner								Jhunjhunu								Delhi								Garhmuktesar																								
	Summer				winter				Summer				winter				Summer				Winter				winter																								
	FF	SPM	PM ₁₀	S. Sed.	FF	SPM	PM ₁₀		FF	SPM	PM ₁₀	S.Sed.	FF	SPM	PM ₁₀		FF	SPM	PM ₁₀	S. Sed. ^a	FF	SPM	PM ₁₀	FF	SPM	PM ₁₀																							
N	2	5	4	4	2	3	3	2	3	3	6	2	2	2	2	4	4	6	2	3	3	2	2	2																									
DLR($\mu\text{g}/\text{m}^3$)	4348-10702			444-2907			-	154-238			169-203			-	1246-2140			752-982			-	203-212			253-287			249-1031			165-410			-	108-259			244-268			-			239-254			165-188		
Avg. Size ⁵	63	18.2	4.9	92	58	17.6	-	60	12.5	4.5	88	54	-	4.3	59	14.5	4.9	55	60	13.4	3.9	60	12.4	-																									
S.D.	8.05	4.25	2.21	8.9	7	5.7	-	9.04	3.5	4.5	9.42	6	-	3.9	10.4	3.9	3	7.8	6.2	4.9	2.8	8.6	6.7	-																									
Modes ⁶	12, 69	13.4, 28.8	1.5, 5.8	41, 108	14.1, 63	12.8, 29.1	-	13.4, 71	7.6, 28	1.3, 6.2	39, 102	12, 62	-	1.5, 5.9	16, 66	9.8, 38	1.5, 7.8	18, 63	16, 71	9.8, 26.5	9, 6.8	15, 68	102, 29.3	-																									
Major Minerals [#]	Qz,Fpar, Cc, Mus, Chl	Qz,Cc,Mus Fpar, Chl	Qz,Cc, Mus, Chl	Qz, Cc, Fpar,Dol, Mus, Chl	Qz,Cc, Fspar, Mus, Chl	Qz, Cc, Mus, Fpar	-	Qz,Mus, Cc, Fpar	Qz, Cc, Mus, Chl	Qz, Cc, Mus, Chl	Qz, par, Fpar,Mus, Chl	Qz, Cc	-	Qz, Mus, Cc,Fpar	Qz, Mus, Cc,Fpar, Chl	Qz, par, Mus	-	Qz,Fpar, Cc,Mus, Chl	Qz, Mus, Fpar, Bt, Cc,Chl	Qz,Mus, Cc,Fpar	Qz,Mus, Cc	Qz,Fpar, Cc,Mus,	-	-																									

FF: Free fall; SPM: Suspended particulate matter; PM₁₀: Particulate matter <10 μm ; S.Sed: Surface sediments; ^a data from Tripathi and Rajamani (1999).

N is no of samples collected; DLR Dust Load Range in $\mu\text{g}/\text{m}^3$ during sampling period.

⁵Average size in μm ; * Bimodal size distribution values in μm observed in each sample type; - data not generated due to sample quantity constraints.

[#] Minerals identified by XRD in order of their decreasing abundance in the samples analysed. Qz=Quartz; Cc=Calcite; Mus=Muscovite; Fpar=Feldspar; Chl=Chlorite; Dol=Dolomite.

Table 4.2 Representative Electron Probe Micro-Analysis (EPMA) data on selected aerosol grains. Digits in parentheses show the number of grains analysed.

Wt % Oxides									Phase (n)
SiO ₂	Al ₂ O ₃	FeO	MgO	MnO	CaO	K ₂ O	Na ₂ O	TiO ₂	
<i>Bikaner SPM</i>									
69.98	19.27	0.07	0.01	0.01	0.16	0.06	10.43	0.01	Albite (5)
0.00	0.42	0.56	1.42	0.04	97.33	0.09	0.00	0.13	Calcite
0.00	0.15	1.59	34.75	0.12	63.27	0.02	0.06	0.04	Dolomite (2)
37.01	20.66	35.39	1.54	1.10	4.23	0.00	0.03	0.04	Garnet
51.08	34.49	1.44	2.18	0.00	0.00	9.18	0.35	1.29	Muscovite
61.87	24.00	0.24	0.02	0.00	6.00	0.29	7.55	0.03	Plagioclase (3)
32.12	8.13	0.47	0.00	0.07	27.21	0.00	0.41	31.59	Titanite
<i>Delhi Freefall</i>									
70.07	19.36	0.07	0.02	0.01	0.03	0.13	10.32	0.00	Albite (3)
41.47	36.86	8.62	8.85	0.04	1.22	0.00	2.11	0.83	Chlorite
50.76	33.14	2.89	1.79	0.01	0.08	10.11	0.83	0.38	Muscovite (3)
60.02	25.02	0.27	0.19	0.00	7.09	0.17	7.19	0.05	Plagioclase (2)
98.48	0.71	0.16	0.15	0.00	0.08	0.13	0.29	0.01	Quartz
30.18	6.78	0.43	0.04	0.06	28.47	0.01	0.00	34.02	Titanite
<i>Jhunjhunu SPM</i>									
42.90	38.10	8.86	6.90	0.05	0.26	0.00	2.37	0.56	Amphibole
0.00	0.31	0.25	0.82	0.06	98.49	0.03	0.04	0.00	Calcite
29.58	25.24	30.09	14.28	0.17	0.16	0.31	0.04	0.14	Chlorite (4)
65.41	18.76	1.24	0.29	0.00	0.37	8.63	5.19	0.10	Feldspar
51.59	37.84	2.83	0.48	0.00	0.04	6.17	0.77	0.29	Muscovite
41.97	32.53	1.38	0.56	0.11	23.14	0.16	0.10	0.06	Plagioclase
30.17	2.59	2.40	0.69	0.00	25.52	0.44	0.00	38.19	Titanite
<i>Jhunjhunu Freefall</i>									
45.78	11.32	16.12	11.81	0.25	12.44	0.75	0.80	0.73	Amphibole
39.12	18.45	16.66	11.81	0.03	0.14	9.63	0.00	4.16	Biotite
0.00	0.06	0.59	1.23	0.02	97.98	0.01	0.07	0.05	Calcite (3)
29.17	25.13	27.41	17.81	0.31	0.01	0.00	0.00	0.15	Chlorite
39.45	24.58	10.02	1.06	0.36	24.01	0.22	0.01	0.29	Garnet (2)
39.27	28.65	7.21	0.03	0.02	24.80	0.00	0.00	0.02	Plagioclase
30.26	5.83	0.47	0.01	0.07	27.89	0.00	0.14	35.33	Titanite (3)

4.5.3 Major and Trace Element Chemistry

Major and trace element data on all samples of aerosols and deposited sediments collected along the sampling transect are given in table 4.3. In addition to this, we also present data on the $> 75 \mu\text{m}$ and $< 75 \mu\text{m}$ fractions of bulk FF samples and the $> 10 \mu\text{m}$ fractions. Major element data reported here are on anhydrous and organic free basis but not on carbonate free basis. Carbonate-free CaO contents in only a few samples are given in table 4.3. As discussed before, the process of air sampling required five to six days of continuous operation of air samplers with frequent changing of filters depending on the dust load at different sites and seasons as indicated in table 4.1. Therefore in almost all cases of SPM and PM₁₀ samples, we have several sub-samples. In table 4.3, we report only the weighted mean

concentration (the sum of the weight fraction of each sub sample multiplied by its concentration) of elements for the various SPM and PM₁₀ samples. We observed that the abundance of elements, particularly certain trace elements, show day-to-day as well as seasonal variability. We illustrate this using samples collected at Delhi in table 4.4 wherein replicate analyses as well as analyses of different samples of the same size fraction are given. The complete chemical analysis of all the samples studied from which weighted averages have been calculated are provided in appendix A-2.

The variation in the chemical make up of aerosol samples, especially in the major elements, is surprisingly limited considering the large physical variables such as sample size, sampling site and time, and wind velocity/meteorological parameters in the sample population. Only certain trace elements, particularly transition metals, show relatively large but systematic variations. The observed variations in the geochemical characteristics of these aerosol samples probably reflect the nature of their sources, aeolian processes and the geochemical behavior of chemical elements during aeolian processes. The overall geochemical features of these aerosols, particularly that of the major elements, are very similar to average granodioritic upper continental crust (UCC of Taylor and McLennan, 1985). Schutz and Rahn (1982) also suggested that the bulk crustal rocks could be used as a suitable reference material for understanding the elemental composition and fractionation in aerosols. Thus, we normalized the concentration of various elements in the aerosol samples with respect to average UCC ($X_{\text{sample}}/X_{\text{UCC}}$) and plotted in figure 4.2. The elements are arranged in the X-axis of figure 4.2 with decreasing mobility during surface denudational processes (Middelburg et al., 1988; Sharma and Rajamani, 2001).

Table 4.3 Texture and chemical composition of aerosols from NW part of India. Major oxides are in % and trace elements (in ppm). REE ratios are on chondrite normalized basis.

	Bikaner								Jhunjhunu								Delhi								Garhmuktesar								
	Summer				Winter				Summer				Winter				Summer				Winter				Winter								
	FF	>75µm	<75µm	SPM	PM ₁₀	>10µm	S.Sed	FF	SPM	PM ₁₀	FF	>75µm	<75µm	SPM	PM ₁₀	>10µm	S.Sed	FF	SPM	PM ₁₀	FF	>75µm	<75µm	SPM	PM ₁₀	>10µm	S.Sed	FF	SPM	PM ₁₀	FF	SPM	PM ₁₀
n [#]	2	2	2	4	4	3	4	2	3	3	2	2	2	3	3	3	6	2	2	2	2	2	2	4	4	3	6	2	3	3	2	2	2
SiO ₂	71.9	77.0	70.0	63.1	59.6	64.4	82.6	70.4	56.1	62.4	75.4	77.2	69.4	62.6	57.4	66.8	76.1	71.1	61.2	62.9	68.5	71.6	66.9	61.5	61.0	66.8	73.5	67.9	65.2	60.0	73.3	64.5	66.8
TiO ₂	0.7	0.4	0.8	0.8	0.7	0.7	0.3	0.5	0.5	0.2	0.6	0.4	0.8	0.7	0.8	0.7	0.7	0.5	0.4	0.2	0.7	0.6	0.8	0.7	0.7	0.7	0.7	0.8	0.4	0.3	0.5	0.3	0.3
Al ₂ O ₃	11.9	10.8	12.4	14.7	15.8	13.7	8.8	10.6	11.2	9.6	11.3	11.0	14.2	15.5	17.2	13.8	12.3	11.1	11.3	8.7	13.5	12.0	13.7	15.9	15.3	13.5	11.9	11.9	10.3	9.6	9.4	8.6	10.4
FeO	3.8	2.6	4.0	4.7	5.3	5.1	1.9	2.7	3.5	1.9	3.1	2.4	4.1	5.3	6.2	4.4	3.3	2.9	3.8	2.5	4.8	4.4	5.3	5.6	6.0	4.8	4.3	4.6	3.0	2.5	2.6	2.3	2.3
MgO	2.2	1.5	2.3	3.0	3.5	3.1	0.8	1.7	2.9	3.8	1.5	1.1	2.0	3.4	3.9	2.6	1.3	1.6	2.8	2.7	2.6	2.4	2.8	3.3	3.3	2.6	2	2.2	2.4	2.8	2.0	2.6	3.6
MnO	0.1	0.1	0.1	0.1	0.1	0.1	0.04	0.1	0.1	0.05	0.1	0.1	0.1	0.1	0.1	0.1	0.1	0.1	0.1	0.04	0.1	0.1	0.1	0.1	0.1	0.1	0.07	0.1	0.1	0.04	0.1	0.04	0.04
CaO _T	4.7	3.0	5.4	8.5	9.5	8.5	1.8	5.7	12.3	13.4	3.3	3.1	3.8	7.0	8.4	5.8	2.2	4.1	8.4	7.0	4.4	3.5	4.8	6.9	6.9	6.7	3.7	4.7	6.1	6.7	5.2	5.6	7.4
Na ₂ O	2.0	1.8	2.3	2.0	2.4	1.5	1.6	5.8	9.1	3.5	2.0	2.0	2.5	2.1	2.0	1.8	1.8	6.0	7.8	10.3	2.1	2.1	2.5	2.9	3.7	1.4	1.5	4.5	9.3	13.6	1.4	11.7	3.3
K ₂ O	2.6	2.6	2.6	2.9	3.0	2.8	2.1	2.4	4.2	5.0	2.4	2.6	2.8	3.1	3.5	3.8	2.0	2.5	4.1	5.3	3.0	3.1	3.0	2.9	2.8	3.2	2.2	2.9	3.2	4.3	4.7	4.2	5.5
P ₂ O ₅	0.2	0.1	0.2	0.2	0.2	0.2	0.1	0.2	0.1	0.2	0.2	0.1	0.2	0.3	0.4	0.2	0.2	0.2	0.2	0.2	0.4	0.2	0.2	0.3	0.3	0.2	0.15	0.3	0.1	0.2	0.8	0.2	0.3
CaO*	1.71	1.77	1.47	1.1	.84	-	-	1.54	-	-	1.91	1.69	1.80	1.01	.95	-	.87	1.43	-	-	0.95	1.04	1.07	1.2	.83	-	1	0.95	-	-	1.4	-	-
CIA	56	55	57	60	59	63	54	42	25	36	55	54	58	60	62	58	60	42	27	19	61	58	60	51	60	63	62	49	23	17	51	17	38
Ba	372	397	350	422	455	409	356	342	610	1687	393	403	438	429	502	535	361	365	929	810	500	633	515	421	530	619	376	533	1087	771	323	803	2367
Sr	185	188	189	198	180	197	177	265	257	258	202	178	202	200	193	213	167	256	208	112	300	320	290	195	155	227	200	255	143	56	119	50	77
Zr	340	145	396	161	131	224	125	-	84	70	301	154	336	175	95	-	441	-	62	35	240	152	259	188	79	-	337	-	89	38	-	-	-
Y	34	19	38	27	29	37	13	-	16	22	30	20	32	32	22	-	28.4	-	13	9	34.6	19.1	35.3	28	23	-	33	-	16	11	-	-	-
Ni	43	28	46	92	82	68	28	61	458	84	32	23	40	89	86	65	60	46	186	66	68	78	65	87	111	66	71	59.6	138	97	53	190	78
Cr	68	49	82	105	115	92	34	77	82	62	72	38	77	124	114	96	81	71	79	52	101	138	88	110	117	110	129	124	95	77	83	74	73
Ce	79.9	45.7	101.0	70.5	64.5	70.4	56.2	26.7	46.2	-	66.7	43.2	97.0	64.3	60.6	64.7	127.9	23.7	44.5	25.2	69.3	41.2	72.9	66.1	60.5	67.2	78.9	66.2	31.3	33.8	52.9	37.1	24.5
Nd	35.0	18.6	42.5	30.3	27.6	29.6	22.2	11.5	18.7	-	32.0	18.4	42.9	27.7	25.4	29.9	56.3	9.8	18.9	9.4	30.4	19.3	32.2	27.7	25.6	27.7	34.8	28.4	12.3	13.6	22.5	14.5	8.7
Sm	6.7	3.3	8.2	6.3	5.8	6.0	4.0	2.2	4.0	-	6.0	3.5	8.1	5.7	5.3	5.6	10.1	2.1	3.7	2.1	5.9	3.6	6.2	5.7	5.2	5.6	6.5	5.5	2.5	2.7	4.3	3.0	1.9
Eu	1.2	0.7	1.5	1.2	1.3	1.2	1.0	0.5	0.8	-	1.1	0.8	1.4	1.2	1.2	1.2	1.8	0.4	0.8	0.4	1.1	0.7	1.2	1.2	1.2	1.2	1.1	1.0	0.5	0.6	0.7	0.6	0.4
Gd	5.8	2.8	7.0	5.8	6.1	5.7	3.8	2.5	4.1	-	5.1	3.1	7.0	5.9	5.9	5.4	8.8	2.5	3.8	2.5	5.4	3.2	5.5	5.3	5.3	6.1	5.2	5.4	2.6	3.0	4.3	3.2	2.2
Dy	4.9	2.4	5.6	4.7	4.4	4.4	3.1	1.8	3.0	-	4.3	2.7	5.8	4.4	4.0	4.4	7.5	1.8	2.8	1.6	4.6	3.0	4.9	4.5	3.8	4.3	4.6	4.4	2.0	2.2	3.2	2.3	1.5
Er	3.0	1.4	3.9	3.4	3.3	2.6	2.2	1.4	2.8	-	2.8	1.6	3.5	3.4	3.2	2.8	5.0	1.4	2.2	1.6	2.8	1.6	2.9	3.3	3.0	2.7	2.9	1.9	2.1	2.2	2.2	1.8	
Yb	2.6	1.2	3.0	2.1	1.9	2.3	1.8	0.9	1.5	-	2.3	1.4	3.0	2.2	2.0	2.3	4.0	0.9	1.0	0.7	2.3	1.4	2.6	2.1	1.8	2.0	2.4	2.3	0.9	1.0	1.6	1.2	0.8
Ce/Yb	7.7	9.4	8.5	8.4	8.5	7.9	8.0	7.2	7.7	-	7.6	7.8	8.3	7.3	7.8	7.2	8.2	6.6	11.4	9.4	7.8	7.6	7.2	8.0	8.5	8.5	8.3	7.5	9.1	8.6	8.5	7.9	7.9
Ce/Sm	2.8	3.3	2.9	2.7	2.6	2.8	3.3	2.8	2.7	-	2.6	2.9	2.8	2.7	2.7	3.0	2.7	2.8	2.9	2.8	2.7	2.8	2.8	2.8	2.8	2.8	2.9	2.8	3.0	3.0	2.9	2.9	3.1
Gd/Yb	1.8	1.8	1.8	2.2	2.5	2.0	1.7	2.1	2.2	-	1.8	1.7	1.9	2.1	2.4	1.9	1.8	2.2	3.1	2.9	1.9	1.9	1.7	2.0	2.4	2.4	1.8	1.9	2.3	2.4	2.1	2.2	2.2
Eu/Eu*	0.6	0.7	0.6	0.6	0.7	0.7	0.8	0.6	0.6	-	0.6	0.7	0.6	0.7	0.7	0.6	0.6	0.6	0.7	0.6	0.6	0.7	0.6	0.7	0.6	0.6	0.6	0.6	0.7	0.6	0.5	0.6	0.6

FF = Freefall, SPM = Suspended particular matter, PM₁₀ = Particulate matter less than 10 µm; S. Sed. = Surface Sediments, CIA = Chemical index of alteration.

[#]Number of the samples analyzed; CaO_T = Total CaO, CaO* = CaO in silicate fraction only; Eu* = (Sm_N × Gd_N)^{1/2}; - data not generated due to quantity constraints.

Table 4.4 Inter and intra sample variability in chemical composition of Delhi aerosols. Major oxides are in % and trace elements (in ppm)

	Summer FF			Summer SPM					Summer PM ₁₀			Winter SPM			Winter PM ₁₀	
	FF-1	FF-1*	FF-2	S-1	S-2	S-2*	S-3	S-4	P-1	P-2	P-3	S-1	S-1*	S-2	P-1	P-2
SiO ₂	69.84	70.20	68.48	63.43	57.92	60.04	64.33	63.22	56.65	63.89	66.67	65.55	66.50	64.33	59.88	60.04
TiO ₂	0.72	0.68	0.72	0.68	0.80	0.75	0.72	0.65	0.74	0.58	0.56	0.48	0.52	0.20	0.36	0.26
Al ₂ O ₃	13.62	13.30	13.49	14.98	17.38	16.90	14.71	15.22	17.69	14.18	11.76	11.34	11.00	7.60	10.57	8.50
FeO	4.23	4.50	4.81	5.25	6.09	5.80	4.97	5.39	7.59	4.64	4.14	3.54	3.60	1.52	2.84	2.10
MgO	2.46	2.50	2.61	3.08	3.65	3.60	2.98	3.15	3.68	3.03	2.73	2.32	2.40	2.56	2.87	2.62
MnO	0.08	0.08	0.09	0.11	0.12	0.10	0.10	0.12	0.13	0.09	0.08	0.06	0.07	0.02	0.05	0.03
CaO _T	3.71	3.80	4.44	6.21	7.71	7.52	6.38	6.41	7.86	5.85	6.12	6.18	6.23	5.76	7.19	6.21
Na ₂ O	2.21	2.60	2.13	2.96	3.06	3.20	2.70	2.84	2.31	4.45	5.63	7.22	7.45	14.66	11.62	15.85
K ₂ O	2.96	2.90	3.04	3.05	2.95	2.89	2.85	2.74	3.00	2.92	2.05	3.16	3.26	3.20	4.42	4.21
P ₂ O ₅	0.18	0.20	0.19	0.25	0.31	0.28	0.26	0.25	0.34	0.36	0.26	0.14	0.19	0.16	0.20	0.19
Ba	530	542	500	416	459	465	369	406	418	591	695	876	880	1625	550	1026
Sr	290	310	300	135	227	230	180	198	141	133	214	172	179	70	50	64
Ni	70.7	65.8	67.7	67	76	80	156	70	144	83	74	126	120	169	96	98
Cr	95.8	97	101	106	112	110	115	105	130	111	96	93	90	100	91	60
Zr	238	249	240	-	188	192	-	-	82	79	-	124	132	-	71	-
Y	32	39	35	-	27.6	30	-	-	25	23.2	-	22	28	-	20	-
Ce	80.4	79.2	69.3	61.2	68.4	69.1	61.2	68.4	60.5	58.9	59	31.3	32.0	47.8	33.8	34.1
Nd	32.6	33.4	30.4	26.5	28.2	28.5	26.5	28.2	25.6	24.9	25.8	12.3	12.5	19.1	13.6	13.5
Sm	6.4	6.8	5.9	5.2	5.8	5.9	5.2	5.8	5.2	4.8	5.1	2.5	2.4	3.8	2.7	2.7
Eu	1.2	1.2	1.1	1.1	1.2	1.1	1.1	1.2	1.2	1.3	1.0	0.5	0.5	0.7	0.6	0.8
Gd	5.7	5.9	5.4	5.0	5.4	5.4	5.0	5.4	5.3	5.4	5.4	2.6	2.8	3.7	3.0	3.0
Dy	4.7	4.8	4.6	4.1	4.6	4.8	4.1	4.6	3.8	4.1	4.1	2.0	1.8	2.9	2.2	2.1
Er	2.8	2.9	2.8	3.2	3.3	3.5	3.2	3.3	3.0	3.1	3.1	1.9	1.8	2.5	2.1	2.1
Yb	2.5	2.5	2.3	2.2	2.1	2.4	2.2	2.1	1.8	1.6	1.8	0.9	0.9	1.5	1.0	1.0

FF= Free fall; SPM= suspended particulate matter; PM₁₀= Particulate matter less than 10 μ m.

Numbers 1, 2, 3 and 4 represent different samples of the same size fraction.

* indicates the replicate analysis of same sample; CaO_T represents total CaO content.

The major element chemistry of FF samples (Fig. 4.2 a) collected during the summer season before the onset of SW monsoon at all sites is remarkably similar to each other and to the UCC. SiO₂ is somewhat enriched in all cases, more so in samples from Jhunjhunu and Bikaner. The lowering of most major constituents relative to UCC is likely related to the dilution effect of silica. Samples collected from the upwind locations had higher SiO₂ contents just as the deposited sediments collected from the surface. Surprisingly, Na shows depletion (in almost all FF samples) suggesting little contribution from sea-spray or from dry lake beds

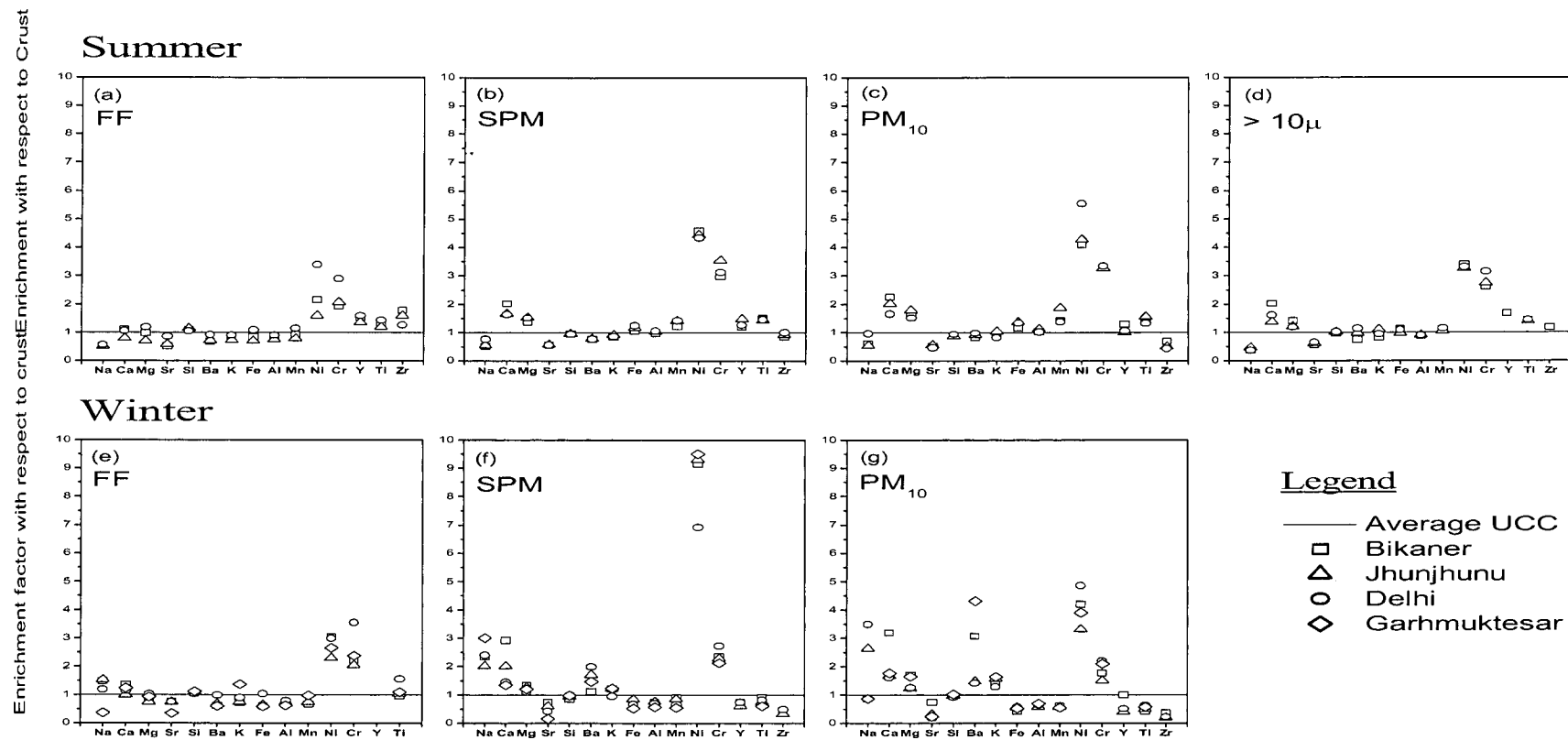


Figure 4.2 Major and trace element abundance in aerosols normalized to the abundance in average upper continental crust ($X_{\text{Aerosol}}/X_{\text{UCC}}$; UCC of Taylor and McLennan, 1985). Actual Ni concentration in Bikaner is 2.5 times to that shown in Figure 2f. FF-free fall; SPM-suspended particulate matter; PM₁₀ – particulate matter less than 10 μm .

to the aerosol budget even in the summer season. This is probably an effect of overwhelming dominance of silicate dust in the summer season diluting the contribution from the non-silicate sources. FF samples collected during winter seasons show a greater variability (Fig. 4.2 e). Ca and Na show noticeable enrichment, suggesting additions from non-silicate sources such as local carbonates, gypsum and halites from the dry lakebeds and Na salts from marine and nonmarine sources. During the winter season, wind direction becomes somewhat northerly and the wind speed decreases, reducing the dominance of coarser silicates in the free-fall samples and therefore causing a greater variability in bulk sample chemistry.

In summer, with decreasing particle size in SPM and PM₁₀ samples (Fig. 4.2 b and 2 c), Ca, Mg, Fe and Al contents increase whereas Si decreases. Appearance of chlorite in these fractions may explain the increased levels of Al, Fe and Mg. The increase in Ca and Mg contents is well in excess of that caused by reduced SiO₂ suggesting a greater contribution from local nonsilicate sources (limestone and gypsum quarrying in the upwind regions and caliche in the soil profiles) to the finer aerosols. This is also evident from the much-lowered CaO contents in silicate phase (Table 4.3). In the winter SPM and PM₁₀ samples, in addition to Ca, Na and Mg, K also shows a significant enrichment. However, Fe and Al show depletion possibly due to dilution by non-silicate sources, which have increased to Ca and Na budget significantly. The addition of K in the winter samples is likely from anthropogenic activities (mostly due to biomass burning; Cooper, 1980; Andreae, 1983). Secondary atmospheric interactions between alkaline particles containing Ca and Mg, and not necessarily natural, and SO₂/sulfate particles in the atmosphere could also have contributed to the total budget of Ca and Mg in aerosols (Andreae et al., 1986). Northern India experiences high SO₄ concentration in aerosols (Kulshrestha et al.,

1998) and temperature inversions in winter (Murthy, 1984), providing favorable conditions for such chemical reactions. Thus, we observe at least three possible sources for the major element chemistry of the aerosols: (1) dominantly UCC and their derivative soils and sediments, (2) minor non-silicate sources such as limestone, gypsum, lakebeds, caliche in the soil profiles and sea salt, and (3) anthropogenic sources.

Trace elements show a much greater variation in terms of particle size, season of sampling and site of sampling (Fig. 4.2). Sr shows a general depletion in all size fractions relative to the UCC. Finer fractions collected during winter show a much greater Sr depletion indicating decoupling from Ca, probably due to differences in their chemical mobility (Kanayama et al., 2002). This suggests that sources responsible for Ca and Mg enrichment in the aerosols during winter are also depleted in Sr. In contrast, Ba shows little size and site dependency and its concentration in summer is similar to that of UCC. However, the finer fractions in winter samples have a strong enrichment of Ba and greater size variability, a behavior similar to that of K. Burning of barium-rich lubricants in motor vehicles could be responsible for such high Ba concentrations (Morawska and Zang, 2001; Singh et al., 2002), as vehicular emissions account for 72% of total pollution in this region (Economic survey of Delhi, 2002).

Other trace elements such as Ni, Cr, Ti, Y and Zr are variably enriched in the FF samples relative to the UCC. With decrease in particle size, Ni and Cr show a larger and more variable enrichment whereas Zr shows depletion, particularly in PM₁₀ aerosols. Ti and Y show depletion only in winter SPM and PM₁₀ samples. Among these transition metals, Ni shows the greatest site dependency. An unusually high concentration of Ni is seen in the winter SPM. Such high Ni would require a large

contribution from anthropogenic sources mixed with natural mineral sources (Reheis et al., 2002). Such contributions show up in the winter months because of much reduced wind velocity and temperature inversions. For trace elements such as Cr, Ti, Y and Zr, accessory/heavy minerals in granitic rocks are the important hosts – zircon for zirconium, titanite and ilmenite for Ti and Y and magnetite for Cr and possibly Ni. Among these, zircon may be concentrated in FF aerosols and its abundance decreases significantly with decreasing size and in the winter. Similarly, concentrations of titanite and ilmenite in the aerosols decrease in the winter. Magnetite, on the other hand, is relatively more uniformly distributed in all size fractions, a feature also observed in the dust of Colorado plateau (Reynolds et al., 2001). However, Cr concentrations suggest an increasing magnetite content with decreasing grain size, provided all Cr is due to magnetite. The mineral chlorite can also contribute to the Cr budget. There is little difference in the Cr concentration of summer and winter samples indicating little anthropogenic contribution to Cr. Ni shows the maximum enrichment, and the largest and unsystematic variations among the elements studied. These variations cannot readily be explained by the observed mineralogy of minor and accessory phases. Also to the best of our knowledge, there is no accessory mineral in granitic rocks, which concentrates only Ni. Therefore, an anthropogenic contribution is required for Ni in the samples studied. Likely anthropogenic sources for Ni include coal/oil combustion processes (Nriagu and Pacyna, 1988) as well as metal plating industries in this region. We have also reported two to three orders of magnitude of enrichment of Cu in the fine fractions of the winter samples at all sites (Yadav and Rajamani, 2003a). From these observations we infer that concentrations of many trace transition metals in the aerosols is controlled by accessory minerals of granitic rocks and by the wind velocity. Because of much reduced wind strength in

the winter months, the uptake and transport of heavy minerals are reduced and that of anthropogenic contribution get enhanced especially for Ni.

4.5.4 REE Geochemistry

The chemistry of rare earth elements (REE), both in terms of their chondrite normalized abundance and patterns in silicate minerals, rocks and sediments provide insight into their sources and processes of formation of these earth materials. The chemical data on rare earth elements (REE) generated on aerosols of different sizes and bulk surface sediments, and collected from different locations are given in table 4.3. The chondrite normalized REE abundance and patterns for these samples are shown in figure 4.3. Similarly, chondrite normalized abundance and patterns of Upper Continental Crust (UCC) and Post Archean Australian Shale (PAAS) (Taylor and McLennan, 1985) and loess (McLennan, 1995) are also shown in figure 4.3 g for the purpose of comparison. All the samples studied have a fractionated REE pattern with LREE enrichment. The LREE show a uniform fractionation with $(Ce/Sm)_N$ ratios ranging between 2.63-3.10. The HREE show a small difference in fractionation between FF and SPM/PM₁₀ samples, with $(Gd/Yb)_N$ values of 1.8 to 2.1 and 1.8 to 3.1 respectively. A striking feature of REE chemistry in our samples is their uniform chondrite normalized patterns which are parallel to those of the UCC, PAAS and Loess. All samples have strong negative Eu anomaly, a feature again similar to UCC, PAAS and Loess with Eu/Eu^* ratios varying between 0.50 and 0.78. $(Ce/Yb)_N$ ratios of 7.47-8.22 for FF samples suggest that free fall samples are less fractionated than SPM and PM₁₀ samples that have ratios between 7.7-11.4. The summer free fall samples from all locations collected in the summer show nearly identical patterns and abundance indicating strong homogeneity among these aerosols. Reheis et al. (2002)

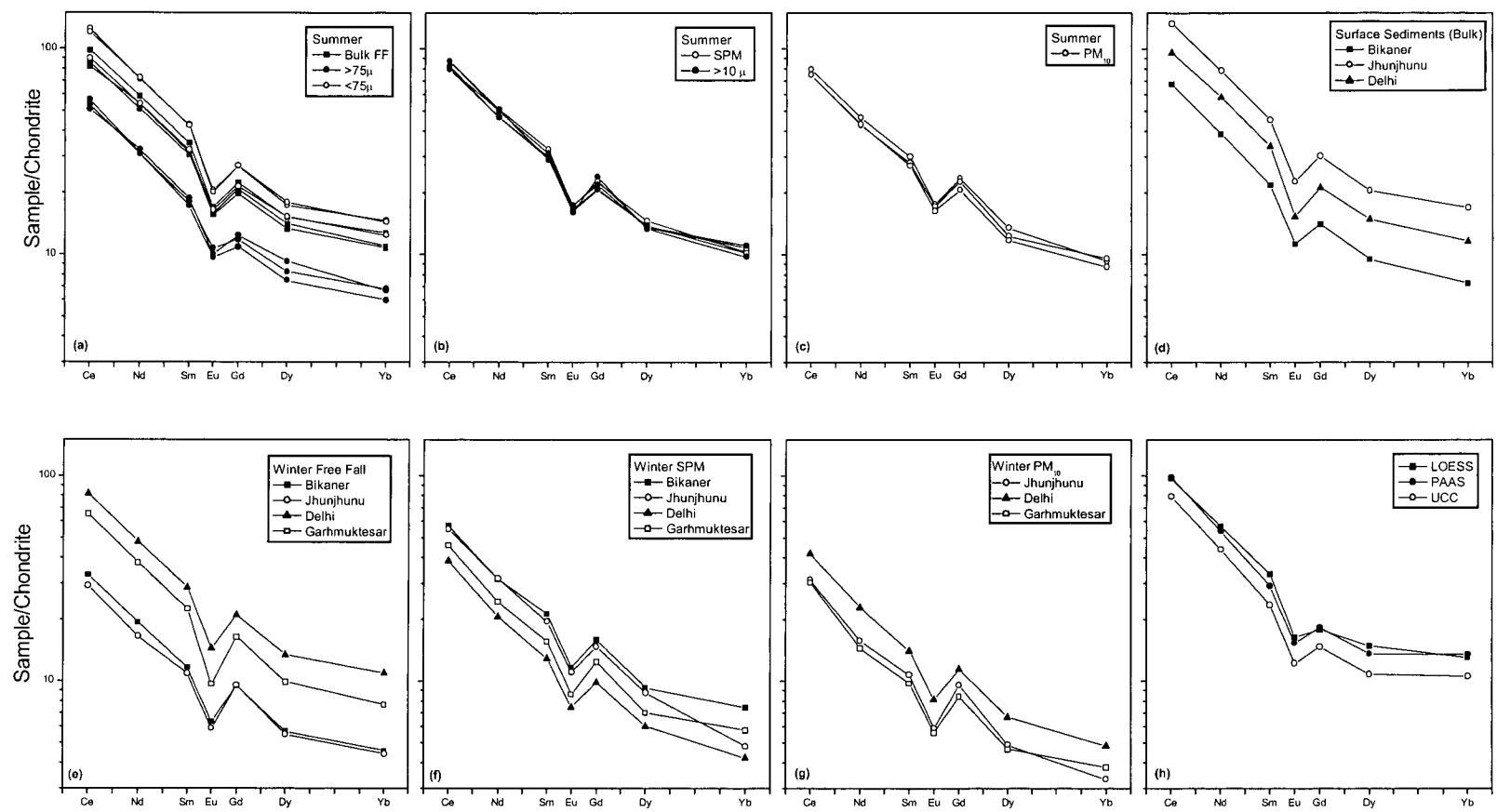


Figure 4.3 Chondrite normalized REE abundance and patterns of aerosol and sediment samples of NW India. Note the uniformity of REE chemistry of summer FF, SPM, PM₁₀, and >10 μ m samples from different stations along the W-E wind corridor. In figure a, b and c, sample sites are not distinguished because of the closeness of abundance in samples collected from different sites. Data source: Loess (McLennan, 1995); Upper Continental Crust UCC and Post Archean Australian Shale (PAAS) (Taylor and McLennan, 1985).

reported similar patterns of REE abundance in the dust Nevada and southern California, USA. These authors observed that the REE abundance in the dust is much lower than that in local alluvial sources and attributed this to the winnowing effect of wind transport on heavy minerals hosting the REE. However, such a simple relation between the dust sources and dust is not observed in the samples studied here. In the upwind Bikaner site, the surface sediments has a much lower REE abundance relative to summer samples of all sizes. In Jhunjhunu, a station located 250 km downwind, the deposited sediments has a higher REE abundance than all size samples. Further downwind at Delhi (540 km), all samples have very similar REE abundance. Clearly, the prevailing summer winds seem to be transporting REE hosting minerals in our sampling domain. This aspect is well illustrated in figure 4.3 a by the abundance and patterns of $+75 \mu\text{m}$ and $-75 \mu\text{m}$ fractions separated from the same FF samples of all the three locations. Samples of $>75 \mu\text{m}$ size show roughly half the abundance present in most of the $<75 \mu\text{m}$ fraction. When we compare this difference (a factor of two) with the silica contents of the same samples (Table 4.3), it strongly suggests that REE-hosting heavy minerals such as titanite, zircon, garnet, and unidentified phosphate minerals, are concentrated in $<75 \mu\text{m}$ fraction, which are transported in the dust by the prevailing summer winds. The REE chemistry of bulk FF samples, therefore, seems to be controlled by the relative proportions of $<75 \mu\text{m}$ and $>75 \mu\text{m}$ fractions.

Surprisingly, the SPM, $>10 \mu\text{m}$ and PM_{10} summer samples have REE patterns identical to themselves as well as to the FF samples. The overlapping abundance and uniformity of REE patterns in all size fractions suggest a well mixing and homogenizing effect of prevailing strong SW-W winds in summer. If anything, PM_{10} samples have slightly lower abundance compared to SPM samples despite the fact

they have lower SiO₂ contents. This suggests a possible decrease in the abundance of REE bearing phases in this fraction. It is important to note that the type of REE-bearing minerals remains the same in all the size fractions, although their proportions may vary. For example, lower zircon content in the PM₁₀ samples (as indicated by lower Zr values, Table 4.3) may reduce the proportions of HREE to yield higher (Ce/Yb)_N ratios compared to the free fall samples. Alternatively, REE bearing phases may also occur as coatings on finer particles as suggested for some riverine sediment (Singh and Rajamani, 2001). We note that the <75 μm fraction has REE abundance similar to or even higher than that in average loess with a mean size between 20–40 μm (McLennan, 1995). SPM and especially PM₁₀ samples have much lower abundance compared to average loess, in spite of their smaller mean grain size, 18 μm and 5 μm respectively. This suggests that REE-hosting minerals in aerosols seem to be concentrated in the size fraction of 20–40 μm and those heavy mineral contents may decrease on either side of this peak size. Similar observations about heavy minerals in dust have also been made by Schutz and Rahn (1982) and Herwitz et al. (1996). The surface sediment samples from Jhunjhunu and Delhi also have higher abundance compared to the free fall samples from the same area probably suggesting their deposition by aeolian processes under similar condition.

Unlike the summer samples, winter FF samples show a much lower and spatially variable REE abundance, although their patterns remain similar to that of the summer samples. Bikaner and Jhunjhunu samples show a large decrease in REE concentration whereas Delhi and Garhmuktesar have somewhat similar abundance compared to the summer samples. During the winter sampling period, we observed a noticeable difference in the wind trajectories of the two sets of stations. At Bikaner and Jhunjhunu, the wind was northerly and blowing only horizontally without much

vertical turbulence. At Delhi and Garhmuktesar, the wind was NW with high turbulence motion. It is not known if the differences in the wind direction and strength between these two sets of stations were responsible for the observed differences in REE through the differential uptake and transport of REE hosting heavy minerals. The finer fractions, SPM and PM₁₀, show a regular decrease in concentration with pattern similar to those of the summer samples as well as winter free fall. The relatively lower abundance in winter SPM and PM₁₀ samples could be related to a dilution effect of non crustal components as well as to a reduction in the content of REE-bearing phases as suggested by lower Zr and Ti contents in these samples (Table 4.3). In the winter season, the wind speed drops significantly and hence its carrying capacity of heavy minerals is reduced. The insufficient power of winds to pick up coarse particles and heavy minerals could be responsible for the spatial heterogeneity in the coarse fraction as well as relatively lower REE abundances in all fractions in winter. It implies that wind velocity plays a vital role in the compositional homogeneity of aerosols, particularly in the components that are hosted in heavy minerals. The source of REE, which is largely crustal at least in this region, remains the same for all sizes, at all times and in all sampling sites. The fact that the pattern and abundance of REE in the aerosols (other than that caused by wind velocity) are similar to that of the UCC indicates that the immediate crustal source has suffered little chemical weathering to cause chemical fractionation in different sizes of aerosols. The observed depletion of HREE in the aerosols here relative to the UCC is more likely a source feature rather than the winnowing effect of wind transport on REE hosting heavy minerals.

4.5.5 Sediment Geochemistry

In order to understand the nature of the sediments on the ground and their relation to aerosol production, transportation and deposition along the summer wind trajectory, their chemical data are plotted in figure 4.4 against those of the UCC. The Thar sediments from Bikaner are enriched in Si relative to the UCC because of selective retention of sand-sized quartz grains. All other components except Ni are depleted. Because Ni shows a large variation among the studied transition metals, an anthropogenic contribution is suspected. There is a depletion of Ti, Zr and Y, elements held in heavy minerals, indicating a wind speed capable of picking and transporting even the heavy minerals. Figure 4.4 b shows the concentration of elements in Thar sediments plotted against those of Jhunjhunu sediments, about 250 km downwind of the Thar desert. Interestingly, the Jhunjhunu sediments show an enrichment in elements commonly carried in silt and heavy minerals relative to the Thar sediments. Thus the prevalent winds are capable of transporting these components from their source in the Thar desert to Jhunjhunu. Delhi and Jhunjhunu surface sediments are compositionally nearly identical (Fig. 4.4 c), suggesting a homogenizing effect of wind transport at least within a distance of about 540 km from the Thar desert. Tripathi and Rajamani (1999) observed that the loessic sediments on the quartzite ridge of the Delhi region (DRS) are compositionally very homogeneous, both laterally and with depth (for more than 10 m). We suggest, therefore, that neither the sediment sources nor the average wind velocity have changed during the depositional period of these sediments.

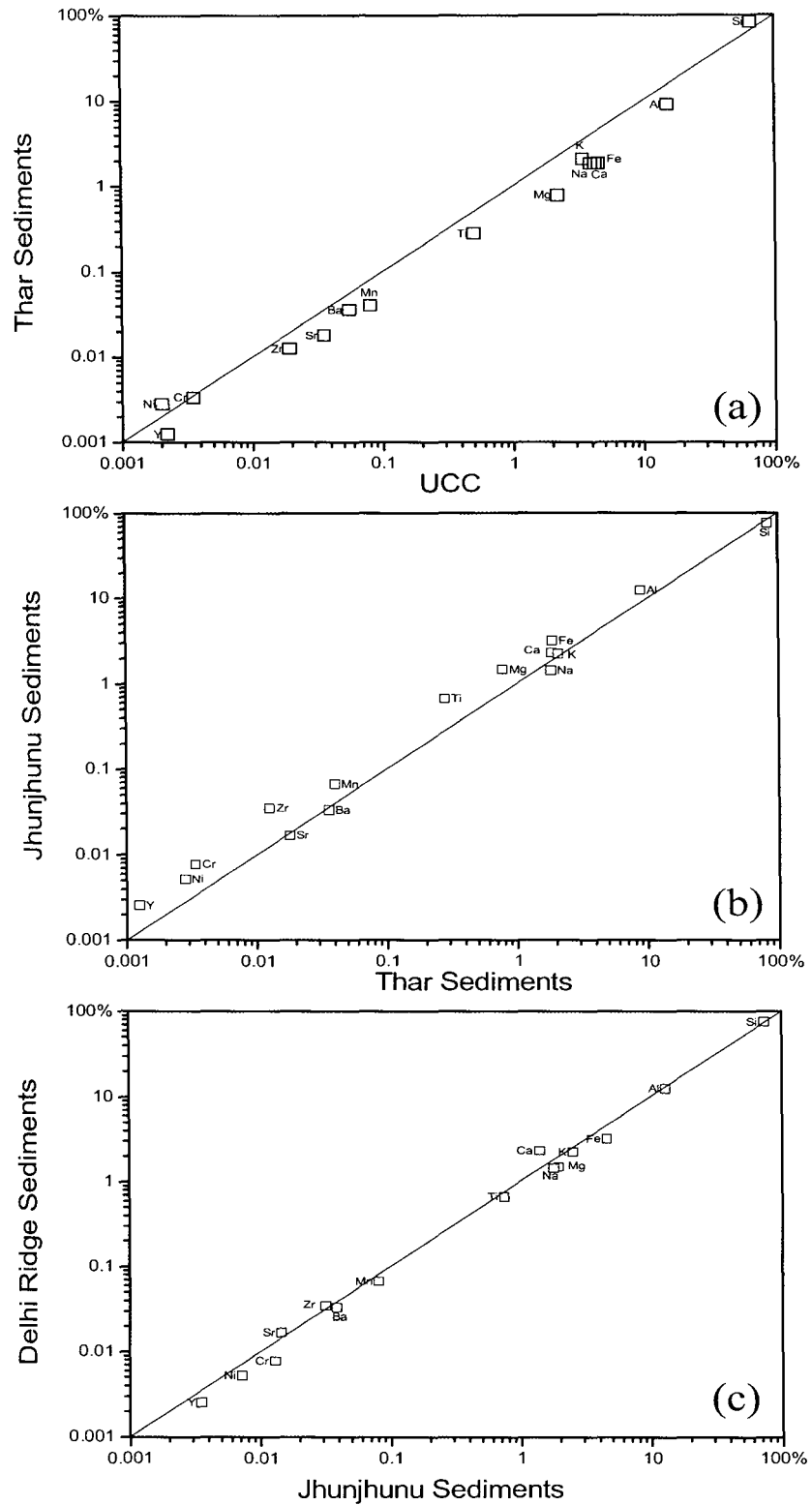


Figure 4.4 Equiline plots of sediment samples and UCC. Note the uniformity of composition of wind deposited Delhi ridge sediments (DRS) and sediment samples from Jhunjhunu.

4.5.6 Chemical Index of Alteration

To evaluate the chemical nature and weathering history of the aerosol sources the chemical index of alteration (CIA) was calculated for all samples using the molar proportions of Al_2O_3 , CaO, Na_2O and K_2O ($\text{CIA} = (\text{Al}_2\text{O}_3 / (\text{Al}_2\text{O}_3 + \text{CaO} + \text{Na}_2\text{O} + \text{K}_2\text{O})) * 100$). For this, only the silicate part of the total CaO is to be considered. Because of the small quantity of the aerosol samples we could not determine the carbonate free CaO for winter SPM and PM_{10} samples. Therefore, we have taken CaO as equal to Na_2O , in cases where CaO in silicate phase could not be determined and where CaO is greater than Na_2O , as suggested by McLennan (1993). Even this correction and calculation could not be done on some winter finer samples (SPM and PM_{10}), because of possible Na addition from secondary sources resulting in Na_2O becoming greater than CaO. The molar proportions are plotted in the A-CN-K diagram of Nesbitt and Young (1984). For comparison, values of UCC, Loess, PAAS and Yamuna alluvium are also plotted in figure 4.5. Unweathered, average granodioritic crustal rocks have CIA values around 50 (Fedo et al., 1995) and plot close to the plagioclase side of the plagioclase and K-feldspar tie line. Loess and average shale have CIA values of about 60 and 70 respectively. Soils and sediments produced by intense chemical weathering would have CIA value close to 100 and would plot near the apex A in the A-CN-K diagram (Fig. 4.5). It has been suggested that chemical fractionation by physical processes during transport and deposition of sediments can also affect the chemistry of river sediments and hence their position in the A-CN-K diagram (Nesbitt and Young, 1996; Nesbitt et al., 1996; Singh and Rajamani, 2001). However the effectiveness of physical sorting in chemical fractionation of sediments mainly depends on the extent of chemical weathering of

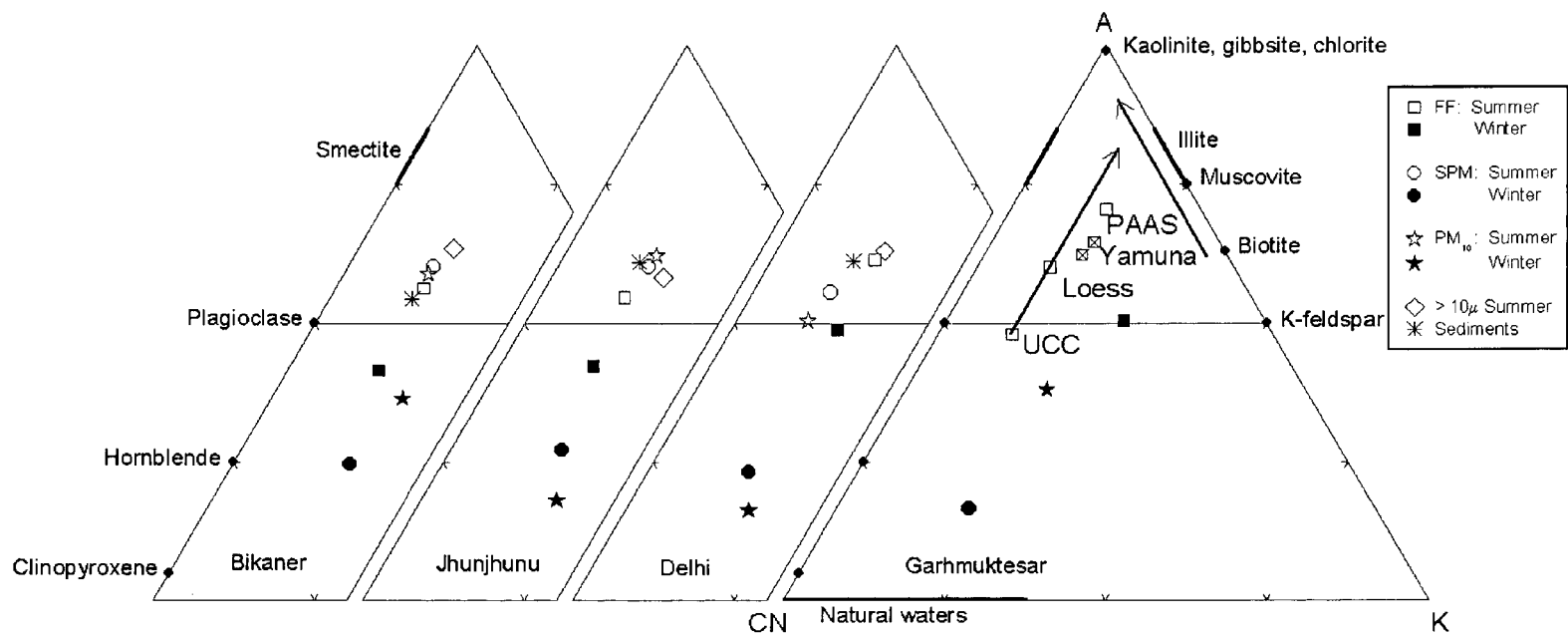


Figure 4.5 A-CN-K ($\text{Al}_2\text{O}_3\text{-CaO} + \text{Na}_2\text{O-K}_2\text{O}$ normalized molecular composition after Nesbitt and Young, 1984) plot of aerosol and sediment samples from NW India. Upper Continental Crust (UCC) and Loess from Taylor and McLennan (1985); Post Archean Australian Shale (PAAS) from McLennan (1995); Yamuna river alluvium from Tripathi et al. (2003).

their source rocks. Both of the processes, i.e. extent of chemical weathering and transport/deposition, together determine the chemistry of deposited sediments. It is important to note that sediments formed by glacial grinding of rocks and transported by fluvial action do not show much change in chemistry, at least in the first cycle of sedimentation (Tripathi and Rajamani, 1999). The CIA values for the entire summer aerosol sample show only a limited spread 57-67. In winter samples, there are large variations in CIA values irrespective of particle size. CIA values are as low as 31 for PM₁₀ winter samples, largely because of Na addition. All summer aerosol samples and deposited sediments plot between UCC and PAAS with a trend similar to the normal weathering trend of common granodioritic type rocks in A-CN-K diagram. This suggests that the aerosols are possibly consanguineous and related to common UCC type crustal rocks. Further, their sources did not suffer a high degree of chemical weathering which would have caused a greater spread in the A-CN-K diagram. Also, a high degree of chemical weathering would have caused significant mineralogical and therefore geochemical variation in different size fractions of aerosols (Schutz and Rahn, 1982). The separation of winter samples of SPM and PM₁₀ in the plot is due to addition of Ca, Na and K from secondary atmospheric reactions and anthropogenic sources. We note that Thar desert material also plots along the trend, defined by aerosol samples (Fig. 4.5) but with a lower CIA value. Tripathi et al. (2003) suggest that the Thar desert sands are river alluvium deposited by now extinct Himalayan rivers. Such alluvial materials are considered to be important dust sources worldwide (Prospero et al., 2002).

4.5.7 $^{87}\text{Sr}/^{86}\text{Sr}$ Isotope Chemistry

To investigate the ultimate source to the aerosols we have obtained limited $^{87}\text{Sr}/^{86}\text{Sr}$ data on the aerosols (Table 4.5). Clearly the leached aerosols have higher radiogenic Sr than the bulk samples, and the difference is greater in the finer aerosols. Therefore,

Table 4.5 $^{87}\text{Sr}/^{86}\text{Sr}$ isotopic ratio of the analyzed aerosol Samples

Sample	Bulk	Leached*
<i>Delhi Summer</i>		
FF	0.719852 (0.000055)	
SPM	0.720140 (0.000044)	0.730751 (0.000005)
PM ₁₀	0.718546 (0.000114)	0.733254 (0.000004)
<i>Jhunjhunu Summer</i>		
FF	0.719430 (0.000098)	0.727526 (0.000004)
SPM	0.715195 (0.000060)	
PM ₁₀	0.716358 (0.000101)	
<i>Bikaner Summer</i>		
FF	0.719153 (0.000078)	

FF=Free fall; SPM=Suspended particulate matter;
 PM₁₀= Particulate matter less than 10 μm diameter.
 Values in parentheses indicate $\pm 2\sigma$ errors.
 (*) Carbonate leached with 1.3N HCl.

the leachable component has much less radiogenic Sr. It is not possible to constrain the source of the leachable component, as there are several possible sources for the leachable component such as Jurassic limestone and Gypsum (that are being quarried in the upwind area near Bikaner), Himalayan carbonates and far traveled dust. For the high-radiogenic ($^{87}\text{Sr}/^{86}\text{Sr} = 0.7275\text{-}0.7332$) silicate fraction of the aerosols, again there are several possible sources in the Indian subcontinent. Among these, only certain lithotectonic units of the Himalayan orogen, such as the Tethyan Sedimentary Series have appropriate Sr isotopic characteristics (Najman et al., 2000). Tripathi et al. (2003) suggested that Thar sediments were most likely to have been deposited by an ancient river draining to the Thar from the Himalayas. The aerosols studied here and

the Thar sediments studied by these authors are geochemically very similar. Thus, the Thar sediments appear to be the major source for the silicate fraction of aerosols, which were ultimately derived from the Himalayan orogen through denudational processes.

4.6 CONCLUSIONS

Hot and arid regions of NW India are witnessing intense aeolian activity resulting in the transport of a large quantity of dust and aerosols. Strong pre-monsoon W to SW winds, aridity, and the presence of loose sands in the Thar region together are responsible for the entrainment and transport of aerosols. Light, northerly winds in the winter seasons seem only to rework the deposited aeolian sediments locally. All of the sample types of aerosols show a bimodal distribution in their particle size, a textural feature commonly reported for world's aerosols (Feng et al., 2002; Goossens et al., 2001). The weighted median size of the aerosols studied here is estimated to range between 20-40 μm similar to that of loess-forming dust that is commonly transported by winds in short term suspension a few meters above ground (Tsoar and Pye, 1987). The source of the aerosols is largely crustal (average UCC) particularly for the coarser fraction. Secondary non-silicate crustal sources, atmospheric reaction products and anthropogenically derived components, particularly product of biomass burning, constitute only minor amounts; they are most noticeable in the finer fractions of winter samples. We also infer from the aerosol chemistry that wind velocity controls the bulk chemistry of aerosols as an intensive variable. Under high velocity conditions in summers (high speed and directional restrictions), the coarser crustal component is so overwhelming that it results in a very uniform chemical composition of the aerosols over a long distance (at least 600 km). When the wind velocity is low, local

contributions to aerosols as well as reworking of deposited sediments make the aerosols compositionally heterogeneous, particularly the finer fractions. The reported textural and geochemical homogeneity in the ~10 m thick lossic sediments on the Delhi Quartzite points to long term stability of the dust transporting winds, both direction and strength in this region (Tripathi and Rajamani, 1999).

Abundance of certain trace elements such as Ti, Cr, Zr, Y and REE in the aerosols show large deviations from their average crustal abundance in all the sample types (FF, SPM and PM₁₀). This is because their host minerals are largely heavy minerals whose concentrations appear to vary with the particle size of aerosols. Although the heavy minerals are present in all the size grades, they seem to have been preferentially concentrated in the size range of 20-40 µm, a feature also observed in desert soils (Schutz and Rahn, 1982). These two physical factors, i. e., higher specific gravity and preferential enrichment in a restricted size range, of the heavy minerals make their distribution and therefore, the abundance of hosted elements more dependent on wind velocity. Thus wind velocity affects the geochemistry of aerosols in at least two different ways; by making secondary non silicate and anthropogenic sources a significant component for some major and trace elements during periods of low velocity and by selective uptake, transport and deposition of accessory heavy minerals for some trace elements.

The REE geochemistry of the aerosols in the NW part of India is surprisingly uniform. Kreutz and Sholkovitz (2000) attribute REE fractionation in cores of Inilchek glacier (Tien Shan Mountains, Kyrgyzstan) to size sorting during aerosol transport or alternatively to multiple sources. Significant distortion in REE abundance and pattern compared to the earth's crust in aerosols can also be caused by anthropogenic sources, particularly by oil fired power plants and vehicular exhaust

(Rahn, 1976 b; Olmez and Gordon, 1985; Wang et al., 2000). We do not observe in our samples any such physical or chemical fractionation of REE. Interestingly, REE patterns in all size fractions at all sites are similar and conform to that of average UCC (Taylor and McLennan, 1985) although the absolute abundance slightly decreases with size. The variations can be explained by quartz and other (REE free) component dilution as well as by the effect of wind velocity on the entrainment and transport of accessory heavy minerals. The observed CIA values on samples free from secondary/anthropogenic sources as well as the coherence of REE geochemistry point to a common, UCC type, crustal source that has suffered only a mild chemical weathering. If the source for the aerosols was previously deposited clastic sediment as appears the case here, then it must have been derived from rapid physical erosion of dominantly upper crustal rocks and deposited as flood plain sediments that have since been little affected by chemical weathering.

The available geochemical data, particularly Sr and Nd isotope data, suggest that the Thar sands are alluvial materials, deposited by paleorivers draining the Himalayas (Tripathi et al., 2003). Thus the various Himalayan lithologies constitute the ultimate source of aerosols in this region. Sediments of flood plains and deltas of the world's rivers are thought to have been deposited by rivers rapidly eroding recently uplifted terrains (Chesworth, 1982; Rajamani, 2002) undergoing little chemical weathering. These sediments are rich in plant nutrients (cations) and therefore are good for agriculture. A large part of the cations is stored in primary minerals present as silt fraction in the alluvial sediments. Consequently, selective uptake and transport of the silt fraction from alluvial sediments by aeolian processes will impoverish the sediments in plant nutrients. In the NW part of India, prevailing aridity, strong south westerly summer winds and the availability of thick alluvial

sediments in the Thar region together act to transport large quantities of silt dominated dust. Removal of nutrient rich silt from the alluvium has impact on climate and vegetation, factors leading to the desertification of the Thar region. The feed back mechanism that exists in dust generation, silt removal and desertification in the alluvial plains needs a detailed study in view of its environmental significance.

Environmental Chemistry

5. ENVIRONMENTAL CHEMISTRY

5.1 INTRODUCTION

Air Pollution is a major cause of concern for deterioration of environmental conditions, particularly in the developing countries. Air borne particles in the atmosphere have serious environmental implications such as the reduction of visibility and the health hazards due to the inhalable fraction, i.e., PM_{10} aerosols. Recently, the national air quality standards in many countries are being reviewed in order to monitor and maintain a healthy environmental quality. United States Environmental Protection Agency (USEPA) has replaced the monitoring of total suspended particulate matter (TSPM) by PM_{10} measurements in United States (USEPA, 1990) and more recently this agency had argued for monitoring of even $PM_{2.5}$ fraction of aerosols (USEPA, 1996). Trace metals introduced into the atmosphere by anthropogenic means affect the life system on earth through their biogeochemical cycling in three spheres (Atmosphere, Hydrosphere, and Geosphere) of earth (Rasmussen, 1998). A number of epidemiological studies report a close relationship between the fine particles in the atmosphere and the mortality rates (Dockery and Pope, 1996; Adler and Fischer, 1994). The present chapter discusses the air quality data on SPM and PM_{10} aerosols and dry accumulation rates of free fall (FF) in N-NW part of India. The trace element chemistry of different size fraction of aerosols collected from different locations is discussed subsequently.

5.2 DEPOSITIONAL FLUX AND THE AIR QUALITY

Free fall accumulation rates and air quality data on SPM and PM_{10} aerosols collected from Bikaner, Jhunjhunu, Delhi and Garhmuktesar in summer and winter seasons are

summarized in table 5.1. The air concentration levels for SPM and PM₁₀ are based on observations made during a week's sampling in summer between 19-26th May 2000 and in winter during 17-26th Jan 2001. FF samples are averaged for two samples, collected for seven days along with SPM and PM₁₀ sampling and other for continuously one month in June, 2000 before the onset of the summer monsoon and in February, 2001 during winter. FF accumulation rates presented here are calculated

Table 5.1 Dry accumulation rates of FF aerosols and the air quality data on SPM and PM₁₀ aerosols for NW India.

	FF(g/m ² /day)				SPM(μ g/m ³)				PM ₁₀ (μ g/m ³)			
	N	Range	GM	GSD	N	Range	GM	GSD	N	Range	GM	GSD
<i>Summer</i>												
Bikaner	2	4.4-21	9.6	8.9	4	4348-10702	6041	2576	4	444-2907	1260	1139
Jhunjhunu	2	2.57-4.3	3.3	0.9	3	1246-2140	1631	368	3	752-982	878	97
Delhi	2	0.5-2.70	1.2	1.2	5	249-1031	540	269	3	269-410	346	60
<i>Winter</i>												
Bikaner	1	0.47			3	154-238	206	40	1	169		
Jhunjhunu	1	0.412			2	203-212	207	5	2	253-287	269	17
Delhi	1	0.318			3	108-259	176	63	3	22-266	251	10
Garhmuktesar	1	0.48			2	165-188	176	12	2	239-254	246	7.5

FF Free fall; SPM suspended particulate matter; PM₁₀ particulate matter less than 10 μ m; N is number of samples collected; Range indicate minimum and maximum concentration levels; GM and GSD indicate Geometric Mean and geometric standard deviation respectively.

from the FF samples collected by the marble dust collectors (MDCs) as described in the methodology. The data represent only dry accumulation rates, as there was no instance of rainfall during sampling. The MDC method has been proposed as the international standard method for FF collection, calculation and comparison of dry accumulation rates (Goossens and Offer 1994; Reheis and Kihl, 1995). There could be small differences in the results when compared with other dust collector data. SPM and PM₁₀ air quality data are based on the sampling done by a high volume air sampler which collects total SPM (0.01-100 μ m) and particles < 10 μ m aerodynamic diameter, respectively. We observe abnormally high concentration levels of all types of air borne particles in the atmosphere at all sites during the summer season

compared to the winter. All fractions studied during summer show more day-to-day variability at all sites (indicated by geometric standard deviation in table 5.1) compared to winter samples. Seasonal variability as well as day-to-day variability in the atmosphere loading of FF, SPM and PM₁₀ are shown graphically in figure 5.1 along with their geometric mean and geometric standard deviation.

All types of aerosols in summer show the highest concentrations in Bikaner, a site situated in the Thar Desert in the upwind region. The concentration levels show a systematic and regular decrease from Bikaner to Delhi through Jhunjhunu. We observe one sudden hike in the concentration levels of all types of aerosols at all sites in the summer season. These observed maxima in the air quality data systematically decrease from Bikaner to Delhi with increasing distance from the upwind region. We attribute this to the heavy dust storm that occurred on 24th May, 2000, which descended down in the downwind direction. It is important to mention here that SPM sample showing the highest SPM levels equal to 10702 $\mu\text{g}/\text{m}^3$ at Bikaner was collected in only six hours during the heavy dust storm on 24th May, 2000 in summer. There was a strong reduction in atmospheric loading before and after this dust storm (Fig. 5.1). Among SPM and PM₁₀ aerosols, the SPM shows the highest concentration at all sites with a smaller day-to-day variability compared to PM₁₀ levels. This suggests that the episodic dust events have rather a strong effect on the SPM levels in the atmosphere as well as on their transport in the downwind direction compared to that on the PM₁₀ levels, even at the desert site of Bikaner. Large standard deviations in FF samples at Bikaner are again related to one of the two samples collected, which represents heavy dust events. From the data presented here, we consider that the severe dust events that took place over the Thar Desert are responsible for the increased levels of aerosol loading in all size fractions in the atmosphere over the

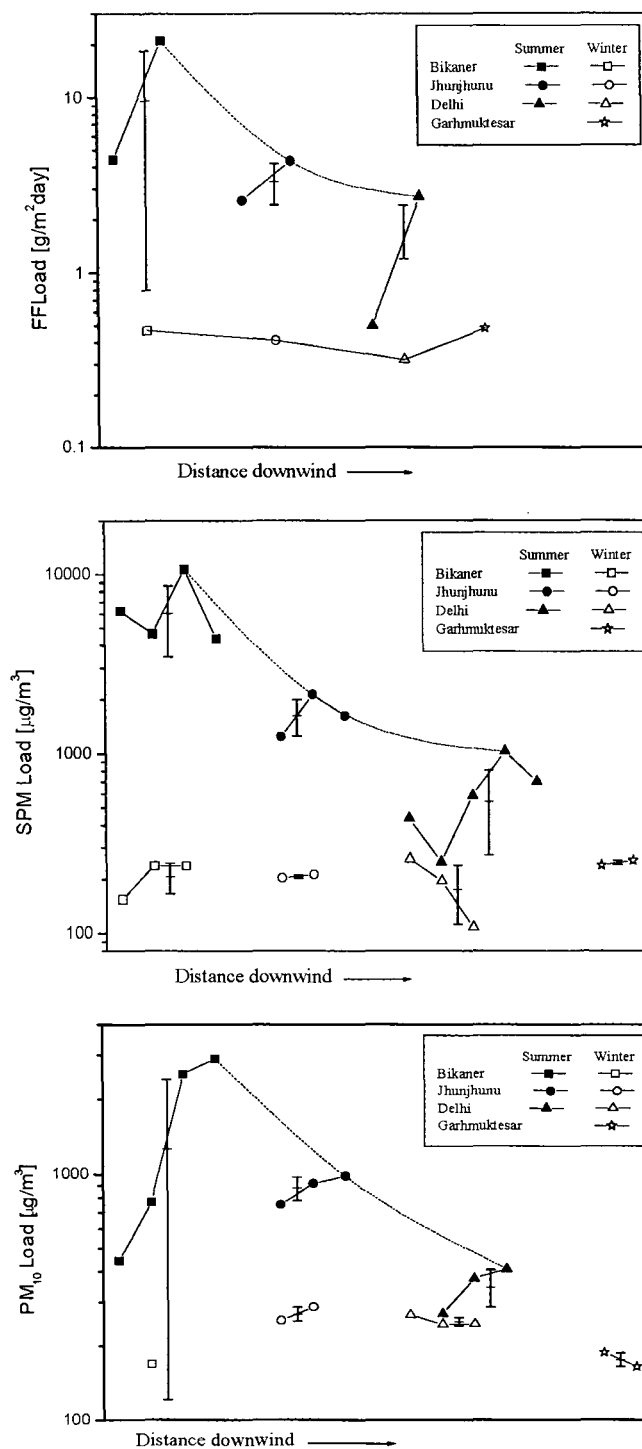


Figure 5.1 Atmospheric loading of free fall (FF), suspended particulate matter (SPM), PM₁₀ aerosols at different locations in summer and winter. Dashed line represents the dust storm event during sampling campaign. Horizontal lines in the error bar indicate geometric mean and the error bar indicate geometric standard deviation.

entire study area. There is a significant drop in atmosphere levels of FF, SPM and PM₁₀ at all sites in winter. The concentration levels of FF decrease from Bikaner to

Delhi and show an increase at Garhmuktesar; SPM levels remain almost same at all sites; PM₁₀ levels are higher at Jhunjhunu and Delhi compared to other two sites. The reduced levels of all types of aerosols in the atmosphere at all site are due to the low wind speed (having insufficient strength to pick up crustal material) and to relatively calm atmosphere in winter compared to summer. The slight increase in FF accumulation rate at Garhmuktesar could be related to the location of the sampling point that was near to the river Ganga and was along the national highway. The elevated air quality data on PM₁₀ aerosols for Jhunjhunu and Delhi suggest the significant contribution from anthropogenic sources to this type of particles. Contributions from the Khetri copper mines, 60 km east of Jhunjhunu or that from the northwest regions (the upwind region in winter) could be the probable sources to PM₁₀ at Jhunjhunu. At Delhi, vehicular exhaust, emissions from thermal power stations and small-scale industries could have contributed significantly to the fine PM₁₀ particles in the atmosphere.

Such higher concentration levels of SPM have also been observed elsewhere in the world, e.g., at Quira in Japan ($6757 \mu\text{g}/\text{m}^3$; Sadayo et al., 2002), at Sede Boger, Israel ($> 3000 \mu\text{g}/\text{m}^3$; Offer and Goossens, 2001). The FF accumulation rates observed here are far higher than that observed in California ($30 \text{g}/\text{m}^2/\text{yr}$; Reheis and Kihl 1995) and in the Neger Desert, Israel ($17 \text{g}/\text{m}^2/\text{m}$; Offer and Goossens, 2001). PM₁₀ values observed in summer season are way higher than other reported values. The winter values are somewhat comparable to other studies. A few studies from India have reported SPM values of $990 \mu\text{g}/\text{m}^3$ and $1305 \mu\text{g}/\text{m}^3$ at Delhi and Agra, respectively (Kulshrestha et al., 1995; Tiwari, 1999). NEERI (1995, 96 and 97) reported the SPM levels between $200\text{-}1000 \mu\text{g}/\text{m}^3$ for ten major cities in India. A recent study by Kumar et al. (2001) on PM₁₀ level at Delhi has reported high values ranging between 5-

1611 $\mu\text{g}/\text{m}^3$, which is near comparison to PM_{10} levels of the present study during summer. No other similar study is available in this region for comparison.

The present study shows that the particulate levels in the ambient air over NW India exceeds the national ambient air quality standards (NAAQS), particularly in the summer season by 1-2 orders of magnitude (Tab. 5.2). In general, NAAQS in India are set higher than that prescribed by USEPA, WHO and European Union (table 5.2), but even these are also not followed. If we ignore the episodic dust events that occur during summer then also the air quality over this region does not meet the

Table 5.2 Reference standards for average ambient air quality.

	SPM($\mu\text{g}/\text{m}^3$)						PM ₁₀ ($\mu\text{g}/\text{m}^3$)				
	Indian ^a			USEPA	WHO ^b	EU ^d	Indian			USEPA	WHO ^c
	IA	RA	SA				IA	RA	SA		
Ann. Avg.	360	140	70	80	60-90	150	12	60	50	50	50
24-H avg.	500	200	100		150-230	300	150	100	75	150	125

SPM suspended particulate matter; PM₁₀ particulate matter less than 10 μm ;

(a) Indian standards given by Central Pollution Control Board, New Delhi.

(b) Not to exceed more than once in a year; (c) WHO guidelines for Europe only; (d) EU limit values IA Industrial area; RA Residential area; SA Sensitive area.

Sources: European Community, 1992 (EU); United States, CFR (USEPA); WHO, 1987; CPCB, 2002.

standard criteria. The higher levels of particles are also a cause of poor visibility in this region. Husar et al. (1997) observed that India has the worst visibility condition compared to the rest of the world. The particles less than 10 μm mostly of anthropogenic origin and rich in toxic metals are directly inhalable while breathing and can have serious health consequences. USEPA has switched over its air quality standard from TSPM to PM_{10} and more recently to PM_5 and $\text{PM}_{2.5}$ in order to avoid the health risk by such fine particles. Therefore, the present study needs immediate attentions of the authorities to monitor the air quality in this region.

The results of the present study are quite useful and realistic in nature due to timely sampling at different locations, covering a total distance of 600 km, along the dominant SW-W wind trajectory in NW India. The observations on FF accumulation

rates, and SPM and PM₁₀ air concentration levels in the atmosphere are demonstration of the effect of prevailing dust storm activities on the air quality during summer in the NW parts of India and of their comparison with no dust storm period and low wind conditions in the winter season. The air quality data for SPM and PM₁₀ are averaged over one week, and FF accumulations are averaged over one week and over the following month, for both summer and winter seasons. Data during summer season are also biased for the episodic events of heavy dust storms, which do not persist all the time and all over India. Therefore, these observations should not be taken as an artifact while calculating the annual accumulation rates as well as the NAAQS for SPM and PM₁₀ for this region, rather they should be considered seriously before driving to any air quality standards for this region. Since we do not have any control on the natural processes of dust storm, the NAAQS needs to be flexible, particularly for the summer season and to be fixed at higher values compared to the rest of the year and rest of India. Detailed sampling is required to establish the real data set and NAAQS in India.

5.3 TRACE METAL CHEMISTRY

5.3.1 Results

The geochemical data on trace elements of environmental concern (Ba, Sr, Ni, Cr, Cu, V, Zn and Pb) for different size fractions of aerosols (FF, SPM and PM₁₀) collected from different locations in summer and winter are given in table 5.3. Elemental concentrations are given in ppm units on weighted mean average of various sub-samples of each type of aerosols (weight fraction of each sub sample × its concentration). We observed a day-to-day variability in trace metal concentrations among the sub-samples collected during the sampling period. Therefore, the

geometric mean and geometric standard deviation (a measure of such variation) are also provided in table 5.3. However, we are using the weighted mean average concentrations in our geochemical discussion here. From the geochemical data plotted in figure 5.2 we observe variations in the elemental abundance as a function of particle size, sampling site and time, and the wind velocity (speed and direction). The elements are arranged in a decreasing order of their crustal abundances in figure 5.2. The observed variations are explained here and are used to understand the causes of variation, source of trace metals and possible consequences.

From the observed variations shown in figure 5.2, trace elements studies can be grouped in three categories such as Sr, V and Cr, Ba and Ni, and Cu, Pb and Zn. Sr, V and Cr show least variations among the sites, between the seasons and among different size fractions of aerosols, if anything elemental abundance decreases in winter season compared to summer. Ba content in aerosols increases with decreasing size in both seasons. This increase is more pronounced in winter samples, and more so in SPM and PM₁₀ aerosols collected from Jhunjhunu and Delhi in the downwind direction. Ni shows maximum abundance in winter SPM samples with high site dependency. The third category elements, Cu, Pb and Zn show maximum variations in terms of particle size, sampling site and season. The relative abundances of these elements in all types of aerosols follow the order $Cu > Pb > Zn$ at all sites. The elemental abundance increases significantly with decreasing size and shows strong dependency on seasons with the highest values in winter samples. Maximum site variability is seen in SPM samples for these elements, particularly in winter.

Table 5.3 Trace element concentration (in ppm) in different size fractions of aerosols and sediment samples collected from different locations.

(A) Bikaner

	Summer Free Fall				Summer SPM				Summer PM ₁₀				>10 μm		S. Sediment		Winter FF		Winter SPM				Winter PM ₁₀				
	W.A	GM	G. S	ER	W.A	GM	G. S	ER	W.A	GM	G. S	ER	WA	ER	WA	ER	WA	ER	W.A	GM	G. S	ER	W.A	GM	G. S	ER	BPW
Ba	372	364	11	0.7	422	409	49	0.8	455	430	106	0.8	409	0.7	356	0.6	342	0.6	610	665	456	1.1	1687	3.1			
Sr	185	184	1	0.5	198	193	19	0.6	180	182	25	0.5	197	0.6	177	0.5	265	0.8	257	262	18	0.7	258	0.7			
Ni	43.1	44	1	2.2	92	92	7	4.6	82	79	9	4.1	68	3.4	28	1.4	61	3.1	458	491	167	22.9	84	4.2			
Cr	68.1	79	16	1.9	105	106	6	3.0	115	110	13	3.3	92	2.6	34	1.0	77	2.2	82	70	31	2.3	62	1.8			
Cu	34.6	20	17	1.4	113	141	241	4.5	1392	1583	1521	55.7	52	2.1	16.5	1.2	36.3	1.5	643	688	224	25.7	22394	895.8			
V	69	72	5	1.2	83	68	27	1.4	73	59	27	1.2	86	1.4	72	1.0	58.7	1.0	47	44	8	0.8	29.4	0.5			
Zn	61.3	56	7	0.9	80	82	50	1.1	182	141	95	2.6	79	1.1	18	0.4	163	2.3	385	413	147	5.4	1333	18.8			
Pb	39	35	6	2.0	35	35	29	1.8	41	41	3	2.1	35	1.8	22	1.2	40	2.0	102	108	117	5.1	524	25.5			

(B) Jhunjhunu

	Summer Free Fall				Summer SPM				Summer PM ₁₀				>10 μm		S. Sediment		Winter FF		Winter SPM				Winter PM ₁₀							
	W.A	GM	G. S	ER	W.A	GM	G. S	ER	W.A	GM	G. S	ER	WA	ER	WA	ER	WA	ER	W.A	GM	G. S	ER	W.A	GM	G. S	ER	W.A	GM	G. S	ER
Ba	393	388	6	0.7	429	414	67	0.8	502	489	81	0.9	535	1.0	331	0.6	365	0.7	929	917	113	1.7	810	813	77	1.5				
Sr	202	200	3	0.6	200	196	19	0.6	193	189	21	0.6	213	0.6	170	0.5	256	0.7	208	206	25	0.6	112	112	26	0.3				
Ni	31.7	39	12	1.6	89	89	0	4.4	86	85	4	4.3	65	3.3	53	2.7	46	2.3	186	156	121	9.3	66	66	5	3.3				
Cr	72	71	1	2.1	124	117	29	3.5	114	113	10	3.3	96	2.7	78	2.2	71	2.0	79	79	4	2.3	52	52	11	1.5				
Cu	30	28	3	1.2	250	238	50	10.0	5541	5486	378	222	33	1.3	28.4	1.1	72	2.9	3741	3444	1585	150	15816	5835	22641	633				
V	58.3	59	1	1.0	84	86	7	1.4	97	98	13	1.6	70	1.2	79.4	1.3	59	1.0	38	38	0	0.6	39	39	9	0.7				
Zn	50.3	64	23	0.7	116	119	75	1.6	147	149	19	2.1	184	2.6	65	0.9	150	2.1	694	698	64	9.8	556	557	126	7.8				
Pb	32	37	7	1.6	35	34	1	1.8	48	49	4	2.4	39	2.0	46	2.3	78	3.9	269	271	38	13.5	448	449	19	22.4				

(C) Delhi

(D) Garhmuktesar

	Summer Free Fall				Summer SPM				Summer PM ₁₀				>10 μm		S.Sediment		Winter FF		Winter SPM				Winter PM ₁₀				Winter FF		Winter SPM				Winter PM ₁₀					
	W.A	GM	G. S	ER	W.A	GM	G. S	ER	W.A	GM	G. S	ER	WA	ER	WA	ER	WA	ER	W.A	GM	G. S	ER	W.A	GM	G. S	ER	W.A	ER	W.A	GM	G. S	ER	W.A	ER	W.A	GM	G. S	ER
Ba	500	515	21	0.9	421	411	37	0.8	530	556	141	1.0	619	1.1	376	0.7	533	1.0	1087	1193	536	2.0	771	751	341	1.4	323	0.6	803	786	304	1.5	2367	4.3				
Sr	300	295	7	0.9	195	182	39	0.6	155	159	45	0.4	227	0.6	200	0.6	255	0.7	143	110	74	0.4	56	57	10	0.2	119	0.3	50	49	20	0.1	77	0.2				
Ni	68	69	2	3.4	87	86	43	4.3	111	96	38	5.5	66	3.3	71	3.6	60	3.0	138	146	30	6.9	97	97	1	4.8	53	2.7	190	181	98	9.5	78	3.9				
Cr	101	98	4	2.9	110	109	5	3.1	117	111	17	3.3	110	3.1	129	3.7	124	3.5	95	96	5	2.7	77	74	22	2.2	83	2.4	74	74	13	2.1	73	2.1				
Cu	64	61	4	2.6	425	417	199	17.0	1895			75.8	165	6.6	35	1.4	130	5.2	1733	1581	410	69.3	15770	12035	17448	631	79	3.2	513	512	27	20.5	4260	170				
V	106	89	22	1.8	55	48	32	0.9	39	39	4	0.7	84	1.4	70	1.2	79	1.3	45	43	5	0.7	36	36	1	0.6	29	0.5	41	41	0	0.7	35	0.6				
Zn	231	166	80	3.3	269	265	146	3.8	503	439	300	7.1	535	7.5	90	1.3	407	5.7	523	557	136	7.4	870	744	570	12.3	162	2.3	890	808	477	12.5	316	4.5				
Pb	221	228	10	11.1	64	61	27	3.2	168	168	63	8.4	264	13.2	55	2.8	380	19.0	354	327	74	17.7	508	497	104	25.4	79	3.9	139	139	4	7.0	633	31.7				

WA and GM indicate weighted average and geometric concentrations respectively; GS- geometric standard deviation; ER- X_{sample}/X_{UCC} ratio (UCC of Taylor and McLennan, 1985). S. Sediment- Bulk surface sediment.

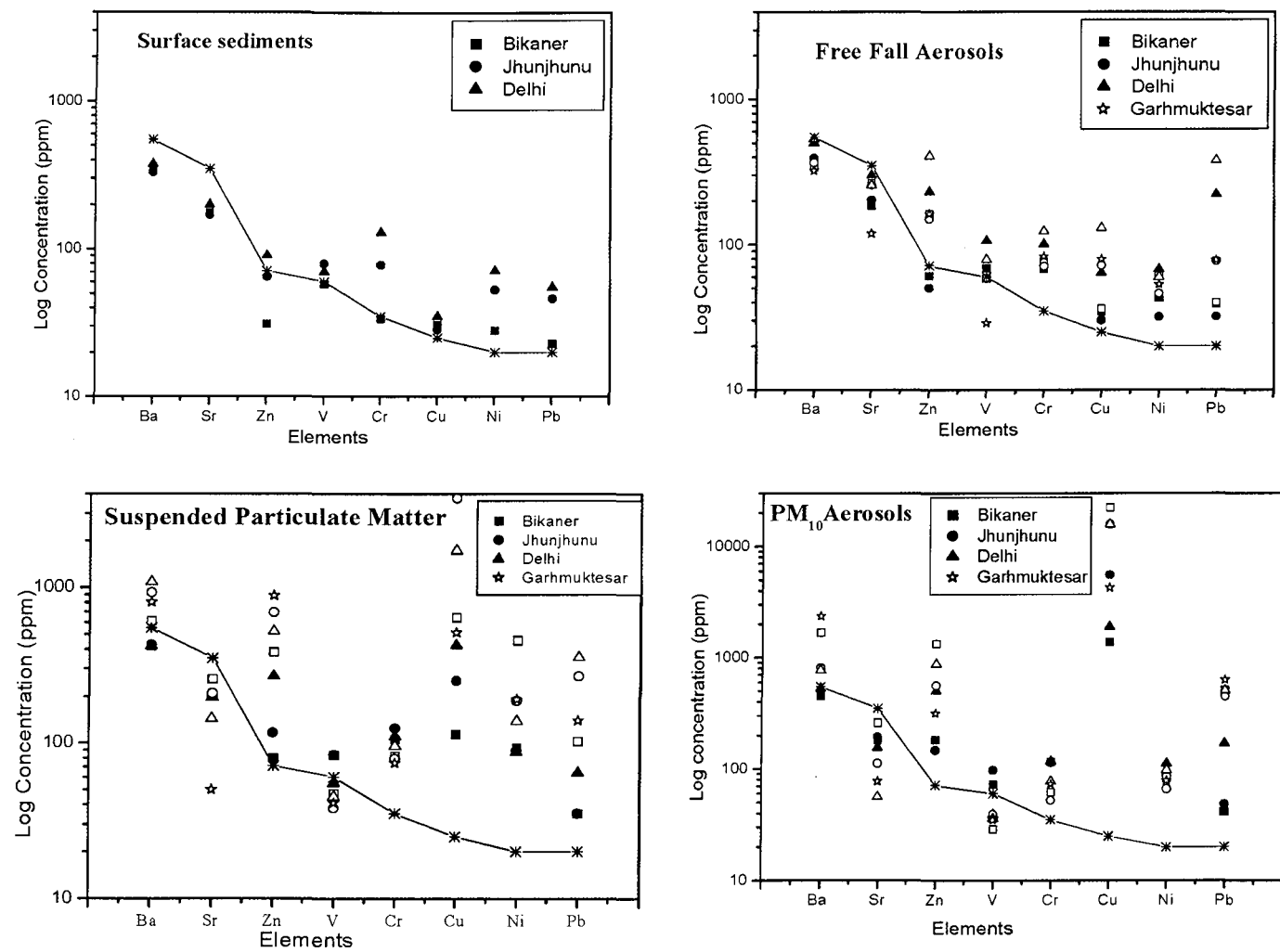


Figure 5.2 Trace element abundance and variations in abundances in aerosols and surface sediment samples of different locations. Closed and open symbols represent summer and winter samples respectively. Line connecting * represent the crustal abundance of trace elements.

5.3.2 Discussion

In order to explain the abundances and their variations as well as the sources of these trace metals in aerosols we have calculated $X_{\text{sample}}/X_{\text{UCC}}$ ratio (UCC of Taylor and McLennan, 1995) as suggested by Rahn (1976 a) and are given in table 5.3. The crustal abundances of these trace elements are also plotted in figure 5.2 for the purpose of comparison of aerosols with UCC. It is observed that low $X_{\text{sample}}/X_{\text{UCC}}$ (1 to 2) ratio would indicate a greater contribution from the crustal sources to the aerosol metal budget while contribution from anthropogenic sources generally tend to increase the ratio to higher values (Nriagu and Pacyna, 1988; Rasmussen, 1998; Reheis et al., 2002).

Among the elements studied here Ba and Sr show depletion in all types of aerosols in summer season compared to the UCC just as the deposited surface sediments. In winter samples, however, Ba contents show significant enrichment in the finer fractions while Sr decreases with decrease in particle size in winter and remains lower than the UCC. The low Ba content in the immediate sediment source (the Thar Desert; Yadav and Rajamani, 2003b) is either an inherited feature or is due to removal of mica, the dominant host mineral for Ba, by aeolian activity. Although chemical weathering of rocks and sediments can also lead to low Sr values due to its high mobility in soil solution, this may not be the case here because the aerosols and surface sediments studied here are known to have undergone only mild chemical weathering (Yadav and Rajamani, 2003 b). The loessic deposits elsewhere in the world are also known to have low Ba and Sr contents (Taylor et al., 1983). The low Ba and Sr contents compared to the UCC in aerosols studied here probably reflect the source feature rather than the depletion caused by aeolian processes. The sediments in the upwind directions are reported to have been derived and transported

by the now extinct rivers from the Himalayas, which have high proportions of intracrustal granites. The high Himalayan granitic rocks are reported to have low Ba and Sr contents equal to 15 and 12 ppm, respectively (Kaur and Chamyal, 1996). Therefore, the low Ba and Sr values in the aerosols likely are a source feature.

The increase in Ba content in winter samples is a result of higher contribution from anthropogenic sources. In the summer season, the effect of anthropogenic sources on Ba content of aerosols remains depressed by the overwhelming contribution and dilution by the crustal sources. Oil and lubricant burnings are the dominant sources of Ba emission in the atmosphere (Morawska and Zang, 2001;

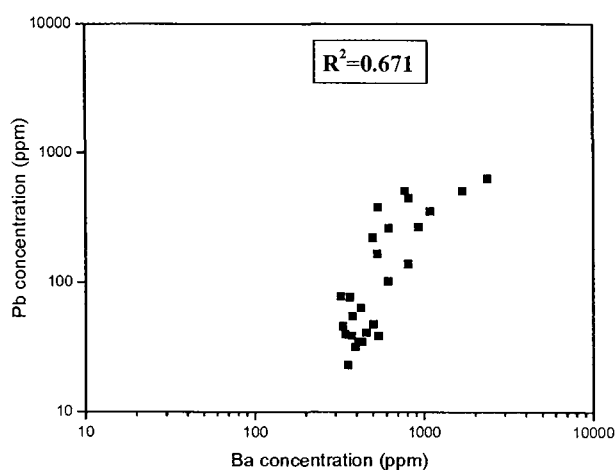


Figure 5.3 Scatter diagram showing correlation between Pb and Ba in our sample population.

($r^2= 0.67$: Fig. 5.3) suggests that Ba is also contributed by the emission sources such as vehicular exhaust which releases Pb to the aerosols. The common anthropogenic sources for Ba and Pb have also been observed elsewhere in the world (Morawska and Zang, 2001; Singh et al., 2002). Unlike Ba, Sr shows no anthropogenic addition and is largely crustally derived. The site dependency and lowering of Sr content in winter compared to summer aerosols is probably due to the dilution effect of increased and variable anthropogenic component in winter samples at different sites. Vanadium is another element of crustal origin. Unlike Sr, all types

Singh et al., 2002). This region also experiences more oil burnings for warming purposes in winter due to near zero temperature conditions. The correlation between Ba and Pb contents in our

of aerosols have higher concentrations of V compared to the UCC just as the deposited sediments have. V behaves similar to Sr in winter samples.

Both Ni and Cr are enriched in aerosols at all sites in both seasons compared to UCC just as the deposited surface sediments. Both aerosols and the deposited sediments show the presence of chlorite and magnetite, the dominant host minerals for Cr and Ni. Chlorite is also observed in the loessic deposits elsewhere in the world (Pye, 1987; Chamley, 1989). The increase in Cr content from coarse to fine aerosols and the decrease in the winter samples at all sites strongly suggest that Cr is controlled by the presence of heavy minerals of crustal origin in aerosols. The variability with particle size and sampling season is probably controlled by different wind strengths in summer and winter seasons. The high wind strength during the summer season is responsible for picking up and transport of heavy minerals in all types of aerosols whereas wind strength to transport the heavy minerals drops significantly in the winter season. In spite of the decrease in the wind speed in winter we observe an increase in the Ni content of the fine aerosols SPM and PM₁₀. This suggests an anthropogenic origin for Ni in the winter season. Metal plating industry could be the dominant source for Ni in these fractions of aerosols (Nriagu and Pacyna, 1988). From the variations it appears that Cr is dominantly crustal in nature while Ni has a mixed origin just as Ba in all type of aerosols at all sites and in both season. Reheis et al. (2002) has observed the mixed origin of Ni and Cr for the dust samples from the southwestern United States.

Cu, Zn and Pb show enrichment in all types of aerosols compared to the UCC in both seasons and in surface sediments except that Zn in Bikaner and Jhunjhunu is lower than UCC. The enrichment ratio compared to UCC increases from coarse to fine aerosols for these three elements at all sites in both seasons. Among the three

elements Cu shows the highest abundance and maximum variability in terms of seasons and sites. Cu content in all types of aerosols collected in the summer season smoothly increases in the downwind direction with the highest concentration observed at Delhi. The winter samples show the maximum concentration at Bikaner, but almost similar concentrations at Delhi and Jhunjhunu. The emissions from the Khetri copper mines (60 km east of Jhunjhunu), the burning of electrical appliances and the metal plating industry are probably responsible for the enrichment of Cu by almost 2.5-3 orders of magnitude compared to UCC in the aerosol over this region (Yadav and Rajamani, 2003 a). Metal plating and waste incineration has been widely recognized as the potential contributors to global Cu budget in the atmosphere (Nriagu and Pacyna, 1988). Zn is also being added to the atmosphere by these sources. We do observe a correlation between Cu and Zn ($r^2 = 0.54$; Fig. 5.4) source in the aerosols studied here suggesting that they are also derived from some common. This must be the reason that the aerosol samples, which have higher concentration of Cu at a given site also, have higher concentration of Zn in them. Pb behaves similar to Ba in all types of aerosols except FF wherein Pb increases and Ba decreases as a function of sampling station in the downwind direction. These

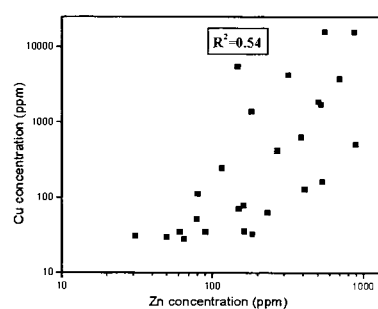


Figure 5.4 Scatter plot of Cu vs. Zn in our sample population.

two elements seem to have been derived from some common anthropogenic sources as depicted by the correlation coefficient ($r^2 = 0.67$, Fig. 5.3). The vehicular exhaust and oil burning are the common sources for Pb and Ba in aerosols on a local as well as global scale (Morawska and Zang, 2001; Singh et al., 2002). The highest traffic density at Delhi among the three sites could be dominantly responsible for higher Pb

content in aerosols at Delhi. At other locations, it could be due to the poor quality of fuel used rather than the higher number of emission sources.

5.3.3 Conclusion

From the discussion above two major sources, crustal and anthropogenic, of trace metals in aerosols are evident. The anthropogenic sources include oil burning, waste incineration, mining and metal industry, and biomass burnings. The crustal sources contribute to all size fractions of aerosols at all sites in both seasons. Among anthropogenic sources oil burning, waste incineration and metal plating industry contribute to SPM and PM₁₀ fractions; metal plating can also contribute to FF samples. Biomass burning contributes exclusively to less than 10 µm fraction only as indicated by higher K content in the fine fraction of these aerosol (Yadav and Rajamani, 2003 b). Interestingly, the trace element chemistry of aerosols is dominantly controlled by the multiplicity of sources, which contribute differently to different size fractions. Therefore, the relative proportion of crustal and anthropogenic inputs to the aerosols are governed by wind speed and direction over the sampling area. Higher the wind strength more will be the crustal contribution; low wind condition will lead to more input from anthropogenic sources. Among the elements studied here Sr, V and Cr are dominantly of crustal origin in all size fractions; summer-winter variability are caused by local wind conditions and the dilution effect of anthropogenic component. Ba is crustal in nature in summer samples only; it is more of anthropogenic nature in winter samples, particularly in SPM and PM₁₀ aerosols. For the finer fraction Ba behaves similar to Pb in both seasons and at all sites. Ni has a mixed origin from crustal and anthropogenic sources. The abundance is controlled by crustal sources in summer season while anthropogenic contribution appears in winter for Ni, a feature similar to Ba. Cu, Zn and Pb are dominantly of

anthropogenic origin in all type of aerosols in both seasons and at all sites. Cu and Zn, and Pb and Ba, respectively, are derived from similar anthropogenic sources, respectively, in this region.

The increased level of these metals in the aerosol compared to the UCC is a serious cause of concern for the environment and the life system. The metals once emitted to the atmosphere settle back to soil and water surface from where it enters into the food chain through plant uptake. Although Cu and Zn are essential micronutrients for the plants, the existing levels of their concentration in the atmosphere will definitely cause a significant increase in the metal content in the soil after deposition (Nriagu, 1988; Kelly et al., 1996). The higher metal content in PM₁₀ aerosols (inhalable aerosols) would directly affect the living organisms through breathing. Ba can cause difficulty in breathing, changes in heart rhythm and blood pressure. Cu can cause headache and irritation to nose, mouth and eye beyond a limit of 0.1 µg/m³ in air (ATSDR 1999). Pb affects almost every organ and system in our body at a level more than 1.5 µg/m³ of the air. The central nervous system is most sensitive to Pb in the body system.

5.4 ENVIRONMENTAL CONSEQUENCES

To understand the effect of atmospheric dry deposition on the soil surface, dry accumulation rates (mg / m²/ day) of trace metals (Br, Sr, Ni, Cr, Pb, Cu, Zn and V) are calculated on a diurnal basis for summer and winter seasons (Tab. 5.4). The atmospheric deposition rates of these show both season and site dependency. The observed variations are shown graphically in figure 5.5. The summer accumulation rates of trace metals are significantly higher than that observed in the winter just as the dry deposition flux. The metal deposition rate decreases along the wind trajectory

Table 5.4 (A) Bulk free fall as well as the trace metal accumulation rates in mg/m²/day on soil/ water surface in NW India; (B) Trace element abundance in surface sediments and the projected percent increase in soil metal contents in next 20 years[#].

(A)

	Bikaner		Jhunjhunu		Delhi		Garhmuktesar	PRD, China ^{\$}	
	Summer	Winter	Summer	Winter	Summer	Winter	Winter	Summer	Winter
BAR*	9.6	0.47	3.3	0.412	1.2	0.318	0.480		
Ba	3.494	0.161	1.282	0.150	0.618	0.169	0.155		
Sr	1.766	0.125	0.660	0.105	0.354	0.081	0.057		
Ni	0.423	0.029	0.130	0.019	0.083	0.019	0.025		
Cr	0.756	0.036	0.234	0.029	0.118	0.039	0.040	11.6-80.5	4.6-22.4
Cu	0.196	0.017	0.092	0.030	0.073	0.041	0.038	43-195	6.3-52.6
V	0.695	0.028	0.195	0.024	0.107	0.025	0.014		
Zn	0.537	0.077	0.212	0.062	0.200	0.129	0.078	159-656	45-454
Pb	0.334	0.019	0.121	0.032	0.273	0.121	0.038	7.25-73.9	5.97-58.6

(B)

	Bikaner		Jhunjhunu		Delhi	
	S. Sed.	%increase	S. Sed.	%increase	S. Sed.	%increase
Ba	356	3.296	361	3.041	376	3.291
Sr	177	5.137	167	4.610	200	2.960
Ni	28.1	7.448	60	2.306	71	1.949
Cr	33.9	7.793	81	2.636	129	2.231
Cu	16.5	7.548	28.4	7.625	35	8.622
V	72	2.797	79.4	2.235	70	2.620
Zn	18	31.070	65	6.941	90	10.498
Pb	22	6.238	35	6.703	55	16.039

PRL- Pearl river delta, china; \$ - data from Wong et al., 2003 for comparison.

* Bulk accumulation rates; S. Sed.- Surface sediments.

Percent increase is calculated for the top 0-5 cm soil, assuming metal accumulation rates equivalent to that of winter season continues for next 20 yrs at respective sites and the soil density equal to 2000 kg/m³ at all sites.

from Bikaner to Delhi in summer for all elements except Pb. Pb shows enhanced levels of deposition at Delhi comparable to that observed at Bikaner. The high traffic density at Delhi and poor quality fuel at Bikaner could be the possible source of higher Pb emissions at these locations compared to Jhunjhunu a small town located in the desert margin area. The overall higher rates for all elements (in summer compared to winter at all sites) are due to the higher bulk accumulation rate of FF particles in summer rather than due to any specific source in the upwind region in summer. The prevailing SW-W winds causing dust storms in the upwind regions are responsible for such increase in the bulk as well as elemental accumulation rates, which subsequently

decreases in the downwind direction just as wind strength decreases from the west to the east.

The accumulation rates of these metals are significantly lower in the winter season compared to that in summer. Unlike in the summer season, rates do not decrease regularly from Bikaner to Delhi in winter, but show site dependency. Ba accumulation rates remain almost unchanged for all locations; Sr decreases from Bikaner to Delhi. Similar Ni rates are observed at Jhunjhunu and Delhi which are lower than the other two sites. Chromium deposits at similar rates at all sites except at the lower rate observed at Jhunjhunu. The other group of trace elements Cu, Zn, Pb and V show a regular increase from Bikaner to Delhi and decrease at Garhmuktesar. Among these elements the accumulation rates vary in the order $Zn > Pb > Cu > V$ at all sites. The observed accumulation rates, and their seasonal and spatial variation points to the crustal source for Ba, Sr, Ni and Cr. Similar behavior of elements is also observed in the deposited surface sediments at these sites. The deposited surface sediments have almost similar Ba and Sr content at all sites whereas other elements show small but regular increase in the downwind direction. This probably reflects the aeolian nature of these sediments and points to the correlation between present day metal accumulation trend and the sediments deposited by such processes over a period of time. The decrease in Sr accumulation rates from Bikaner to Delhi is consistent with the decreasing wind strength and therefore, exclusively suggests a crustal source for Sr or dilution by high Ca content as Ca and Sr in the aerosols of this region show a decoupling with each other (Yadav and Rajamani, 2003b). The small spatial variability in Ni and Cr accumulation rates points to the mixed crustal as well as anthropogenic origin for these elements and are related to the local wind conditions at

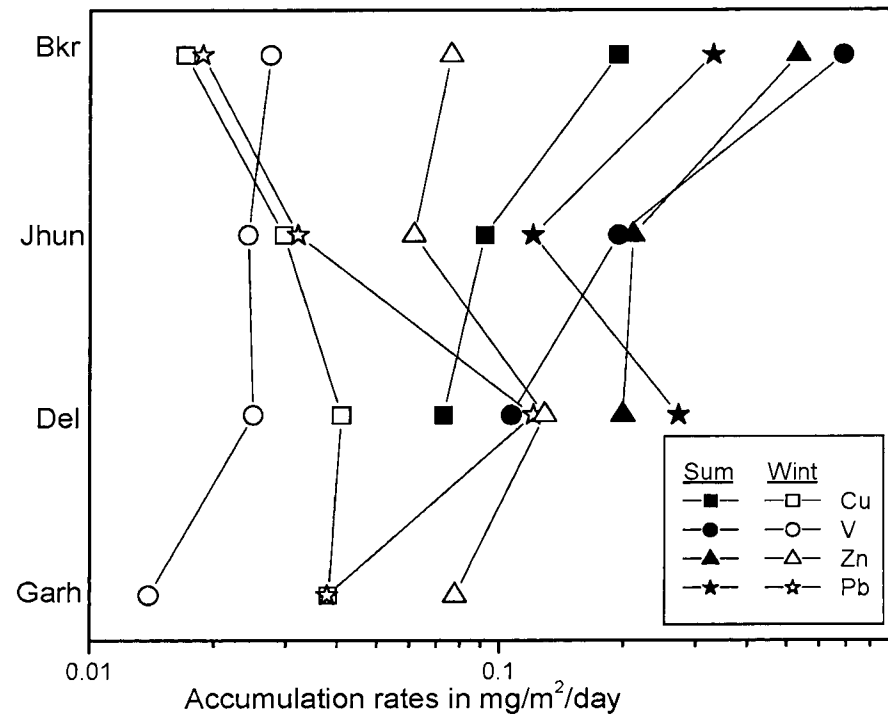
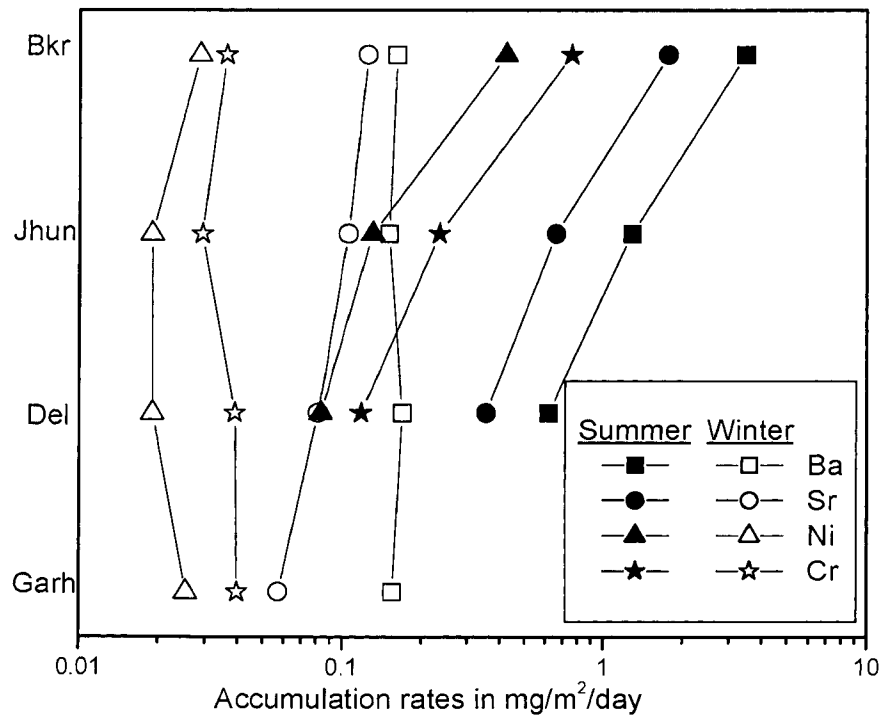


Figure 5.5 Site and seasonal variations in the accumulation rates of trace elements at Bikaner (Bkr), Jhunjhunu (Jhun), Delhi (Del) and Garhmuktesar (Garh) in NW India.

different sampling locations. The low speed and the more spatially variable winds could be responsible for such different Ni and Cr rates, through differential picking of heavy minerals hosting Ni and Cr such as magnetite at different sites in winter. Anthropogenic sources for Ni and Cr include metal plating, non-ferrous metal industry on small scale and local levels. The increment in the accumulation rates of Pb, Cu, Zn and V from Bikaner to Delhi in winter suggests the significant contribution from anthropogenic sources to these elements even under low wind conditions over this region. Pb, Cu, Zn and V show highest rates at Delhi just as it has the highest pollution emitting sources (Vehicular exhaust, waste incineration, metal plating, oil burning, non-ferrous metal industry, etc.) for these elements compared to all other sampling sites.

Vehicular exhaust and coal burning are the dominant sources of Pb, Cu and Zn, and Pb in aerosols are also contributed by the non-ferrous metal industry. Waste incineration releases Cu and Zn. Burning of electrical appliances, Khetri copper mines (60 km east of Jhunjhunu) and metal plating industry are dominantly responsible for the enhanced levels of Cu in the atmosphere in this region (Yadav & Rajamani, 2003 a). Although the anthropogenic sources are significant contributors of these toxic metals and are responsible for their enhanced levels of concentration in the atmosphere, it is unlikely that the trace metals are released to this size fraction, i.e., FF with mean size $\sim 63 \mu\text{m}$ by these sources. The surface coatings, either of fine particles directly emitted to the atmosphere or of the gaseous emissions enriched with these metals from human activities, on the coarse crustal particles could be the possible mechanism for such increment in heavy metal content of free fall aerosols. The detailed mechanism is still poorly understood and calls for further study.

Also, the probable anthropogenic sources for these metals in the atmosphere seem to be operational throughout the year and therefore, could not be responsible for seasonal variations in the dry accumulation rates of the trace metals studied with the maximum rate in summer. The seasonal variation in wind speed and direction is significant in this region. The heavy dust storms during summer contribute overwhelmingly to the total dry accumulation rate and thus to the highest metal accumulation rates in summer. In winter, wind speed and strength to pick the large crustal particle decreases significantly. This could have resulted in the relatively low bulk sample as well as metal accumulation rates in winter compared to summer, which dominantly include anthropogenic emissions. Therefore, the seasonal variations in accumulation rates are governed by the meteorological parameters, particularly the wind speed and direction in this region rather than by the emission sources.

To evaluate the long-term effect of atmospheric deposition of trace metals on the surface soil composition, annual accumulation rates and the percent increase in the metal content of soil by atmospheric deposition were calculated for the next 20 years (Table 5.4 b). The percent increase in the metal content of soil is calculated for the top fertile layer of soil (0-5cm), assuming soil density equal to 2000 Kg/m³ in this region. Among the different locations, Delhi soil will be worst affected by atmospheric deposition of these metals. For different elements studies, Delhi soil will have maximum concentration of Pb, followed by Zn and Cu in the next 20 yrs. Pb content in the topsoil (0-5cm) of Delhi is likely to increase by 16% if the accumulation rate of 0.379 mg/m²/day continues for the next 20 yrs. Zn and Cu show an enrichment of 10.4 and 8.6%, respectively, in total metal concentration of topsoil at Delhi. All other metals studied show an increase of 1-3% at all sites.

The estimated increase in metal contents (Pb, Cu, and Zn) of topsoil at Delhi in next 20 yrs is significant, but lower than that estimated for the Pearl River delta, China (Table 5.4; Wong et al., 2003). These authors also observed the seasonal variation of the accumulation rates with maximum in summer compared to winter as observed here. However, the causes of these variations are different. There is no other data available from N-NW India for comparison. The annual accumulation rates in $\text{mg/m}^2/\text{yr}$ calculated here are based on the winter dry accumulation rates of metals. The summer data were not used as they are biased due to heavy dust storms during May-June in this region. This is only an attempt to see the likely scenario after 20 yrs, if at least the low levels of atmospheric deposition equal to winter season continues for the next 20 yrs, which are even likely to increase with time and increasing industrialization. Therefore, these estimates are tentative and the minimum possible, and need to be understood through more monthly and yearly sampling. It is recommended to monitor such atmospheric processes at this stage through detailed sampling and data generation. Once the accumulated metals in the soil become a part of the ecosystem through geochemical cycling, they can impose serious environmental implications as well as threat to life system.

Aerosols: A Potential Cu Source!

6. AEROSOLS: A POTENTIAL Cu SOURCE!

Degradation of air quality, particularly in urban areas of developing countries, is one of the most alarming problems of modern civilization. Human activities today release a variety of gases and liquid/solid particles (aerosols) to the atmosphere. The cumulative effect of all these air pollutants on the climate of the earth and on the health of its life system are topics of intensive research. As a part of our research on the geochemistry of dust materials in the northwestern part of India, which witnesses frequent dust storms in summer times (Sikka, 1997), we studied the concentration of certain heavy metals such as Cu, Pb, Cr, V and Ni in three different size fractions, PM₁₀, suspended particulate matter (SPM) and dry-deposition dust. We observed abnormally high concentration of Cu in the aerosols and thought it appropriate to report this academically and economically interesting finding. We also speculate on the possible causes and consequences of this finding.

The northwestern part of India including parts of Gujarat, Rajasthan, Haryana, Punjab and western UP witnesses regular dust storms just as the rest of India witnesses summer monsoon. A lot of dust materials is transported by SW- W summer winds in the Thar desert and adjoining regions. These dust storms apparently deposited silty materials in the downwind direction, as, for example, on the quartzite ridge in the Delhi area (Tripathi and Rajamani, 1999). The deposited Delhi ridge aeolian sediments, as well as the falling dust captured in the present study are geochemically very similar to average upper continental crust (UCC; Tripathi and Rajamani, 1999; Taylor et al., 1983). In order to geochemically characterize the aerosols in different size fractions along the dominant SW-W wind trajectory, sampling sites were planned along Bikaner in Thar desert, Jhunjhunu, Delhi and east

of Delhi at Garhmuktesar located on the bank of Ganga, covering a distance of 600 km from west to east (fig.6.1). Although sampling duration was limited in all the sites along the transect because of limitations of infrastructure required for air sampling, the spacing and location of sampling sites, the type of samples collected

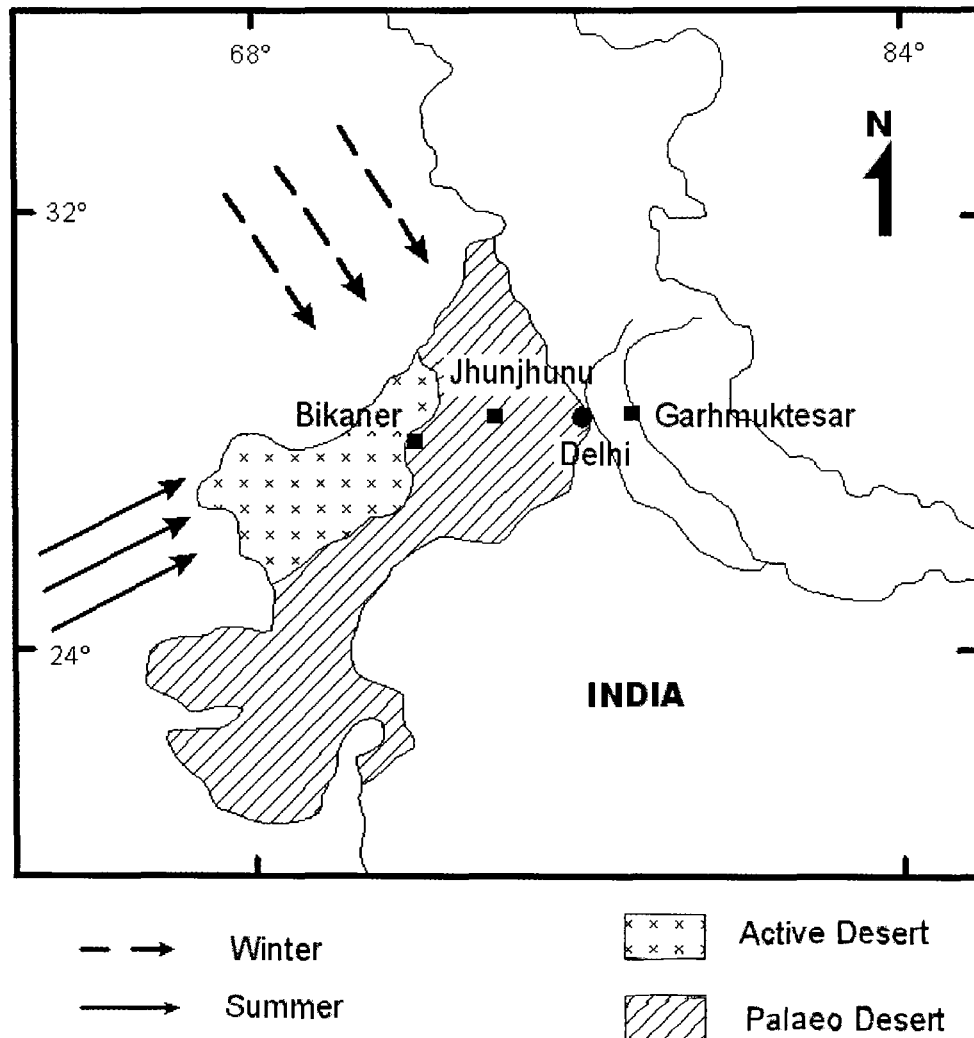


Figure 6.1 Sample locations of the present study. Map also shows the dominant wind trajectory in summer and winter months in the study area.

and the data and its quality all make the findings interesting and worth exploring further in details.

Different size fractions of aerosols were collected using different sampling techniques. Freely falling dust particles (dry deposition) were collected in all the

stations using plastic trays filled with two layers of glass marble balls kept at a height of 20 meters from the ground level. The second type of samples includes the suspended particulate matter (SPM, with a size range of 0.1-100 μm). This size fraction was collected using high volume air samplers, model PEM HVS-1 (Polltech instruments) fitted with EPM 2000 glass micro fiber kept at a height of 20 meters from the ground level. The airflow was kept at an average rate of 1.2 lit/min. Sampling simultaneously at all sites, was done for a few days between 19-26th May, 2000 and 17-27th Jan 2001. Because the filter papers got choked within a period of 24 hrs or less, we could collect different samples for the same size fraction from a given site and this enabled us to see the variability of aerosol chemistry in a matter of few days. A similar procedure was adopted for the finest size fraction PM_{10} (<10 μm in size) using the high volume air samplers, model PEM HVF-1 (Polltech instruments) kept at the same height at a constant flow rate of 1.2 lit/min. At each site we have also collected surface sediments which were used as reference materials. The two finer types of aerosols SPM and PM_{10} collected on glass micro fiber filter papers were in dry powder form and therefore were easily scrapped off the filters. These powders as well as powdered dry-deposition samples and deposited surface sediments (-200 mesh size) were digested in open beakers using a combination of $\text{HF}+\text{HNO}_3+\text{HClO}_4$. These solutions were analyzed for copper using a Labtam 8440 ICP-AES at a wavelength of 324.754 nm using international and laboratory internal standards. The precision and accuracy of our analysis were better than 4% and 2%, respectively.

At each sampling site and for each season, 5-7 samples of each size fraction were collected as constrained by the sampling process. Minimum and maximum concentrations of Cu during the sampling period at each site for each size fraction is presented in table-6.1. The weighted mean concentration for each size fraction is

given as average concentration (obtained by the sum of weight fraction of each sample and multiplied by its concentration). Because the number of samples in each fraction is small and the variation in Cu concentration is large, geometric mean and geometric standard deviation were calculated for PM₁₀, SPM and dry deposition and are given in table 6.1. In figure 6.2, we show the variation of Cu concentration as a

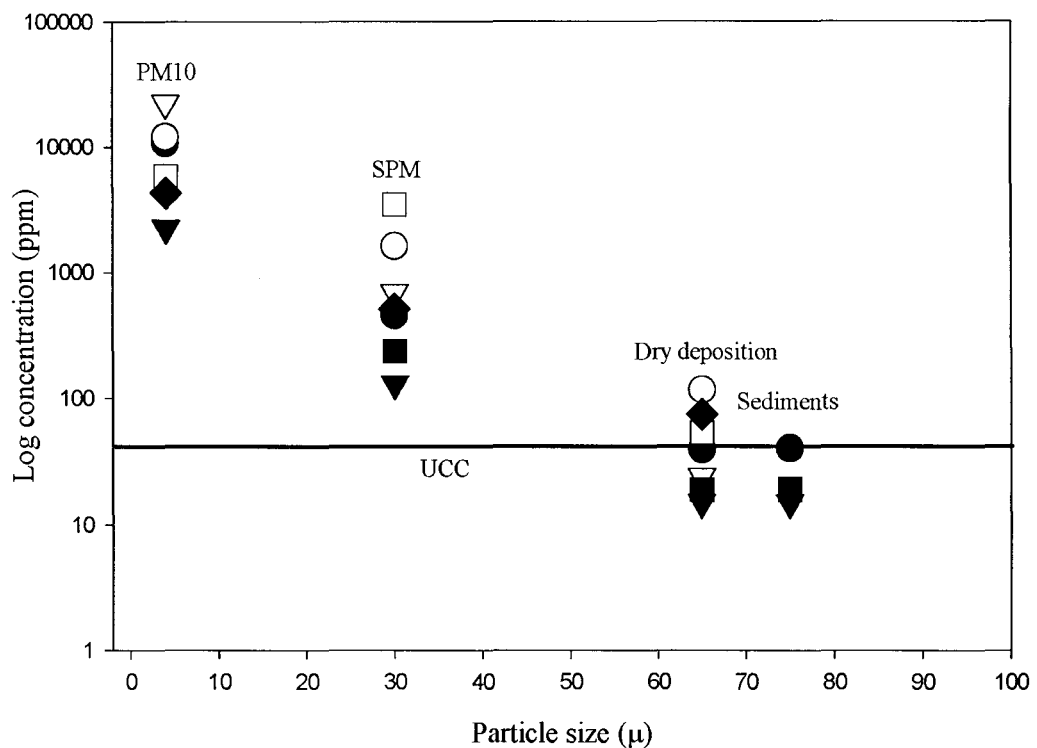


Figure 6.2 Dependency of Cu concentration on the particle size of aerosols in NW India. Open and filled symbols represent summer and winter samples. Bikaner: ▽, Jhunjhunu: □, Delhi: O, Garhmuktesar: ◇.

function of mean particle size of different size fractions. Summer and winter samples collected from different sites are also distinguished. Also Cu concentration in deposited sediments as well as the average Cu in the upper continental crust (UCC of Taylor et al., 1983) are shown. We could infer several features from the plot in figure 6.2. First, the PM₁₀ size fraction everywhere has the highest Cu concentration relative

Table 6.1 Cu concentration (ppm) in the aerosol samples of NW India (values in parentheses are in $\mu\text{g}/\text{m}^3$ of air).

PM₁₀ (<10 μm size aerosols)

	Bikaner		Jhunjhunu		Delhi		Garhmuktesar	
	summer	winter	summer	Winter	Summer	Winter	Summer	Winter
Range (max.-minim.)	1251-4100 (1.653-3.636)		5225-5760 (3.92-5.28)	1216-28000 (.348-7.084)	8437-13000 (2.9-5.33)	5160-28072 (1.37-6.84)	-	-
Average conc.	1862 (3.2831)	22394 (3.784)	5540.5 (4.7271)	15816 (4.0202)	11408 (4.165)	15762 (3.906)	-	4260 (.8008)
Geometric mean	2232 (2.8129)		5486 (4.55)	5835 (1.572)	10655 (3.688)	12035 (3.0661)	-	-
Geometric Std Deviation	1586 (.8873)		378 (.959739)	22614 (5.69085)	2298 (1.3196)	17449 (4.1452)	-	-

SPM (0.1-100 μm size aerosols)

	Bikaner		Jhunjhunu		Delhi		Garhmuktesar	
	summer	winter	summer	Winter	summer	Winter	Summer	Winter
Range (max.-minim.)	53-400 (.3269-1.739)	548-563 (.1304-1329)	205-276 (.334-5906)	2511-4725 (.53-.95)	206-677 (.1435-.4536)	1319-1896 (.1424-.491)	-	493-531 (.117-1348)
Average conc.	105 (.872)	643 (.13115)	250 (.4805)	3741 (.7694)	425 (.31548)	1733 (.3928)	-	513 (.1268)
Geometric mean	130.4 (.7878)	688 (.13165)	238 (.4442)	3445 (.7146)	417 (.2730)	1581 (.2645)	-	511.65 (.1246)
Geometric Std Deviation	164 (1.994)	224 (.001752)	50.32 (.18232)	1585 (.30502)	199 (.221688)	410 (.25735)	-	29 (.01229)

Dry Deposition samples (mean size between 60-80 μm)

	Bikaner		Jhunjhunu		Delhi		Garhmuktesar	
	summer	winter	summer	Winter	summer	Winter	Summer	Winter
Range (max.-minim.)	11.1-20.3	-	13-26.7	-	34.4-45.4	116	-	-
Geometric mean	15	24	18.6	53	40	-	-	74
Geometric Std Deviation	6.58	-	9.85	-	7.78	-	-	-
Reference material (local sediments)	19		30		35		-	

to the other size fractions. A general decrease in Cu concentration with increasing particle size diameter is observed. Also samples collected during winter have higher Cu concentrations relative to the summer samples. Site dependency of Cu concentration does not appear to be very significant, although a small variation is seen from Bikaner to Delhi, particularly in the winter season. Finally, the deposited surface sediments have the lowest concentration of Cu, even lower than that in the average UCC.

All the aerosol samples particularly PM_{10} and SPM show very significant enrichment of Cu relative to UCC. This suggests a non-crustal source of Cu to the aerosols. This is also supported by the size dependency of Cu concentration in aerosols. It is well known that anthropogenically generated heavy metals in atmospheric aerosols are commonly enriched in the finest fraction (Al-Rajhi et al., 1996). Crustal sources to aerosols/sediments are commonly coarser grained and should have the crustal level concentration of various elements. Surface sediments and samples of dry deposition represent such a crustal component. The observed enrichment of Cu in the finest fraction, PM_{10} , is a combined effect of high Cu content in aerosols of anthropogenic origin and lack of dilution by the crustal component. As the grain size of the aerosols increases the relative contribution of anthropogenic component decreases. Also because on an average, wind velocity is much reduced during the wintertime, the dilution effect by coarser crustal component is minimal in the winter season. Greater stability and poorer dispersion of pollutants due to local temperature inversions observed over Indian cities (Murthy, 1984) are also responsible for the winter maxima in the Cu concentration of anthropogenic aerosols. Thus the observed concentration of Cu and its variation in different samples point to an anthropogenic source of Cu in aerosols in the north-west parts of India.

In the present study, the sampling site Jhunjhunu is located 60 kms west of the Cu mining township of Khetri. However we did not observe any exceptionally high concentration in Jhunjhunu samples, nor did we observe the lowest concentration in the Bikaner samples, as this site is located in the upwind direction. Therefore a large part of Cu in these aerosols is likely unrelated to Cu mining or smelting activity. It is very tempting to suggest that the major contributor to the Cu in aerosols in this region could be electric power sector, including power transmission, power consumption and all the materials/ appliances associated with this human activity. Surprisingly we also observe high concentration in Bikaner samples, although relatively lower concentration compared to the other sites. Unfortunately, we do not know what is the relative contribution from local sources and from the cities located in the upwind direction (Karachi in summer time air back trajectory and Islamabad in winter time air back trajectory). Some high concentrations of Cu in SPM samples are reported from Kanpur (Sharma et al., 1983); however, at Jaipur, Mumbai, Nagpur, Bangalore and Agra (Negi et al., 1987; Sadasivan and Negi, 1990; Kulshrestha et al., 1994) reported Cu concentrations in SPM samples are lower than the present study. Observed Cu concentration in PM₁₀ here on an average is the highest reported so far in India. High concentrations of Cu ($\sim 3\mu\text{g}/\text{m}^3$) in PM₁₀, similar to observed here, was reported near a Cu mining area in Chile (Romo-Kroger et al., 1994) but not so high as observed here. This also supports our thinking that the anthropogenic source of Cu in the aerosols of NW India could be dominantly the power sector- production, transmission and consumption. On a global scale, Cu takes only the fourth position among Pb, Zn, Ni and Cu in terms of atmospheric emission from anthropogenic sources (Nriagu and Pacyna, 1988). However, in the present study we observed that Cu is the most abundant among the four trace metals in the aerosols. It is possible that this high

levels of abundance of Cu could be related to its chemical affinity to organic phases (Fergusson and Kim, 1991) present in large amounts in the atmosphere of this region (the so called Asian Brown Cloud; Srinivasan and Gadgil, 2002), in addition to its anthropogenic emission.

The PM₁₀ dust samples studied have an average of 6000 and 15000 ppm concentration of Cu in the summer and winter time, respectively. This level of concentration, nearly 1.5 % Cu in the aerosols, suggests that they are better than Cu ores in terms of Cu content (any rock containing >0.5% Cu is a potential Cu ore today). The economics of Cu recovery from the aerosols need to be understood. Similarly environmental and health consequences of such high Cu concentration in the air need to be investigated. Although Cu is an essential nutrient required by plants and animals in very small amounts, the observed levels of Cu concentration in the respirable fraction of aerosols i.e. PM₁₀ could cause gastrointestinal disturbances including nausea, vomiting and liver or kidney damage depending on exposure time. We need to generate a sound scientific knowledge of causes and consequences of heavy metal concentration in aerosols at a local, regional and global level for better policy options of development and environment.

Conclusions

7. CONCLUSIONS

Different size fractions of aerosols (FF, SPM, PM₁₀ and >10µm) as well as the surface sediment samples, collected from Bikaner, Jhunjhunu, Delhi and Garhmuktesar, situated along the dominant S-SW wind trajectory for about 600 km were characterized for their texture, mineralogy and geochemistry including REE and Sr isotopes. The minor conclusions drawn from this study are given in the previous chapters of this thesis. Some of the major and important findings of the present work on "*Aerosol Geochemistry*" are given here.

1. The geochemical nature of aerosols is as a function of source (s), wind strength (speed and direction), particle size, and sampling site and season. The aerosols are generated from two dominant sources, crustal and anthropogenic. The crustal materials themselves have two components, the Thar silicate sediments derived from the Himalayas and the non silicate, such as, soil carbonates in the Thar sediments and the dry lakebeds in the desert regions. The anthropogenic sources again include contributions from vehicular exhaust, oil/coal combustion, metal and mining industry, and biomass burnings.
2. Geochemical coherence among aerosols, deposited surface sediments and the Thar sands, and the limited Sr isotopic data indicate that the Thar sediments and certain lithotectonic units of the Himalayan orogen are the proximal and distal crustal sources, respectively, for the aerosols in this region. Prevailing aridity and strong summer winds, and the presence of river alluvium in the Thar act together to transport silt rich dust, the removal of which could be a possible mechanism of the ongoing desertification.

3. The different sources identified contribute differently to the chemistry of different fractions of aerosols for the different elements and in different seasons. Whereas crustal sources are dominant in all the size grades, anthropogenic components show up in the finer fractions; metal and mining industry to size fractions \leq free fall aerosols, coal/oil combustion and vehicular exhaust to particles of size \leq suspended particulate matter, and biomass burnings to fractions \leq PM_{10} . The crustal components are somewhat diluted by the anthropogenic inputs in the finer fractions, particularly in the winter season and vice versa happens in the summer season.
4. The wind strength (speed and direction) acts as an intensive variable in deciding the chemistry of aerosols. Strong winds make the crustal component a very large part of the aerosols and therefore, result in the very homogeneous and uniform chemistry in different fractions of aerosols in different regions. During periods of low wind strength, the aerosols become heterogeneous in their chemistry, particularly in that of the trace elements which have been contributed by the anthropogenic sources and in the winter season. Wind strength also indirectly controls the trace element chemistry of the crustal component in aerosols through differential lifting, transportation and deposition of the heavy minerals hosting the trace elements present in the silicate sediments.
5. The observed aerosol chemistry has both positive and negative impact on the environment. The dominant crustal component would buffer the rain water pH by providing cation rich aerosols. Presence of some of the nutrient cations such as Ca, K and Mg in aerosols may be responsible for the enhanced or at least self sustained fertility of the soil system in the down wind region and for the removal

of fertility in the upwind region. The high levels of accumulation of some of the toxic trace elements such as Ba, Pb, Zn, Ni and Cu in the soils of the semi-arid and monsoonal climatic regions of N-NW India may get into the water and soil systems which are detrimental to terrestrial and aquatic life systems.

References

REFERENCES

- Abbey S., Aslin G. E. M. and Lachances G. R (1977) Recent developments in silicate rocks and minerals. *Rev. Analyt. Chem.* **III**, 181-248.
- Ackerman S. A. (1997) Remote sensing aerosols using satellite infrared observations. *J. Geophys. Res.* **102**, 17069-17079.
- Ackerman S. A. and Cox S. K. (1989) Surface weather observations of atmospheric dust over the southwest summer monsoon region. *Meteorol. Atmos. Phys.* **41**, 19-34.
- Adler K. B. and Fischer B. M. (1994) Interaction between respiratory epithelial cells and cytokines: relationships to lung inflammation. *Annals New York Acad. Sci.* **725**, 128-145.
- Allen A. G., Nemitz E., Shi J. P., Harrison R. M. and Greenwood J. C. (2001) Size distributions of trace metals in atmospheric aerosols in the United Kingdom. *Atm. Environ.* **35**, 4581-4591.
- Al-Rajhi M. A., Al-Shayeb S.M., Seowarad M. R. D. and Edwards H. G. M. (1996) Particle size effect for metal pollution analysis of atmospherically deposited dust. *Atmos. Environ.* **30**, 145.
- Andreae M. O. (1983) Soot carbon and excess fine potassium: Long-range transport of combustion-derived aerosols. *Sci.* **220**, 1148-1151.
- Andreae M. O. (1995) Future climate of the world: A modeling perspective. In: World Survey and Climatology, Henderson S. A. eds. 16, Elsevier.
- Andreae M. O., Charlson R. J., Bruynseels F., Storms H., Grieken R. Van and Maenhaut W. (1986) Internal mixture of sea salt, silicate and excess sulfate in marine aerosols. *Sci.* **232**, 1620-1623.
- Applin K. R. and Jersak J. M. (1986) Effect of airborne particulate matter on the acidity of precipitation in central Missouri. *Atmos. Environ.* **20** (5), 965-969.
- Arimoto R., Duce R. A., Ray B. J., Ellis Jr., W. G., Cullen J. D. and Merrill J. T. (1995) Trace elements in the atmosphere over the North Atlantic. *J. Geophys. Res.* **100**, 1199-1214.
- Arimoto R., Duce R. A., Savoie D. L., Prospero J. M., Talbot R., Cullen J. D., Tomza U., Lewis N. F. and Ray B. J. (1996) Relationships among aerosols constituents from Asia and the North Pacific during PEM-West. *J. Geophys. Res.* **101**, 2011-2024.
- ATSDR (1999) Toxicological profiles for lead, barium and copper. U.S. Department of health and human services, Public health services Atlanta, GA.

- Birkland P. W. (1974) *Pedology, Weathering and Geomorphological research*, Oxford university press, London.
- Broecker W. S. (2000) Abrupt climate change: causal constraints provided by the paleoclimate record. *Earth Sci. Rev.* **51**, 137-154.
- Brooks N. and Legrand M. (2000) Dust variability over northern Africa and rainfall in the Sahel. In: *Linking land surface change to climate change*, S. J. Mc Laren and D. Kniverton, eds., Kulwer Acad., Norwell Mass, 1-27.
- Buseck P. R. and Posfai M. (1999) Airborne minerals and related aerosol particles: effects on climate and environment. *Proc. Natl. Acad. Sci. USA* **96**, 3372-3379.
- Carroll D. (1970) Clay minerals: A guide to their X-ray identification. Special Paper 126, *Geol. Soc. America*, Boulder, Colorado, pp 80.
- Chamley H. (1989) *Clay sedimentology*, Springer Verlag, Berlin, pp. 623.
- Chan Y. C., Vowles P. D., McTainsh G. H., Simpson R. W., Cohen D. D., Bailey G. M. and McOrist G. D. (2000) Characterisation and source identification of PM₁₀ aerosol samples collected with a high volume cascade impactor in Brisbane (Australia). *The Sci. Tot. Environ.* **262**, 5-19.
- Chen W., Fryrear D. W. and Yang Z. (1999) Dust fall in the Takla Makan desert of China. *Phys. Geogr.* **20**, 189-224.
- Chesworth W. (1982) Late Cenozoic geology and the second oldest profession. *Geosci. Canada* **9**, 54-61.
- Chibbar R. K. (1985) Soils of Delhi and their management. In: *Soils of India and their management*, B. C. Biswas, D. S. Yadav and S. Maheshwari, eds., Fertiliser Assoc. of India, New-Delhi, 72-86.
- Choi J. C., Lee M., Chun Y., Kim J. and Oh S. (2001) Chemical composition and source signature of spring aerosol in Seoul, Korea. *J. Geophys. Res.* **106(D16)**, 18067-18074.
- Choudhary A. K., Gopalan K. and Sastry C. A. (1984) Present status of geochronology of the Precambrian rocks of Rajasthan. *Tectonophysics* **105**, 131-140.
- Chun Y., Boo K., Kim J., Park S. and Lee M. (2001) Synopsis, transport, and physical characteristics of Asian dust in Korea. *J. Geophys. Res.* **106(D16)**, 18,461-18,469.
- Cooper J. A. (1980) Environmental impact of residential wood combustion emissions and its implications. *J. Air Poll. Control. Asses.* **30**, 855-861.
- CPCB (2002) National ambient air quality standards on the website http://envfor.nic.in/cpcb/aaq/aaq_std.html.

- Darzi M. and Winchester J. W. (1982) Aerosol characteristics at Mauna Loa observatory, Hawaii, after East Asian dust storm episode. *J. Geophys. Res.* **88**, 5321-42.
- DasGupta S. K. (1975) A revision of Mesozoic Tertiary stratigraphy of Jaisalmer basin, Rajasthan, India. *Earth Sci.* **2** (1).
- Dentener F. J., Carmichael G. R., Zhang Y., Lelieveld J. and Crutzen P. J. (1996) Role of mineral aerosol as a reactive surface in the global troposphere. *J. Geophys. Res.* **101**, 22869-22889.
- Dhir R. P. (1977) Western Rajasthan soils. In: Desertification and its control, P. L. Jaiswal, eds, I.C.A. R., New Delhi, 102-115.
- Dickerson R. R., Kondragunta S., Stenchikov G., Civerolo K. L., Doddridge B.G. and Holben B.N. (1997) The impact of aerosols on solar ultraviolet radiation and photochemical smog. *Sci.* **278**, 827-830.
- DiTullio G. R., Hutchins D. A. and Bruland K. W. (1993) Interaction of iron and major nutrients controls phytoplankton growth and species composition in the tropical North Pacific Ocean. *Limnol. Oceanogr.* **38**, 495-508.
- Dockery D. and Pope A. (1996) Epidemiology of acute health effects: summary of time-series studies. In: Particles in our air: Concentration and health effects, Wilson R. and Spengler J. D., eds., Harvard university press, Cambridge, MA, USA, 123-147.
- Dockery D., Pope C. A., Xiping X., Spengler J., Ware J., Fay M., Ferris B. and Spiezer F. (1993) An association between air pollution and mortality in six U. S. cities. *New England J. Med.* **329**(24), 1753-59.
- Donaghay P. L., Liss P. S., Duce R. A., Kester D. R., Hanson A. K., Villareal T., Tindale N. W. and Gifford D. G. (1991) The role of episodic atmospheric nutrient inputs in the chemical and biological dynamics oceanic ecosystems. *Oceanogr.* **4**, 62-70.
- Drees L. R., Manu A. and Wilding L. P. (1993) Characteristics of aeolian dust in Niger, West Africa. *Geoderma* **59**, 213-233.
- Duce R. A. (1995) Sources, distributions, and fluxes of mineral aerosols and their relationship to climate. In Dahlem Workshop on Aerosol Forcing of Climate, Charlson R. J. and Heintzenberg J., eds, John Wiley, New York, 43-72.
- Duce R. A., Unni C. K., Ray B. J., Prospero J. M. and Merrill J. T. (1980) Long range transport of soil dust from Asia to the tropical north Pacific: Temporal variability. *Sci.* **209**, 522-524.
- Economic Survey of Delhi (2002) Government of National Capital Territory, Delhi.
- European Community (1992) European Community Deskbook. Washington, D. C.: *Environ. Law Institute.*

- Falkowski P. G., Barber R. T. and Smetacek V. (1998) Biogeochemical controls and feedbacks on ocean primary production. *Sci.* **281**, 200-206.
- Fedo C. M., Nesbitt H. W. and Young G. M. (1995) Unraveling the effects of potassium metasomatism in the sedimentary rocks and paleosols, with implications for paleoweathering conditions and provenance. *Geol.* **23**, 921-924.
- Fedo C. M., Eriksson K. A. and Krogstad E. J. (1996) Geochemistry of shales from the Archean (~3.0 Ga) Buhwa Greenstone Belt, Zimbabwe: Implication for provenance and source-area weathering. *Geochim. Cosmochim. Acta* **60**, 1751-63.
- Feng Q., Endo K. N. and Cheng G. D. (2002) Dust storms in china: a case study of dust storm variation and dust characteristics. *Bull. Eng. Geol. Environ.* **61**, 253-261.
- Fergusson J. E. and Kim N. D. (1991) Trace elements in street and house dusts: Sources and speciation. *The Sci. Tot. Environ.* **100**, 125-150.
- Fung I., Meyn S., Tegan I., Doney S. C., John J. and Bishop J. K. B. (2000) Iron supply and demand in the upper ocean. *Global Biogeochem. Cyc.* **14**, 281-296.
- Gale S. J. and Hoare P. G. (1991) Quaternary Sediments—Petrographic methods for the study of unlithified rocks, eds, Belhaven Press, London, pp 323.
- Galloway J. N., Thornton J. D., Norton S. A., Volchok H. and McLean R. A. N. (1982) Trace metals in atmospheric deposition: a review and assessment. *Atmos. Environ.* **16**, 1677-1700.
- Gao Y., Kaufman Y. J., Tanre D., Kolber D. and Falkowski P. G. (2001) Seasonal distribution of aeolian iron flux to global ocean. *Geophys. Res. Lett.* **28**, 29-32.
- Gardner I. R. (1972) Origin of the Mormon Misa caliche, Clark County, Nevada. *Geo. Soc. Am. Bull.* **83**, 143-156.
- Gillette D. A. and Sinclair P. C. (1990) Estimation of suspension of alkaline material by dust devils in the United States. *Atmos. Environ.* **24A**, 1135-1142.
- Gillette D. A. (1981) Production of dust that may be carried great distance. In: Desert Dust: Origin, Characteristics, and Effect on Man, Pewe T. L., eds., *Spec. Pap. Geol. Soc. Am.* **86**, 11-26.
- Gillette D. A. (1999) A qualitative geophysical explanation for “hot spot” dust emitting source regions. *Contrib. Atmos. Phys.* **72**, 67-77
- Ginoux P., Chin M., Tegen I., Prospero J. M., Holben B., Dubovik O. and Lin S. -J. (2001) Sources and distribution of dust aerosols simulated with the GOCART model. *J. Geophys. Res.* **106**, 20255-20274.
- Goossens D. and Offer Z. Y. (1994) An evaluation of the efficiency of some eolian dust collectors. *Soil Techn.* **7**, 25-35.

- Goossens D., Gross J. and Spaan W. (2001) Aeolian dust dynamics in agricultural land areas in lower Saxony, Germany. *Earth Surf. Proc. Landforms*. **26**, 701-720.
- Goudie A. S. (1983) Dust storms in space and time. *Prog. Phys. Geogr.* **7**, 502-530.
- Goudie A. S. and Middleton N. J. (1992) The changing frequency of dust storms through time. *Clim. Change* **20**, 197-225.
- Griffin G. M. (1971) Interpretation of X-ray diffraction data. In Procedures in sedimentary petrology, Carver R. E., ed., John Wiley, New York, 641-659.
- Grousset F. E., Biscaye P. E., Revel M., Petit J-R, Pye K., Joussaume S. and Jouzel J. (1992) Antarctic (Dome C.) ice core dust at 18 k. y. B. P.: isotopic constraints on origins. *Earth Planet. Sci. Lett.* **111**, 175-182.
- Gupta S. N., Arora Y. K., Mathur R. K., Iqballuddin, Prasad B., Sahay T. N. and Sharma S. B. (1980) Lithostratigraphic map of Aravali region, southern Rajasthan and northeastern Gujarat. *Geol. Surv. India*.
- Guerzoni S. and Chester R. (1996) The impact of desert dust across the Mediterranean, eds, Kluwer Acad., Norwell Mass, 389-402.
- Handa B. K., Kumar A. and Goel D. K. (1982) Chemical composition of rainwater over Lucknow in 1980. *Mausam* **33**, 485-488.
- Harrison S. M. (1986) Nitrogen and sulphur compounds. In Handbook of air pollution analysis, Harrison R. M. and Perry R. eds., Chapman and Hall, 2nd ed., London.
- Harrison S. P., Kohfeld K. E., Roelandt C. and Claquin T. (2001) The role of dust in climate changes today, at the Last Glacial Maximum and in the future. *Earth Sci. Rev.* **54**, 43-80.
- Haywood J. and Boucher O. (2000) Estimates of the direct and indirect radiative forcing due to tropospheric aerosols. *Rev. Geophys.* **38**, 513-543.
- Hedin L. O. and Likens G. E. (1996) Atmospheric dust and acid rain. *Sci. Am. Dec.* 88-92.
- Herman J. R. and Celarier E. A. (1997) Earth surface reflectivity climatology at 340-380 nm from TOMS data. *J. Geophys. Res.* **102**, 28003-28012.
- Heron A. M. (1936) Synopsis of the pre-Vindhyan geology of Rajputana. *Trans. Nat. Inst. Sci. India* **1(2)**, 17-33.
- Heron A. M. (1953) The geology of central Rajputana. *Mem. Geol. Surv. India* **79**, pp 389.
- Herwitz S. R., Muhs D. R., Prospero J. M., Mahan S. and Vaughn B. (1996) Origin of Bermuda's clay rich quaternary paleosols and their paleoclimatic significance. *J. Geophys. Res.* **101**, 23389-23400.

- Hileman B. (1981) Particulate matter: the inevitable variety. *Environ. Sci. Tech.* **15**, 983-986.
- Hlavay J., Polyak K. and Wesemann G. (1992) Particle size distribution of mineral phases and metals in dusts collected at different workplaces. *Fresenius J. Anal. Chem.* **344**, 319-321.
- Husar R. B., Prospero J. M. and Stowe L. L. (1997) Characterisation of tropospheric aerosols over the oceans with the NOAA advanced very high resolution radiometer optical thickness operational product. *J. Geophys. Res.* **102**, 16889-16909.
- Igarashi Y., Aoyama M., Hirose K., Miyao T. and Yabuki S. (2001) Is it possible to use ^{90}Sr and ^{137}Cs as tracers for the Aeolian dust transport? *Water, Air, and Soil Poll.* **130**, 349-354.
- International Panel on Climate Change (IPCC) Climate Change 1994, J. T. Houghton et. al., eds., Camb. Univ. Press, New York, 1995.
- IPCC (1995) IPCC second assessment report: climate change. *IPCC, Geneva, Switzerland*, pp 64.
- Johnson W. B. and Maxwell J. A. (1981) *Rocks and Minerals Analysis*, Willey Interscience Inc. New York, pp. 489.
- Kanayama S., Yabuki S., Yanagisawa F. and Motoyama R. (2002) The chemical and strontium isotope composition of atmospheric aerosols over Japan: the contribution of long-range transported Asian dust (Kosa). *Atm. Environ.* **36**, 5159-5175.
- Kar A. (1995) Geomorphology of Arid Western India. In Quaternary Environments and Geoarchaeology of India, Statira Wadia, Ravi Korisettar and V.S. Kale, eds., *Memoirs of Geol. Soc. of India* **32**, 168-190.
- Kaur M. and Chamayal L. S. (1996) The granitoids of Pinder-sarju-Ramganga and Goriganga valleys of Higher Kumaun Himalaya. *J. Geol. Soc. India* **47**, 665-674.
- Kelly J, Thornton I. and Simpson P. R. (1996) Urban geochemistry: a study of the influence of anthropogenic activity on the heavy metal content of soils in traditionally industrial and non - industrial areas of Britain. *App. Geochem.* **11**, 363-370.
- Khemani L. T., Naik M. S., Momin G. A., Kumar R., Chatterjee R. N., Singh G. and Ramana Murthy Bh. V. (1985) Trace elements in the atmospheric aerosols at Delhi, North India. *J. Atmos. Chem.* **2**, 273-285.
- Khemani L. T., Momin G. A., Rao P. S. P., Safai P. D., Singh G. and Kapoor R. K. (1989) Spread of acid rain over India. *Atm. Environ.* **23 B (4)**, 757-762.
- Knap A. H. (1990) The long range transport of natural and contaminant substances, eds. Kluwer Acad. Pub. 59-86.

- Kohfeld K. E. and Harrison S. P. (2001) DIRTMAP: The geological record of dust. *Earth Sci. Rev.* **54**, 81-114.
- Kreutz K. J. and Sholkovitz E. R. (2000) Major element, rare earth element, and sulfur isotopic composition of a high elevation firn core: sources and transport of mineral dust in Central Asia. *Geochem. Geophys. Geosyst.* **1**, 2000GC000082.
- Kulshrestha U. C., Saxena A., Kumar N., Kumari K. M. and Srivastava S. S. (1994) Measurement of heavy metals in the ambient air of Agra. *Ind. J. Environ. Prot.* **14** (9), 685-687.
- Kulshrestha U. C., Kumar N., Saxena A., Kumari K. M. and Srivastava S. S. (1995) Identification of the nature and source of atmospheric aerosols near the Taj Mahal, India. *Environ. Monitor. Asses.* **34**, 1-11.
- Kulshrestha U. C., Sarkar S. K., Srivastava S. S. and Parashar D. C. (1996) Investigation into atmospheric deposition through precipitation studies at New Delhi, India. *Atmos. Environ.* **30**, 4194-4154.
- Kulshrestha U. C., Saxena A., Kumar N., Kumari K. M. and Srivastava S. S. (1998) Chemical composition and association of size differentiated aerosols at a suburban site in a semi-arid tract of India. *J. Atm. Chem.* **29**, 109-118.
- Kumar A., Phadke K. M., Tazne D. S., and Hasan M. Z. (2001) Increase in inhalable particulates concentration by commercial and industrial activities in the ambient air of a select Indian metropolis. *Environ. Sci. Tech.* **35**, 487-492.
- Larocque A. C. L. and Rasmussen P. E. (1998) An overview of trace metals in the environment, from mobilisation to remediation. *Environ. Geol.* **33**(2/3), 85-91.
- Lasaga A. C. (1984) Chemical kinetics of water rock interactions. *J. Geophysics Res.* **89**, 4009-40025.
- Legrand M., Plana-Fattori A. and N'Doumé C. (2001) Satellite detection of dust using the IR imagery of Meteosat, 1, Infrared difference dust index. *J. Geophys. Res.* **106**, 18251-18274.
- Leinen M., Prospero J. M., Arnold E. and Blank M. (1994) Mineralogy of aeolian dust reaching the North Pacific Ocean, 1, Sampling and analysis. *J. Geophys. Res.* **99**, 21017-21024.
- Leon J. -F. (2001) Large scale advection of continental aerosols during INDOEX. *J. Geophys. Res.* **105**, 28427-28439.
- Leon J. -F. and Legrand M. (2003) Mineral dust sources in the surroundings of the north Indian Ocean. *Geophys. Res. Lett.* **30**(6), 1309, doi: 10.1029 / 2002 GL 016690.
- Levin Z., Ganor E. and Gladstein V. (1996) The effects of desert particles coated with sulfate on rain formation in the eastern Mediterranean. *J. Appl. Meteorol.* **35**, 1511-1523.

- Likens G. E., Driscoll C. T. and Buso D. C. (1996) Long-term effects of acid rain. *Sci.* **272**, 244-246.
- Lewis W. H. (1984) Pollen allergy. In: Allergy theory and practice, Korenblat P. E. and Wedner H. J., eds. Grune and Startlon, Orlando, pp 353.
- Lundholm B. (1979) In Saharan dust-Mobilization, Transport and Deposition, Morales C., eds., Wiley, New York, SCOPE 14, 61-68.
- Mahadevan T. N., Negi B. S. and Meenakshy V. (1989) Measurements of elemental composition of aerosol matter and precipitation from a remote background site in India. *Atmos. Environ.* **23(4)**, 869-74.
- McDonald C. and Duncan H. J. (1979) Atmospheric levels of trace elements in Glasgow. *Atmos. Environ.* **13**, 413-417.
- McKendry I. G., Hacker J. P., Stull R., Sakiyama S., Mignacca O. and Reid K (2001) Long range transport of Asian dust to the lower Fraser Valley, British Columbia, Canada. *J. Geophys. Res.* **106**, 18361-18370.
- McLennan S. M. (1993) Weathering and global denudation. *J. Geol.* **101**, 295-303.
- McLennan S. M. (1995) Sediments and soils: Chemistry and abundances. In Rock Physics and phase relations, a handbook of physical constants, A. G. U. reference shelf-3, *Am. Geophys. Un.* 8-19.
- Michaels A. F., Olson D., Sarmiento J. L., Ammerman J. W., Fanning K., Jahnke R., Knap A. H., Lipschultz F. and Prospero J. M. (1996) Inputs, losses and transformations of nitrogen and phosphorus in the pelagic north Atlantic Ocean. *Biogeochem.* **35**, 181-226.
- Middelburg J. J., Van der weijden C. H. and Woittiez J. R. W. (1988) Chemical processes affecting the mobility of major, minor and the trace elements during weathering of granitic rocks. *Chem. Geol.* **68**, 253-273.
- Middleton N. J. (1986) A geography of dust storms in south-west Asia. *J. Climatol.* **6**, 183-196.
- Middleton N. J. (1989) Climatic controls on the frequency, magnitude and distribution of dust storms: examples from India/ Pakistan, Mauritania and Mongolia. In: Paleoclimatology and paleometeorology: modern and past patterns of global atmospheric transport, Leinen M. and Sarnthein M., eds. Kluwer Acad. 97-132.
- Mikami M. (2000) Proposal of an international joint program on the evaluation of aeolian dust outbreak from the continents and its impact to the climate. *J. Desert Res.* **10**, 232-234.
- Misra J. S., Srivastava B. P. and Jain S. K. (1962) Discovery of marine Permo-Carboniferous in western Rajasthan. *Curr. Sci.* **130**.

- Molnar A., Meszaros E., Bozo L., Borbely-kiss I., Koltay E. and Szabo G. (1993) Elemental composition of atmospheric aerosol particles under different conditions in Hungary. *Atmos. Environ.* **27(A)**, 2457-2461.
- Monna F., Joel Lance O. T., Croudace I. W., Cundy A. B. and Lewis J. T. (1997) Pb isotopic composition of air borne particulate material from France and the Southern United Kingdom: implications for Pb pollution sources in urban areas. *Environ. Sci. Tech.* **31**, 2277-2286.
- Morawska L. and Zang J. (2002) Combustion sources of particles: Health relevance and source signatures. *Chemosphere* **49**, 1045-1058.
- Mortimore M. (1998) *Roots in the African dust: sustaining the sub-Saharan drylands*, Cambridge Univ. Press, New York, 219.
- Murthy B. P. (1984) Meteorological potential for urban air pollution in India. *Mausam* **35**, 237-239.
- Najman Y., Bickle M. and Chapman H. (2000) Early Himalayan exhumation: isotopic constraints from the Indian fore land basin. *Terra Nova* **12**, 28-34.
- Nambi K. S. V. and Sapra B. K. (1998) *Aerosols: generation and role in medicine, industry and Environment*, eds. Allied Pub. Ltd. New Delhi, XX.
- Narayanan K. (1964) Stratigraphy of Rajasthan self. *Proc. Symp. Problems of Indian Arid Zone*, Govt. of India and UNSCO, CAZRI, Jodhpur, 92-100.
- Natusch D. F. S., Wallace J. R. and Evans Jr. C. A. (1974) Toxic trace elements: preferential concentration in respirable particles. *Sci.* **183**, 202-204.
- NEERI (1995, 96 and 97) Status reports on air pollution aspects in 10 Indian major cities, National Environmental Engineering Research Institute, Nagpur, India.
- Negi B. S., Sadasivan S. and Mishra U. C. (1987) Aerosol composition and sources in urban areas in India. *Atmos. Environ.* **21 (6)**, 1259-1266.
- Nesbitt H. W. and Young G. M. (1984) Prediction of some weathering trends of plutonic and volcanic rocks based on thermodynamic and kinetic considerations. *Geochim. Cosmochim. Acta* **48**, 1523-1534.
- Nesbitt H. W. and Young G. M. (1996) Petrogenesis of sediments in the absence of chemical weathering: effects of abrasion and sorting on composition and mineralogy. *Sediment.* **43**, 341-358.
- Nesbitt H. W., Young G. M., McLennan S. M. and Keays R. R. (1996) Effects of chemical weathering and sorting on the petrogenesis of siliciclastic sediments, with implications for provenance studies. *J. Geol.* **104**, 525-542.
- Nesbitt H.W. and Young G. M. (1989) Formation and diagenesis of weathering profiles. *J. Geol.* **97**, 129-147.

- Nickling W. G. (1983) Grain-size characteristics of sediments transported during dust storms. *J. Sediment. Petrol.* **53**, 1011.
- Nriagu J. O. (1988) A salient epidemic of environmental metal poisoning? *Environ. Poll.* **50**, 139-161.
- Nriagu J. O. and Pacyna J. M. (1988) Quantitative assessment of worldwide contamination of air, water and soils by trace metals. *Nature* **320**, 735-738.
- Nriagu J. O. (1989) A global assessment of natural sources of trace metals. *Nature* **338**, 47-49.
- Offer Z. Y. and Goossens D. (2001) Ten years of aeolian dust dynamics in a desert region (Negev desert, Israel): analysis of airborne dust concentration, dust accumulation and the high-magnitude dust events. *J. Arid Environ.* **47**, 211-249.
- Olmez I. and Gordon G. E. (1985) Rare Earths: Atmospheric signatures for oil-fired power plants and refineries. *Sci.* **229**, 966-968.
- Ostro B. (1994) Estimating the health effects of air pollutants: a method with an application to Jakarta. Policy research working paper, 1301, World Bank, Policy research dept., Washington, D.C.
- Pant R. K. (1993) Spread of loess and march of desert in western India. *Curr. Sci.* **64**, 841-47.
- Pareek H. S. (1981) Basin configuration and sedimentary stratigraphy of western Rajasthan. *J. Geol. Soc. Ind.* **22** (11).
- Pillai A. G., Naik M. S., Momin G. A., Rao P. S. P., Safai P. D., Ali K., Rodhe H. and Granat L. (2001) Studies of wet deposition and dustfall at Pune, India. *Water, Air and Soil Poll.* **130**, 475-480.
- Pinnick R. G., Fernandez G., Martinez- Andazola E., Hinds B. D., Hansen A. D. A. and Fuller K. (1993) Aerosols in the arid southwestern United states: Measurements of mass loading, volatility, size distribution, absorption characteristics, black carbon and vertical structure to 7 km above sea level. *J. Geophys. Res.* **98**, 2651-2666.
- Prospero J. M. (1981) Eolian transport to the world ocean. In *The oceanic lithosphere*, Emiliani C., eds., **7**, The Sea. John Wiley, New York, 801-874.
- Prospero J. M., Charlson R. J., Mohnen V., Jaenicke R., Delaney A. C., Mayer J., Zoller W. and Rahn K. (1983) Atmospheric aerosol system: An overview. *Rev. Geophys.* **21**, 1607-1630.
- Prospero J. M., Uematsu M. and Savoie D. L. (1989) Marine aerosol transport to the north Pacific Ocean. In *Chemical Oceanography*, Riley J. P., Chester R. and Duce R. A., eds., **10**, Acad. Press, San Diego, 188-218.

- Prospero J. M. (1996 a) The atmospheric transport of particles to the ocean. In Particle Flux in the Ocean, V. Ittekkott, S. Honjo, and P. J. Depetris, eds., SCOPE Rep. 57, John Wiley, New York, 19-52.
- Prospero J. M. (1996 b) Saharan dust transport over the North Atlantic Ocean and Mediterranean: An overview. In The Impact of Desert Dust Across the Mediterranean, (S. Guerzoni and R. Chester, eds), 133-151, Kluwer acad., Norwell, Mass.
- Prospero J. M. (1999) Long-range transport of mineral dust in the global atmosphere: Impact of African dust on the environment of the southeastern United States. *Proc. Natl. Acad. Sci. USA* **96**, 3396-3403.
- Prospero J. M., Barrett K., Church T., Dentener F., Duce R. A., Galloway J. N., Levy II H., Moody J. and Quinn P. (1996) Atmospheric deposition of nutrients to the North Atlantic Basin. *Biogeochem.* **35**, 27-73.
- Prospero J. M., Ginoux P., Torres O., Nicholson S. E. and Gill T. E. (2002) Environmental characterization of global sources of atmospheric soil dust identified with the nimbus 7 total ozone mapping spectrometer (TOMS) absorbing aerosol product. *Rev. Geophys.* **40(1)**, 1002, doi: 10.1029/2000RG000095.
- Pye K. (1987) *Aeolian dust and dust deposits*. Acad. Press, London, pp. 121.
- Pye K. and Tsoar H. (1987) The mechanics and geological implications of dust transport and deposition in deserts with particular reference to loess formation and dune sand diagenesis in the northern Negev, Israel. In: Desert sediments: Ancient and Modern, Frostick L. and Reid I., eds., *Geol. Soc. Spl. Publ.* **35**, 139-156.
- Rahn K. A. (1976 a) The chemical composition of the atmospheric aerosols. Technical Report, University of Rhode Island, Narragansett, 151- 177.
- Rahn K. A (1976 b) Silicon and aluminum in atmospheric aerosols: crust-air fractionation? *Atmos. Environ.* **10**, 597-601
- Rahn K. A., Borys R. D., Shaw G. E., Schutz L. and Jaenicke R. (1979) Long range impact of desert aerosol on atmospheric chemistry: two examples. In: Saharan dust: Mobilization, Transport, Deposition, Morales C. ed. John Wiley, New York, 243-266.
- Rajamani V. (2002) Farmland geology – an emerging field in sustainability science. *Curr. Sci.* **83**, 557-559.
- Rasmussen P. E. (1998) Long-range atmospheric transport of trace metals: the need for geoscience perspectives. *Environ. Geol.* **33 (2/3)**, 96-108.
- Raychaudhury S. P. (1963) Soils of India. ICAR, New Delhi, pp 495.

- Rea D. K. (1994) The paleoclimatic record provided by eolian deposition in the deep sea: the geologic history of wind. *Rev. Geophys.* **32**, 159-195.
- Reheis M. C. and Kihl R. (1995) Dust deposition in southern Nevada and California, 1984-1989: Relations to climate, source area, and source lithology. *J. Geophys. Res.* **100**, 8893-8918.
- Reheis M. C., Budahn J. R., and Lamothe P. J. (2002) Geochemical evidence for diversity of dust sources in the southwestern United States. *Geochim. Cosmochim. Acta* **66**, 1569-1587.
- Reheis M. C., Goodmacher J. C., Harden J. W., McFadden L. D., Rockwell T. K., Shroba R. R., Sowers J. M. and Taylor E. M. (1995) Quaternary soils and dust deposition in southern Nevada and California. *Geol. Soc. Am. Bull.* **107**, 1003-1022.
- Reynolds R., Belnap J., Reheis M., Lamothe P. and Luiszer F. (2001) Aeolian dust in Colorado plateau soils: Nutrient inputs and recent change in source. *Proc. Natl. Acad. Sci. USA* **98**, 7123-7127.
- Romo-Kroger C. M., Morales J. R., Dinator M. I., Llona F. and Eaton L. C. (1994) Heavy metal in the atmosphere coming from a copper smelter in Chile. *Atmos. Environ.* **28** (4), 705-711.
- Ross M., Nolan R. P., Langer A. M. and Cooper W. C. (1993) Health effects of mineral dusts other than asbestos. In *Health Effects of Mineral Dust*, G. D. J. Guthrie and B. T. Mossman, eds., *Rev. Mineral.* **28**, 361-407.
- Sadasivan S. and Negi B. S. (1990) Elemental characterisation of atmospheric aerosols. *The Sci. Tot. Environ.* **96**, 269-279.
- Sadayo Y., Shinji K., Fengfu Fu, Masatoshi H., Fumitaka Y., Wenshou Wei, Fanjiang Z., Mingzhe Liu, Zhibao Shen and Lichao Liu (2002) Physical and chemical characteristics of aeolian dust collected over Asian dust sources regions in China – comparison with atmospheric aerosols in an urban area at Wako, Japan. *J. Arid Land. Stud.* **14**, 273-289.
- Satheesh S. K., Ramanathan V., Li-Jones X., Lobert J. M., Podgorny I. A., Prospero J. M., Holben B. N. and Loeb N. G. (1999) A model for the natural and anthropogenic aerosols over the tropical Indian Ocean derived from Indian Ocean Experiment data. *J. Geophys. Res.* **104**, 27421-27440.
- Saxena A., Kulshrestha U. C., Kumar N., Kumari K. M. and Srivastava S. S. (1996). Characterisation of precipitation at Agra. *Atmos. Environ.* **30**, 3405-12.
- Saxena S. K. (1977) Vegetation and its succession in the Indian Desert. In: *Desertification and its control*, Jaiswal P. L., eds., ICAR, New Delhi, 177-92.
- Schutz L. and Rahn K. A. (1982) Trace elements concentration in erodible soils. *Atm. Environ.* **16**, 171-176.

- Schwartz J. (1991) Particulate air pollution and daily mortality: a synthesis. *Public Health Rev.* **19**, 39-60.
- Schwartz J. and Dockery D. W. (1992) Particulate air pollution and daily mortality in Steubenville, Ohio. *Am. Rev. Respiratory Disease* **135**(1).
- Shapiro L. and Brannock W. W. (1962) Rapid chemical analysis of silicate, carbonate and phosphate rocks. *US Geol. Surv. Bull.* **1144 A**, 56.
- Sharma V. K. and Patil R. S. (1992) Size distribution of atmospheric aerosols and their source identification using factor analysis in Bombay, India. *Atmos. Environ.* **26**, 135-140.
- Sharma A. and Rajamani V. (2001) Weathering of charnockites and sediment production in the catchment area of the Cauvery River, southern India. *Sed. Geol.* **143**, 169-184.
- Sharma V. P., Arora H. C. and Gupta R. K. (1983) Atmospheric pollution studies at Kanpur-suspended particulate matter. *Atmos. Environ.* **17** (7), 1307-1314.
- Sharma H. S., Dhir R. P. and Joshi D. C. (1985) Available micro nutrients status of some soils of Arid zones. *J. Indian Soc. Soil Sci.* **33**, 50-55.
- Sheehy D. (1992) A perspective on desertification of grazingland and ecosystems in North China. *Ambio.* **21**, 303-307.
- Shinji K., Sadayo Y., Fumitaka Y. and Osamu A. (2002) Geochemical features and source characterization from Sr isotopes of "Kosa" particles in Red Snow that fell on Yamagata Prefecture, NE Japan in January and March, 2001. *J. Arid Land Stud.* **11**, 291-300.
- Sikka D. R. (1997) Desert climate and its dynamics. *Curr. Sci.* **72**, 35-46.
- Singh A. B. and Malik P. (1994) Pollen aerobiology and allergy- an integrated approach. *Ind. J. Aerobio.* **7**, 1.
- Singh A. B. and Singh A. (1994) Pollen allergy- a global scenario. In: Recent trends in Aerobiology, Allergy and Immunology, Agashe S. N., eds., Oxford IBH, New Delhi.
- Singh M., Jaques P. A. and Sioutas C. (2002) Size distribution and diurnal characteristics of particle-bound metals in source and receptor sites of the Los Angeles Basin. *Atm. Environ.* **36**, 1675-1689.
- Singh P. and Rajamani V. (2001) REE geochemistry of recent clastic sediments from Kaveri flood plains, Southern India: Implications to source area weathering and sedimentary processes. *Geochim. Cosmochim. Acta* **65**, 3093-3108.
- Singh I. B. (1978) Some problems concerning the study of sedimentary rocks in the Precambrian. *Geophytology* **8**, 10-18.

- Singhvi A. K. and Kar A. (1992) In: Thar desert in Rajasthan, land, man and environment, eds., *Geol. Surv. India*.
- Srinivasan J. and Gadgil S. (2002) Asian Brown Cloud-fact and fantasy. *Curr. Sci.* **83(5)**, 586-592.
- Srivastava A. K. (1988) Geoscientific appraisal of Najafgarh depression and related environmental problems of Delhi. In: Geomorphology and Environment, Singh S. and Tewari R. C., eds., *The Allahabad Geographical Society*, Allahabad, India, 631-642.
- Sturges W. T. and Barrie L. A. (1989) The use of stable lead 206/207 isotope ratios and elemental composition to discriminate the origins of lead in aerosols at rural site in eastern Canada. *Atmos. Environ.* **23**, 1645-1657.
- Subbaraya B. H., Jayaraman A., Krishnamoorthy K., and Mohan M. (2000) Atmospheric Aerosol studies under ISRO'S Geosphere Biosphere Programme. *J. Ind. Geophys. Union* **4(1)**, 77-90.
- Swap R., Garstang M. and Greco S. (1992) Saharan dust in the Amazon basin. *Tellus* **44(b)**, 133-149.
- Taylor S. R., McLennan S. M. and McCullah M. T. (1983) Geochemistry of loess, continental crustal composition and crustal model ages. *Geochim. Cosmochim. Acta* **47**, 1897-1905.
- Taylor S. R. and McLennan S. M. (1985) The continental crust: Its Composition and evolution. Blackwell, London, pp.311.
- Taylor S. R. and McLennan S. M. (1996) The evolution of continental crust. *Sci. Am Jan.* 76-81.
- Taylor S. R. and McLennan S. M. (1995) The geochemical evolution of the continental crust. *Rev. Geophys.* **33**, 241-265.
- Tegen I. and Fung I. (1994) Modelling of mineral dust in the atmosphere: Sources, transport, and optical thickness. *J. Geophys. Res.* **99**, 22897-22914.
- Tegen I., Lacis A. A. and Fung I. (1996) The influence on climate forcing of mineral aerosols from disturbed soils. *Nature* **380**, 419-422.
- Thomas D. S. G. and Middleton N. J. (1994) *Desertification: Exploding the Myth*, eds., John Wiley, New York, 194.
- Thussu J. L. (1995) Quaternary stratigraphy and sedimentation of the Indogangetic plains, Haryana. *J. Geol. Soc. India* **46**, 533-544.
- Tiwari S. (1999) Chemistry of atmospheric aerosols at Delhi. *Vayu Mandal* 376-380.

- Tripathi J. K. and Rajamani V. (1999) Geochemistry of the loessic sediments on Delhi ridge, eastern Thar desert, Rajasthan: Its implication to exogenic processes. *Chem. Geol.* **155**, 265-278.
- Tripathi J. K., Bock B., Rajamani V. and Eisenhauer A. (2003) Isotopic ($^{87}\text{Sr}/^{86}\text{Sr}$ and $^{143}\text{Nd}/^{144}\text{Nd}$) evidence for the Thar desert sediment's provenance and its implications. XVI INQUA congress, Reno, USA (Poster).
- Tsoar H. and Pye K. (1987) Dust transport and the questions of desert loess formation. *Sedimentology* **34**, 139-153.
- Uematsu M., Duce R. A., Prospero J. M., Chen L., Merrill J. T. and McDonald R. L. (1983) Transport of minerals aerosol from Asia over the north Pacific ocean. *J. Geophys. Res.* **88**, 5343-52.
- Uematsu M. (1998) Distribution and characterization of Asian aerosols over the western North Pacific region. *Global Environ. Res.* **2**, 39-45.
- United States. CFR (Code of Federal Regulations). Washington D. C.: Govt. Printing Office.
- USEPA (United States Environmental Protection Agency;1996) Air quality criteria for particulate matter. US Environmental Protection Agency, EPA/600/P-95/001F.
- USEPA (1990) Review of the national ambient air quality standard for particulate matter: Assessment of scientific and technical information. Research triangle park, N. C.
- Verma G. S. (1989 a) Impact of soil derived aerosols on precipitation acidity, in India. *Atm. Environ.* **23**, 2723-2728.
- Verma G. S. (1989 b) Background trends of pH of precipitation over India. *Atmos. Environ.* **23**(4), 747-51.
- Wadhawan S. K. (1990) Quaternary geology, Morphostratigraphy and neotectonism in parts of Nagaur district, Rajasthan. *Records Geol. Surv. India* **123** (7), 53-54.
- Walker A. S. (1982) Deserts of China. *Sci. Am.* **70**, 366-376.
- Walsh J. N. (1980) The simultaneous determination of the major, minor and trace constituents of silicate rocks using Inductively coupled plasma spectrometry. *Spectrochimica Acta* **35B**, 107-111.
- Wang M. X., Wnchester J. W., Cahill T. A. and Ren L. X. (1982) Chemical elemental composition of windblown dust. *Kexue Tongbao.* **27**, 1193-1198.
- Wang Chunxia, Zhu W., Wang Zijian and Guicherit R. (2000) Rare earth elements and other metals in atmospheric particulate matter in the western part of the Netherlands. *Water, Air and Soil Pollut.* **121**, 109-118.

- Wilson R. and Spengler J. (1996) Particles in our Air concentration and Health Effects. Harvard Univ. Press, Cambridge, MA.
- Wong C. S. C., Li X. D., Zhang G., Qi S. H. and Peng X. Z. (2003) Atmospheric deposition of heavy metals in the Pearl river delta, China. *Atmos. Environ.* **37**, 767-776.
- Wood J. M. (1974) Biological cycles for toxic elements in the environment. *Sci.* **183**, 1049.
- World Health Organisation (1987) Air quality guidelines for Europe. Copenhagen: WHO regional office for Europe.
- Wurzler S., Reisin T. G. and Levin Z. (2000) Modification of mineral dust particles by cloud processing and subsequent effects on drop size distributions. *J. Geophys. Res.* **105**, 4501- 4512.
- Xiaoqing G., Sadayo Y., Zhang Q. U. and Zhenan QIAN (2002) Some Characteristics of Dust Storm in Northwest China. *J. Arid Land Stud.* **11**, 235-243.
- Yaalon D. H. and Ganor T. (1973) The influence of dust on soils in the quaternary. *Soil Sci.* **116**, 146-155.
- Yadav S. and Rajamani V. (2003 a) Aerosols of NW India-a potential Cu source! *Curr. Sci.* **84(3)**, 278-280.
- Yadav S. and Rajamani V. (2003 b) Geochemistry of aerosols of northwestern part of India adjoining the Thar desert. *Geochim. Cosmochim. Acta* (accepted)
- Young J. R., Ellis E. C. and Hidy G. M. (1988) Deposition of air borne acidifiers in western environment. *J. Environ. Qual.* **17**, 1-26.

Appendices

DIFFERENT FORMS OF AEROSOLS

1. SOLID FORMS:

Fly ashes: Finely divided particles of ash entrained in the flue gases arising from the combustion of fuel.

Fumes: The solid particles generated by condensation from gaseous state and often accompanied by a chemical reaction such as oxidation.

Smokes: Finely divided aerosol particles, which mainly consists of carbon and other products of incomplete combustion or condensation of super-saturated vapors.

Soot: Agglomeration of particles of carbon impregnated with tar, formed by the incomplete combustion of carbonaceous materials.

Carbonaceous aerosols: This fraction comprises carbonate, a wide range of organic compounds (OC) and so called elemental carbon (EC). EC is an inert tracer of primary combustion aerosols whereas OC is a result of secondary interactions and the fuel burnings.

2. LIQUID FORMS:

Fog and mist: suspension of liquid droplets formed by atomization or vapour condensation. Like smokes, mist consists of very high concentration of small particles.

3. MIXED FORMS:

Smog: Mixture of smoke and fog, and byproduct of their chemical interactions.

DEFINITIONS FOR AEROSOL SIZES

- Equivalent volume diameter** : diameter of the sphere having same volume as the given irregular particle.
- Stoke's diameter** : diameter of the sphere having same density and falling velocity as the given particle.
- Aerodynamic diameter** : diameter of the sphere of unit density but having same falling velocity as the given particle (useful for characterising filtration and respiratory depositions).
- PM₁₀** : Mass concentration of particles collected by a sampler with a 50% cut-point at an aerodynamic particle diameter of 10 micrometers, mostly particles with aerodynamic particle diameters of 10 micrometers or less.
- PM_{2.5}** : Mass concentration of particles collected by a sampler with a 50% cut-point at an aerodynamic particle diameter of 2.5 micrometers, mostly particles with aerodynamic particle diameters of 2.5 micrometers or less.

NOMENCLATURE OF ATMOSPHERIC PARTICLES

A. METEOROLOGICAL STUDIES

According to Junge:

Aitken particles	:	from approx. 1 nm to 100nm
Large particles	:	from 0.1 μm to 1 μm
Giant particles	:	larger than 1 μm upto approx. 100 μm

According to Whitby:

Nucleation mode particles	:	from approx. 1 nm to 100nm
Accumulation mode particles	:	from 0.1 μm to 1 μm
Coarse mode particles	:	larger than 1 μm up to approx. 100 μm

B. AIR ELECTRICITY STUDIES:

Small ions	:	approx. 0.1 nm
Large ions	:	from approx. 1 nm to 100 nm

C. ATMOSPHERIC OPTICS STUDIES:

Haze particles	:	approx. 10 μm to approx. 1 μm
----------------	---	---

D. CLOUD PHYSICS:

Active condensation nuclei	:	approx. 10 nm to approx. 1 μm
----------------------------	---	--

E. AIR CHEMISTRY AND POLLUTION STUDIES:

Particles containing main aerosol mass:	:	approx. 100nm to approx. 10 μm
---	---	---

Details of Mineralogy

The complete X-ray diffractograms of different size fractions of aerosols collected from different locations are given in figures AF.2.1–2.4. The major mineral phases identified in aerosol samples are quartz, followed by K-feldspar, mica, calcite, chlorite and plagioclase. The dominant minerals, quartz and feldspar show a decrease from coarse to fine size fractions at all sites. A decrease in these minerals is also noticed within a given size fraction of aerosols with distance in the downwind direction. However calcareous and micaceous minerals such as chlorite, muscovite and biotite are enriched in PM₁₀ samples at all sites. Among the different sampling locations, Bikaner samples show more calcite concentration in all size ranges. This could be due to the local contribution from calcareous concretions and gypsum quarries in the Thar desert region. Compared to summer, micaceous minerals are more abundant in winter; particularly, quartz and feldspar show a significant drop. Also the intensity (counts) of different minerals drops significantly, especially in winter PM₁₀ samples compared to summer samples (Fig. AF.2.3). The mineral peaks are broader with larger background counts in winter samples (Fig. AF.2.3 and 2.4). This indicates the presence of extremely fine grained amorphous phases in winter aerosols and a significant contribution from anthropogenic sources compared to crystalline crustal sources. This can be attributed to the low carrying capacity of winds due to poor wind speed in winter. Interestingly, calcite is very poorly represented in our winter FF samples (Fig. AF.2.2) inspite of higher CaO content (Table 4.3). This implies that CaO in winter samples is predominantly derived from additional secondary sources other than primary crustal sources and is amorphous in

nature. In addition to the mineral phases identified from XRD data, heavy minerals like sphene, amphibole, garnet and zircon also have been recognized from EPMA analysis. The elemental analysis and calculated formula of the mineral phases present in the probed aerosol samples are given in table 4.2 (chapter 4). Figures AF.2.5 and 2.6 display the back-scattered electron images of a few selected grains in Jhunjhunu free fall and SPM samples. We notice coarser grains to have suffered rounding because of abrasion during aerosol transport. The sharp edges and crystal outline in the SPM indicate less abrasion compared to FF samples. Small sized grains ($\sim 20 \mu\text{m}$) of sphene are found to be associated with coarser grain size aerosol because of its high density. Schutz and Rahm (1982) have made similar observations for heavy minerals in the Saharan dusts.

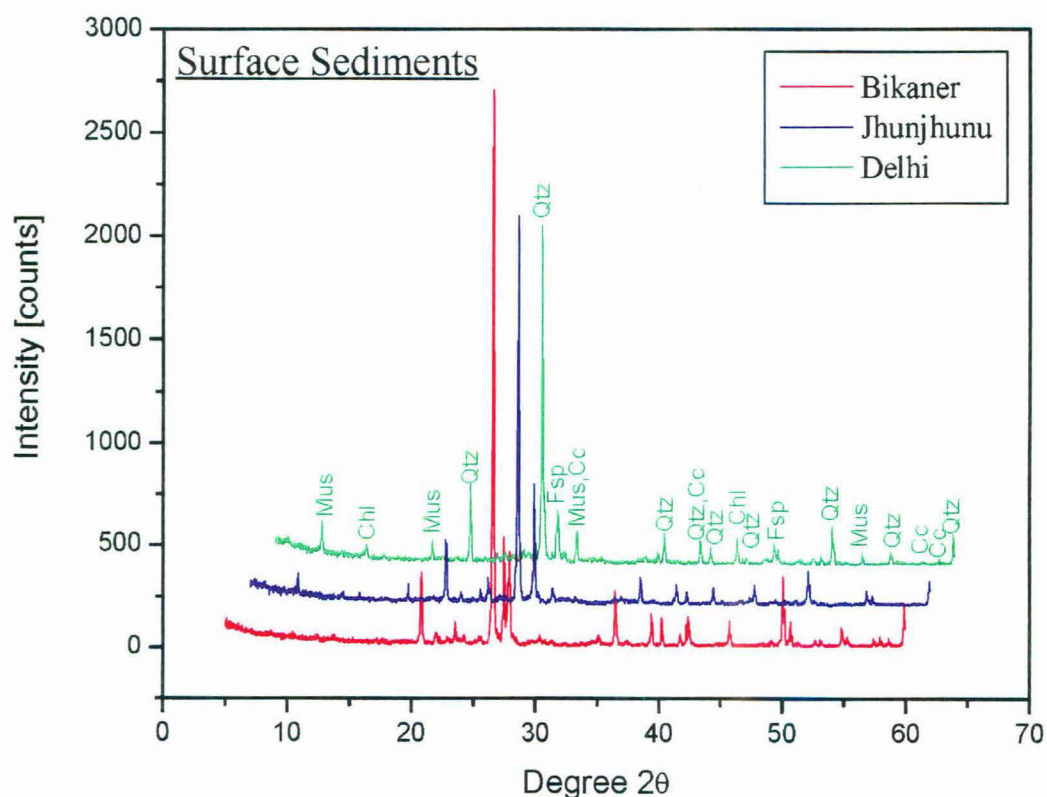


Figure AF.2.1 X-ray diffractograms of sediment samples. Scans are shifted by 200 counts and 2° 2θ from each other for better comparison.

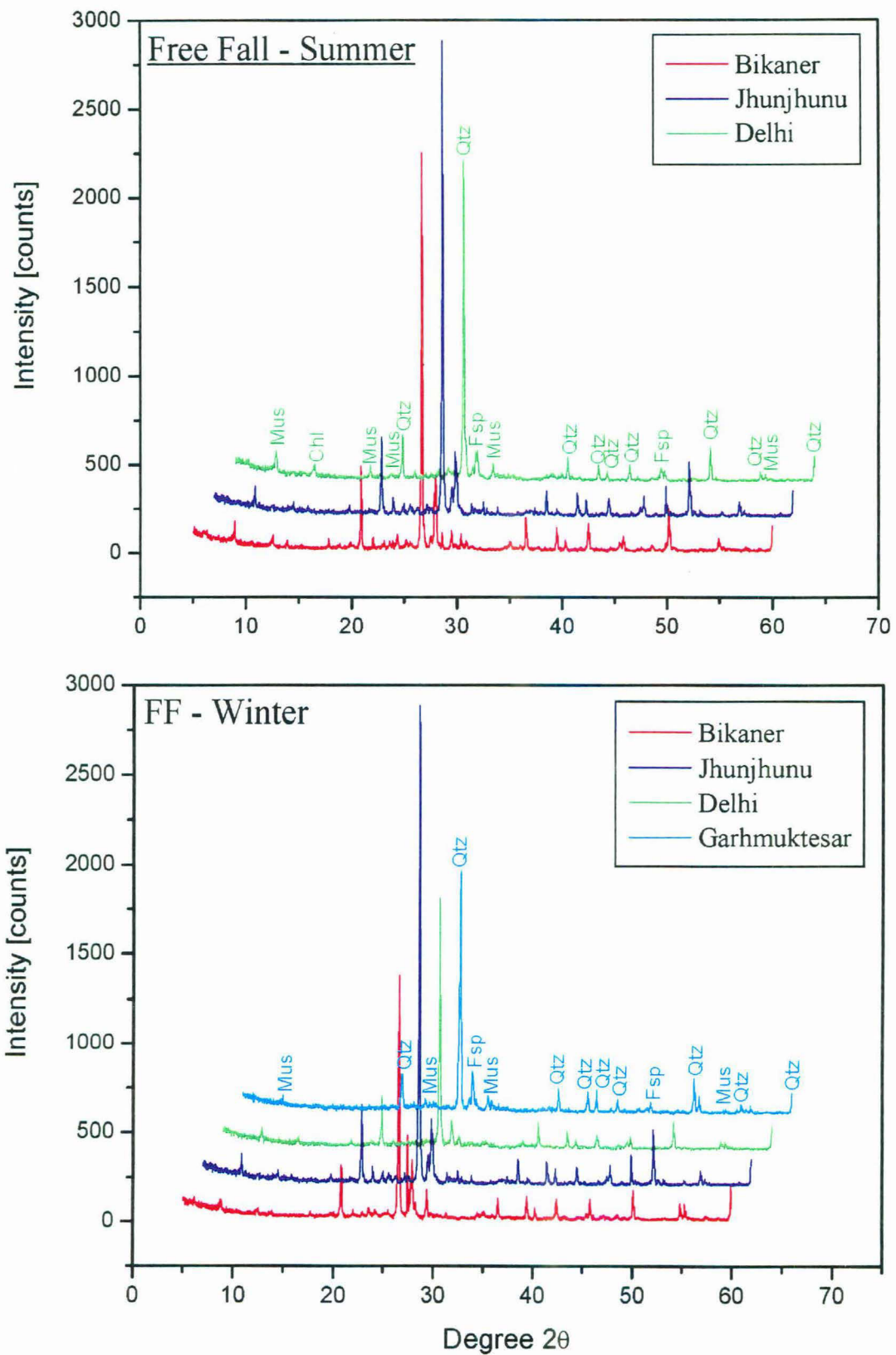


Figure AF.2.2 X-ray diffractograms of summer and winter FF samples. Scans are shifted by 200 counts and 2° 2θ from each other for better comparison.

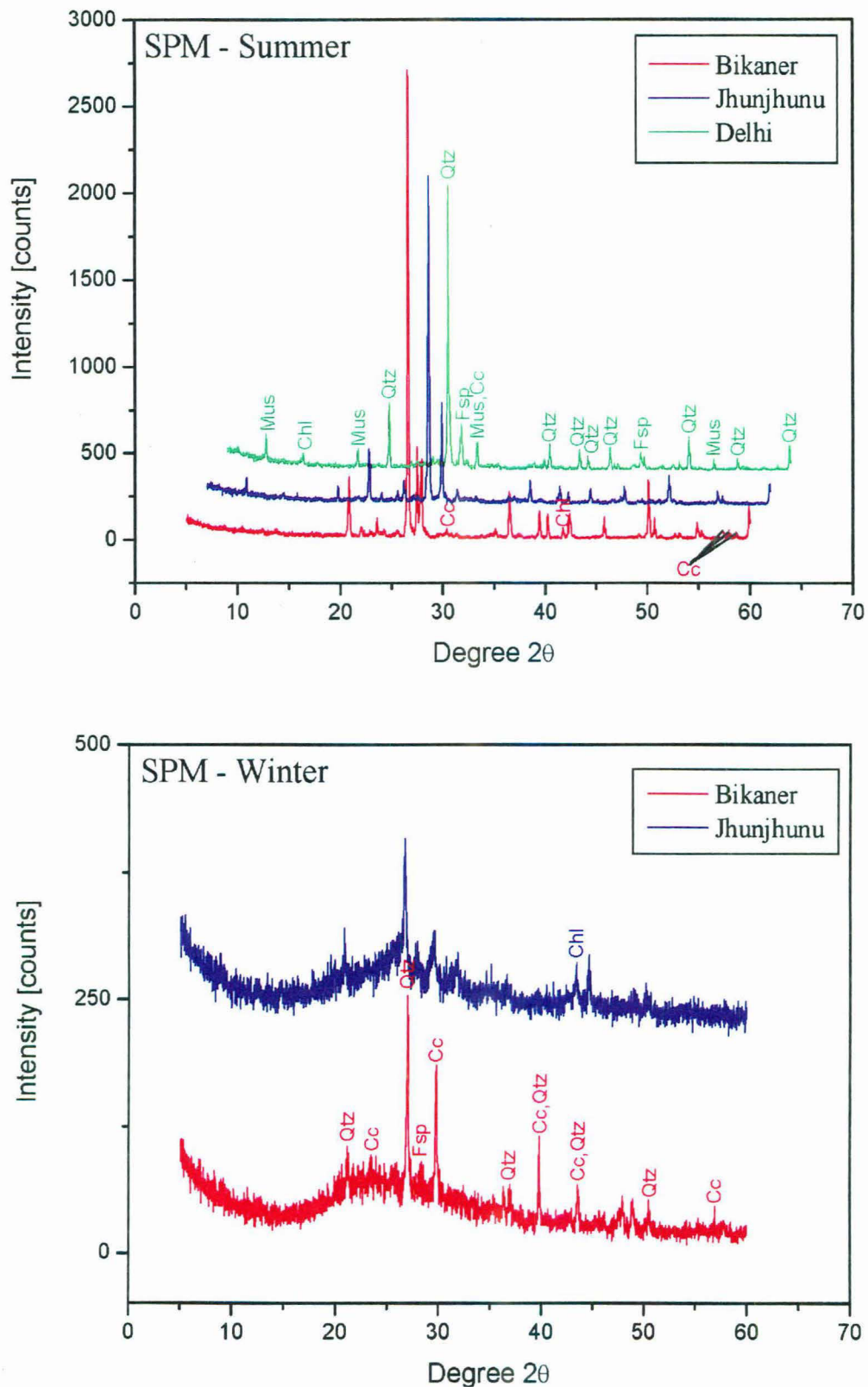


Figure AF.2.3 X-ray diffractograms of summer and winter SPM samples. Scans are shifted by 200 counts and 2° 2θ from each other for better comparison. Note the significant drop of intensity in the winter samples.

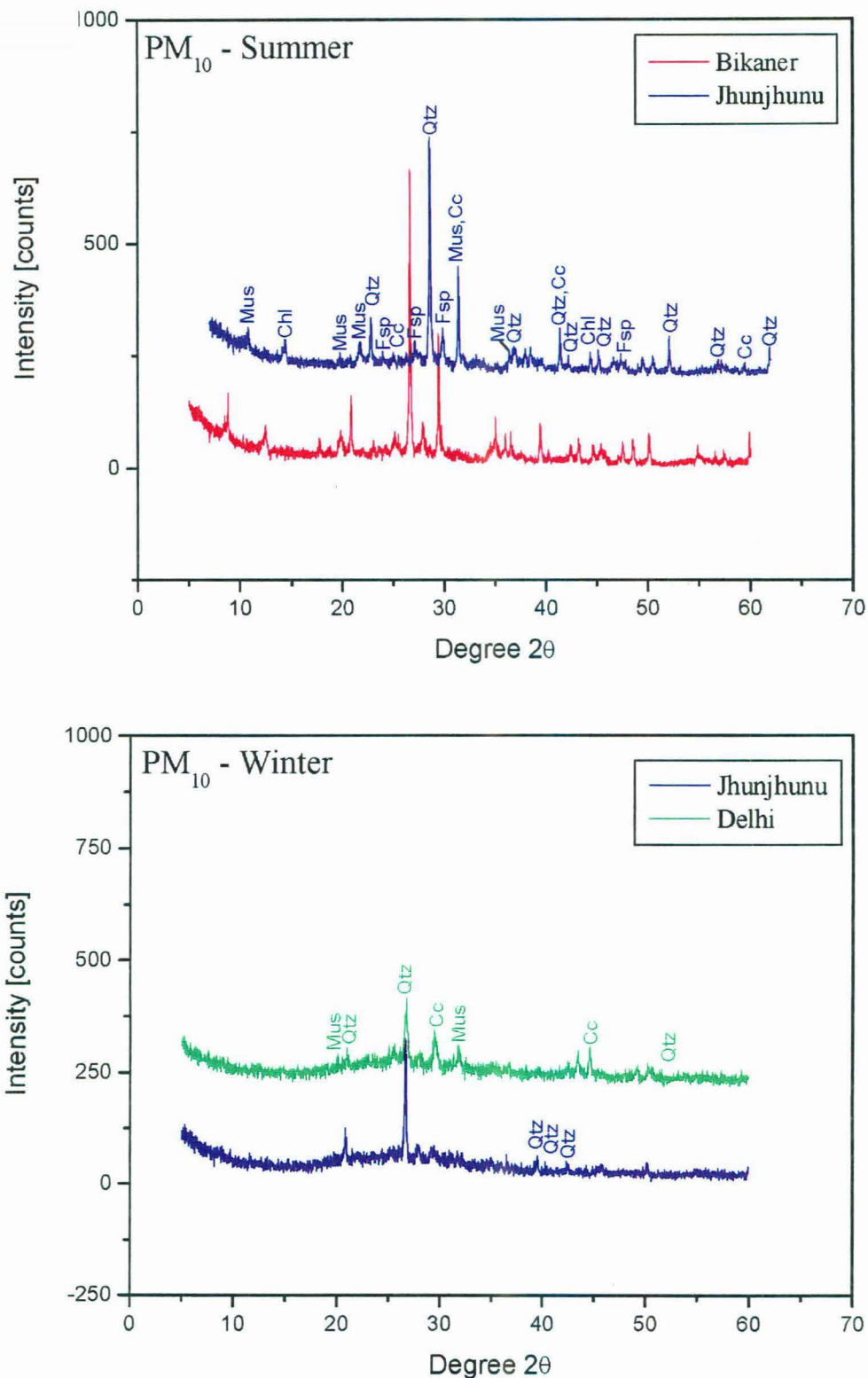


Figure AF.2.4 X-ray diffractograms of summer and winter PM₁₀ samples. Scans are shifted by 200 counts and 2° 2θ from each other for better comparison. Note the significant drop of intensity compared to FF and SPM samples from all sites.

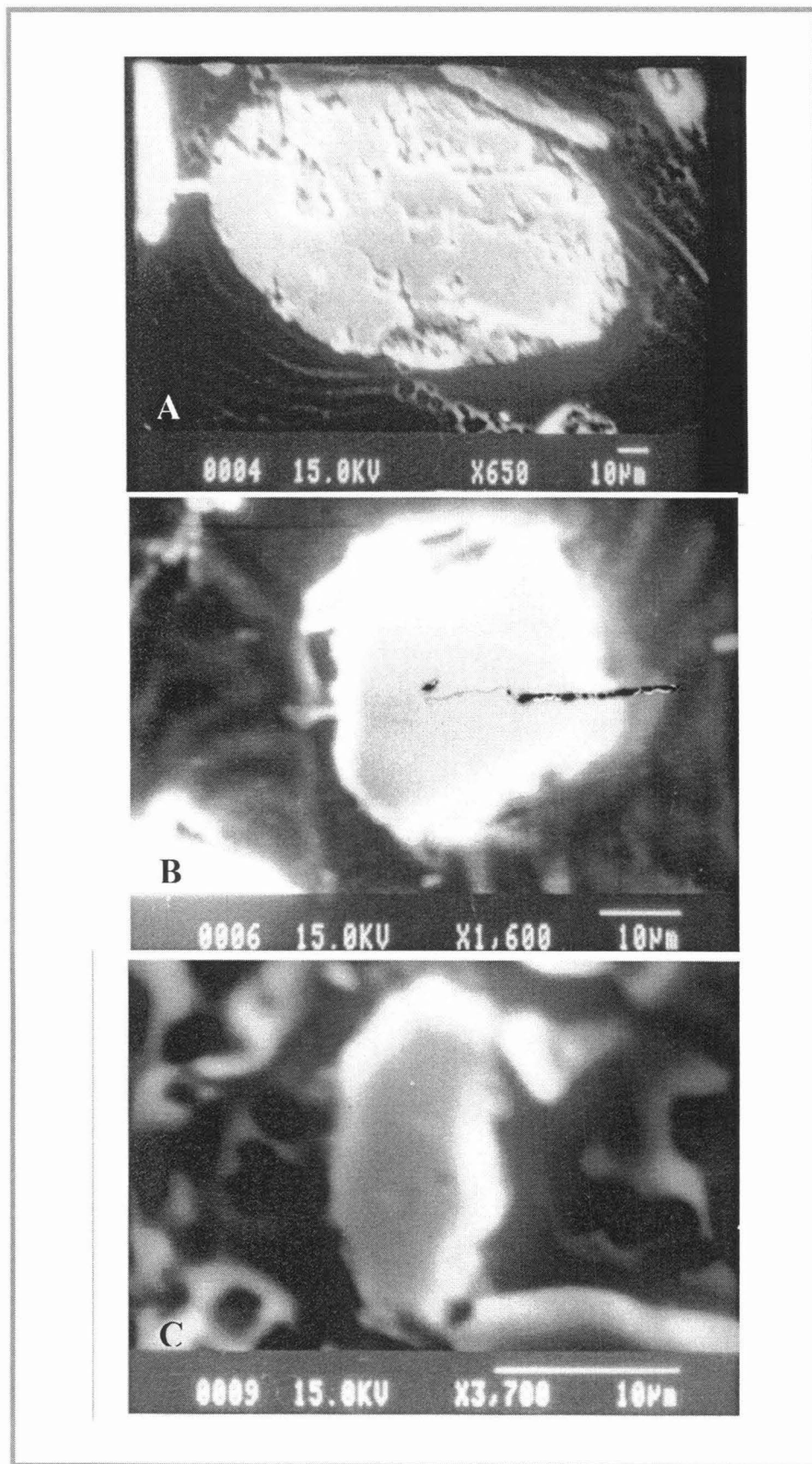


Figure AF-2.5 Backscattered electron images of different free-fall grains collected from Jhunjhunu. (A) rounded amphibole, (B) rounded chlorite, (C) sphene.

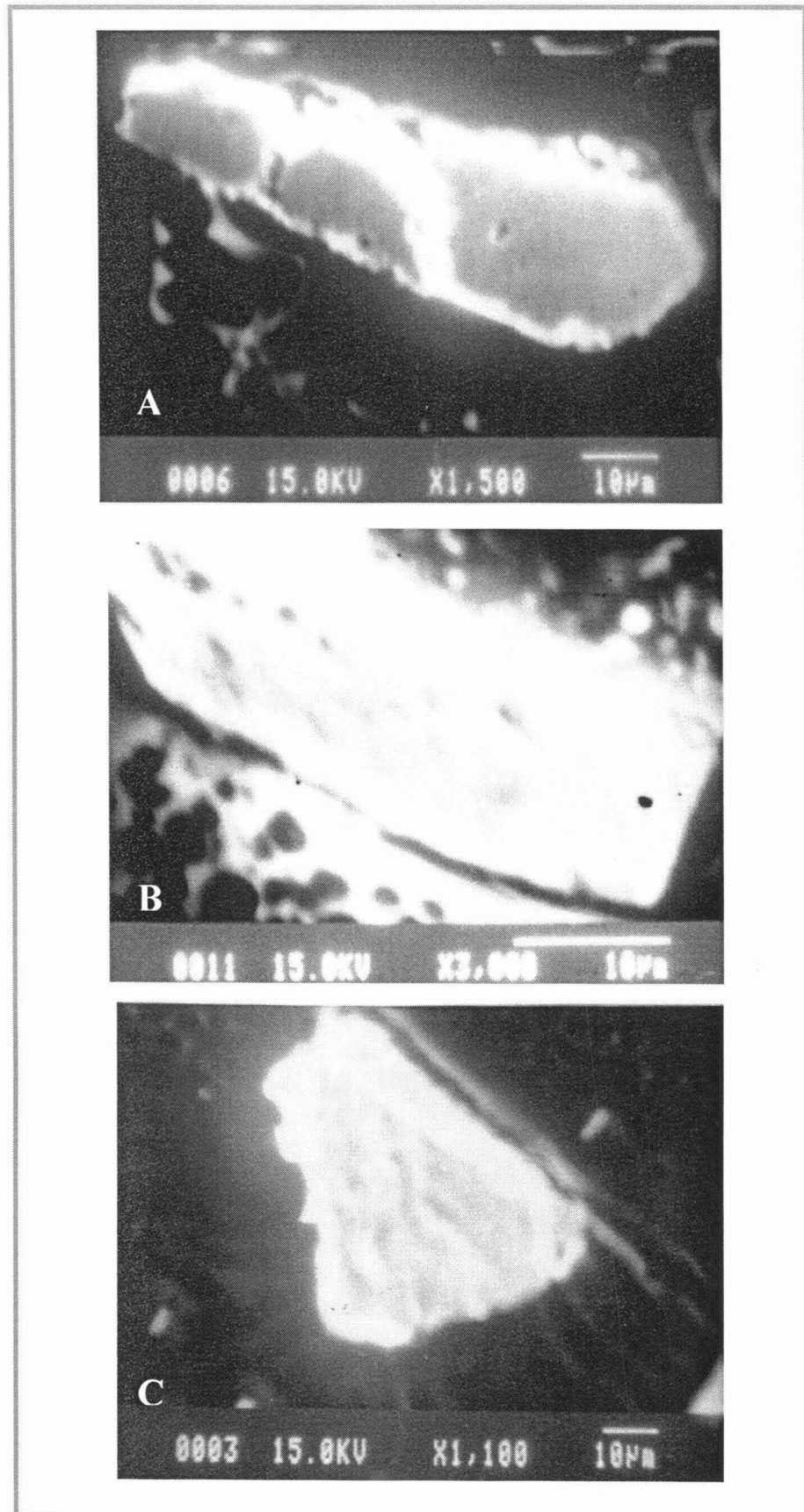


Figure AF-2.6 Backscattered electron images of different free-fall (A) and SPM (B & C) grains collected from Jhunjhunu. (A) elongated calcite, (B) lathe-shaped feldspar, (C) diamond-shaped amphibole showing cleavage at 120 degree.

Table AT 2.1 Geochemical analysis of aerosols of NW India.

Cont.-----

	Summer Free Fall															Summer Suspended Particulate matter												
	Bikaner						Jhunjhunu						Delhi						Delhi				Jhunjhunu		Bikaner			
	B 1	B1a	B1b	B2	B2a	B2b	J1	J1a	J1b	J2	J2a	J2b	D1	D1a	D1b	D2	D2a	D2b	A	B	C	D	A	B	A	B	C	D
SiO ₂	73.4	76.2	71.5	71.9	77.0	70.0	74.5	76.9	73.4	75.4	77.2	69.4	69.8	70.7	69.0	68.5	71.6	66.9	63.4	57.9	64.3	63.2	62.0	63.0	62.3	64.2	62.9	66.1
TiO ₂	0.7	0.5	0.8	0.7	0.4	0.8	0.6	0.4	0.7	0.6	0.4	0.8	0.7	0.6	0.8	0.7	0.6	0.8	0.7	0.8	0.7	0.7	0.7	0.7	0.8	0.8	0.8	0.6
Al ₂ O ₃	11.4	11.0	12.3	11.9	10.8	12.4	11.4	10.6	12.0	11.3	11.0	14.2	13.6	13.0	13.8	13.5	12.0	13.7	15.0	17.4	14.7	15.2	15.1	15.7	15.1	14.9	14.7	11.7
FeO	3.5	2.8	3.7	3.8	2.6	4.0	3.3	2.5	3.5	3.1	2.4	4.1	4.2	3.8	4.3	4.8	4.4	5.3	5.3	6.1	5.0	5.4	5.4	5.2	4.8	4.5	4.9	4.1
MgO	2.1	1.6	2.2	2.2	1.5	2.3	1.9	1.4	2.1	1.5	1.1	2.0	2.5	2.2	2.5	2.6	2.4	2.8	3.1	3.7	3.0	3.2	3.4	3.4	3.1	2.9	3.1	2.7
MnO	0.1	0.1	0.1	0.1	0.1	0.1	0.1	0.1	0.1	0.1	0.1	0.1	0.1	0.1	0.1	0.1	0.1	0.1	0.1	0.1	0.1	0.1	0.1	0.1	0.1	0.1	0.1	0.1
CaO	4.1	2.9	4.6	4.7	3.0	5.4	3.3	3.3	3.4	3.3	3.1	3.8	3.7	3.2	4.1	4.4	3.5	4.8	6.2	7.7	6.4	6.4	7.6	6.6	8.6	8.2	8.5	8.8
T																												
Na ₂ O	2.2	2.0	2.2	2.0	1.8	2.3	2.1	2.0	2.0	2.0	2.0	2.5	2.2	2.1	2.3	2.1	2.1	2.5	3.0	3.1	2.7	2.8	2.6	1.8	2.0	1.5	2.1	3.4
K ₂ O	2.3	2.7	2.4	2.6	2.6	2.6	2.8	2.7	2.7	2.4	2.6	2.8	3.0	4.0	3.0	3.0	3.1	3.0	3.0	2.9	2.8	2.7	3.0	3.2	3.0	2.8	2.8	2.4
P ₂ O ₅	0.2	0.1	0.2	0.2	0.1	0.2	0.1	0.1	0.2	0.2	0.1	0.2	0.2	0.2	0.2	0.2	0.2	0.2	0.2	0.3	0.3	0.3	0.2	0.3	0.2	0.2	0.2	0.2
Ba	356	471	259	372	397	350	384	397	380	393	403	438	530	337	446	500	633	515	416	459	369	406	369	464	473	427	366	380
Sr	183	179	178	185	188	189	198	212	203	202	178	202	290	219	234	300	320	290	135	227	180	198	183	210	213	207	180	176
Ni	45	34	46.4	43	28	46	49	38	41	32	23	40	71	106	71	68	78	65	67	76	156	70	89	88.4	88	101	93	85
Cr	91	56	59	68	49	82	70	55	66	72	38.3	77.3	95.8	164	89	101	138	88	106	112	115	105	98	139	108	111	97	110
Zr				340	145	396				301	154	336				240	152	259		188		179	173		153	165		
Y				33.8	19	38				30	20	32				35	19	35		27.6		34	31.2		23	28.4		
Cu	12	27	15	34.6	28	20	26	22	21	30	18	30	58	122	46	64	62	80	677	440	492	206	205	276	52.4	150	91.3	545
V	76	78	67	69	37	93	60	42	67	58	37	76	75	46	77	106	96	112	36.7	36.3	40	100	91	80.7	81.4	76.8	96.7	35.3
Zn	51	88	63	61	66	51	82	99	70	50.3	41	60	120	183	110	231	305	260	442	251	370	120	182	78.3	75.5	68.5	106	
Pb	31			39	38	34	42			32	37	29	235			221	576	216	60	72	97	34	34	35		32	39	
Ce	94.6	40.8	94.3	79.9	45.7	101	73.6	22.1	79.9	66.7	43.2	97.0	80.4	39.2	83.9	69.3	41.2	72.9	61.2	68.4	61.2	68.4	63.3	64.4	71.8	64.6	72.2	30.7
Nd	42.8	17.5	43.1	35.0	18.6	42.5	33.0	9.0	34.8	32.0	18.4	42.9	32.6	15.9	34.1	30.4	19.3	32.2	26.5	28.2	26.5	28.2	28.0	28.1	31.1	26.5	31.4	71.1
Sm	7.9	3.3	8.1	6.7	3.3	8.2	6.2	1.8	6.7	6.0	3.5	8.1	6.4	3.1	6.8	5.9	3.6	6.2	5.2	5.8	5.2	5.8	5.6	5.8	6.4	6.0	6.3	30.7
Eu	1.4	0.7	1.4	1.2	0.7	1.5	1.2	0.4	1.3	1.1	0.8	1.4	1.2	0.8	1.3	1.1	0.7	1.2	1.1	1.2	1.1	1.2	1.3	1.2	1.3	1.1	1.2	6.2
Gd	6.8	2.8	6.8	5.8	2.8	7.0	5.5	1.7	6.0	5.1	3.1	7.0	5.7	3.2	6.0	5.4	3.2	5.5	5.0	5.4	5.0	5.4	5.7	6.1	5.9	5.2	6.0	1.4
Dy	6.0	2.4	5.9	4.9	2.4	5.6	4.9	0.0	5.1	4.3	2.7	5.8	4.7	3.0	4.9	4.6	3.0	4.9	4.1	4.6	4.1	4.6	4.3	4.5	4.7	4.2	5.0	6.6
Er	3.7	1.5	3.6	3.0	1.4	3.9	3.1	0.8	3.2	2.8	1.6	3.5	2.8	1.6	2.9	2.8	1.6	2.9	3.2	3.3	3.2	3.3	3.2	3.4	3.4	3.1	3.5	4.6
Yb	3.1	1.2	3.1	2.6	1.2	3.0	2.5	0.5	2.8	2.3	1.4	3.0	2.5	1.4	2.8	2.3	1.4	2.6	2.2	2.1	2.2	2.1	2.3	2.2	2.0	1.9	2.5	3.7

	Summer PM ₁₀										Winter Suspended Particulate matter								Summer PM ₁₀					
	Delhi			Jhunjhunu		Bikaner					Delhi		Jhunjhunu		Bikaner		Garhmuktesar		Delhi		Jhunjhunu		Bikaner	Garhmuktesar
	a	b	c	a	b	a	b	c	d	a	b	a	b	a	b	a	b	a	b	a	b	a	b	er
SiO ₂	56.7	63.9	66.7	55.9	58.4	63.7	57.5	58.4	54.0	65.5	64.3	60.3	61.9	57.0	55.6	65.1	64.0	59.9	60.0	63.2	62.5	54.2	60.4	
TiO ₂	0.7	0.6	0.6	0.7	0.8	0.6	0.8	0.7	0.7	0.5	0.2	0.4	0.3	0.3	0.5	0.3	0.3	0.4	0.3	0.2	0.3	0.2	0.3	
Al ₂ O ₃	17.7	14.2	11.8	16.6	17.7	13.6	17.0	16.7	17.6	11.3	7.6	12.2	10.6	9.5	12.0	8.8	8.4	10.6	8.5	7.7	9.9	8.4	9.4	
FeO	7.6	4.6	4.1	6.4	6.0	4.8	5.5	5.3	6.0	3.5	1.5	4.1	3.5	2.7	3.9	2.3	2.4	2.8	2.1	2.0	3.0	1.6	2.1	
MgO	3.7	3.0	2.7	4.1	3.8	3.1	3.7	3.5	3.9	2.3	2.6	2.9	2.7	3.1	2.9	2.7	2.6	2.9	2.6	2.6	2.8	3.3	3.3	
MnO	0.1	0.1	0.1	0.1	0.2	0.1	0.1	0.1	0.1	0.1	0.0	0.1	0.1	0.0	0.1	0.0	0.0	0.1	0.0	0.0	0.1	0.0	0.0	
CaOT	7.9	5.9	6.1	9.7	7.6	8.4	10.0	9.9	11.5	6.2	5.8	8.3	8.5	12.9	12.0	5.9	5.3	7.2	6.2	7.2	6.8	11.7	6.7	
Na ₂ O	2.3	4.4	5.6	2.7	1.6	2.9	2.0	1.8	2.7	7.2	14.7	7.6	8.0	10.1	8.7	10.6	12.7	11.6	15.9	10.6	9.8	16.1	12.6	
K ₂ O	3.0	2.9	2.1	3.4	3.6	2.6	3.2	3.1	3.2	3.2	3.2	3.9	4.3	4.2	4.2	4.2	4.1	4.4	4.2	6.0	4.5	4.3	5.0	
P ₂ O ₅	0.3	0.4	0.3	0.3	0.4	0.2	0.3	0.3	0.3	0.1	0.2	0.2	0.2	0.2	0.1	0.1	0.2	0.2	0.2	0.5	0.3	0.2	0.3	
Ba	418	591	695	435	549	356	539	523	341	876	1625	840	1000	1050	421	1027	601	550	1026	760	869	1687	2367	
Sr	141	133	214	175	205	152	196	209	175	172	70	189	224	275	249	65	37.2	50	64	95	132	258	77	
Ni	144	83	74	82	88	89.3	79.6	80.5	67	126	169	94	260	622	388	262	125	96	98	63	70	84	78	
Cr	130	111	96	106	120	119	116	116	92	93	100	76	82	52	95	84	65	91	60	45	61	62	73	
Zr		79		112	83.6		135	128		124			112		120		71			76	70			
Y		23.2		26	19.2		29	28.4		22			24		23		20			19	22			
Cu			8437	5225	5760	941	1300	1251	4100	1896	1319	2511	4725	863	548	493	531	516	28072	28000	1216	22394	4260	
V	40	35	43	108	89.1	64.3	86.4	80.3	27.8	46.7	39	38.1	38.2	39.4	50.1	40.5	41	37	35	33.5	45.6	29.4	34.8	
Zn	446	810	234	163	136	296	127	98.5	108	469	661	744	654	529	323	542	1204	123	449	475	652	1333	316	
Pb	127	246	153	52	46	39	41.6	40	45	384	279	299	245	212	55	142	137	576	429	436	463	524	633	
Ce	60.5	58.9		61.0	60.4	61.6	68.3	60.0	65.1	31.3	47.8	44.5		32.0	52.4	36.9	37.3	33.8		19.2	32.4		24.5	
Nd	25.6	24.9		26.7	24.7	26.7	28.8	25.8	27.9	12.3	19.1	18.9		12.3	21.5	14.8	14.3	13.6		7.2	12.0		8.7	
Sm	5.2	4.8		5.4	5.3	5.6	6.1	5.3	5.8	2.5	3.8	3.7		2.7	4.6	3.0	3.0	2.7		1.5	2.7		1.9	
Eu	1.2	1.3		1.2	1.2	1.2	1.3	1.2	1.3	0.5	0.7	0.8		0.5	1.0	0.6	0.6	0.6		0.3	0.5		0.4	
Gd	5.3	5.4		5.6	6.0	6.1	6.3	5.4	6.2	2.6	3.7	3.8		3.1	4.6	3.1	3.3	3.0		2.1	3.0		2.2	
Dy	3.8	4.1		4.2	3.8	4.3	4.6	3.9	4.2	2.0	2.9	2.8		2.2	3.4	2.4	2.2	2.2		1.2	2.0		1.5	
Er	3.0	3.1		3.3	3.2	3.2	3.5	3.0	3.4	1.9	2.5	2.2		2.2	3.0	2.2	2.1	2.1		1.4	1.9		1.8	
Yb	1.8	1.6		2.2	1.9	2.0	1.9	1.9	1.9	0.9	1.5	1.0		1.1	1.7	1.3	1.1	1.0		0.6	0.8		0.8	

CaOT indicate total calcium; a, b, c and d represent the different samples analyzed; 1a and 1b in free fall samples represent <75 µm and >75 µm fractions of bulk respectively.